Dimerization of the Fbw7 ubiquitin ligase impacts substrate regulation, tumor suppressor activity

Elizabeth Anne Larimore

A dissertation

submitted in partial fulfillment of the

requirements for the degree of

Doctor of Philosophy

University of Washington

2012

Reading Committee:

Bruce Clurman, Chair

Susan Biggins

Ning Zheng

Program Authorized to Offer Degree:

Molecular and Cellular Biology

University of Washington

Abstract

Dimerization of the Fbw7 ubiquitin ligase impacts substrate regulation, tumor suppressor activity

Elizabeth Anne Larimore

Chair of Supervisory Committee
Professor Bruce E. Clurman
Department of Pathology

The SCF (Skp1-Cullin1-F-box protein) is a multi-protein ubiquitin ligase that regulates the abundance of proteins involved in myriad cellular processes. The system uses interchangeable F-box proteins to impart substrate specificity to the ligase. Fbw7, the human ortholog of yeast Cdc4, is an F-box protein and the SCF^{Fbw7} complex regulates a number of proto-oncoprotein substrates including cyclin E, c-Myc, Notch, and c-Jun. Accordingly, Fbw7 is a tumor suppressor and is mutated in approximately ten percent of human malignancies.

Fbw7 binds its substrates after they become phosphorylated within a consensus sequence called a Cdc4 phospho-degron (CPD). CPD phosphorylation creates a high-affinity binding site for Fbw7, which sets into motion the process of substrate ubiquitylation and subsequent degradation by the proteasome. Although phosphorylation of high-affinity CPDs regulates several Fbw7 substrates, our data suggest this model of regulation may be incomplete. A dimerization domain found in Fbw7 is evolutionarily conserved from yeast to human, and the domain is also found in several other F-box proteins.

In this thesis I present my work studying the functions of Fbw7 dimerization. Using AAV-mediated gene-targeting, I generated a human cell line in which the dimerization of Fbw7 is ablated, and used this as a tool to study the effects on substrate turnover. I also present my novel purification of recombinant dimeric Fbw7 and my efforts to crystallize the complex. *In vitro* studies using purified Fbw7 dimers and monomers showed that a dimeric ubiquitin ligase can interact with two substrate degron sequences

simultaneously while the monomer cannot. The dimeric ligase can also attach ubiquitin to more substrate lysine residues than can a monomeric ligase.

TABLE OF CONTENTS

LIST OF FIGURES ..... **iii**

CHAPTER 1: Introduction **1**
Elimination of short-lived proteins is a crucial aspect of various cellular processes 1
The ubiquitin-proteasome system regulates cell cycle transitions 2
The oncoprotein cyclin E is a crucial cell cycle protein and its destruction is phosphorylation-dependent 3
Fbw7, the ortholog of yeast Cdc4, is the F-box protein that recognizes phosphorylated cyclin E 5
Multiple site recognition accounts for degradation of some SCF substrates and may demand F-box protein dimerization 6
Dimerization may partially explain the cancer-associated selection for point mutations at critical arginines in Fbw7 7
A model for Fbw7 dimer function: separate contacts to separate degrons 9
Aims of dissertation research 9

CHAPTER 2: Disruption of Fbw7 in human cells leads to dereguation of substrates cyclin E and Myc **17**
Rationale behind engineering a human cell line that lacks Fbw7 dimers 17
Adeno-associated virus is an efficient method for gene-targeting in human cells 17
Generation of AAV targeting vector 18
Generation of AAV virus 20
Targeting and confirming proper engineering of Fbw7 21
Introducing the ΔD mutation does not alter total Fbw7 levels, causes the endogenous protein to form monomers 23
Analysis of cyclin E levels in Fbw7 ΔD cells 25
Analysis of c-Myc stability in Fbw7 ΔD cells 25
Cell cycle analysis of ΔD cells 26
Conclusions and future directions 27

CHAPTER 3: Purification of recombinant Fbw7 dimer and crystallography efforts **34**
Fbw7 has been largely studied as a monomer 34
The structural knowledge of cyclin E is incomplete 35
An F-box protein dimer structure (with or without substrate) would greatly inform our understanding of substrate interaction 35
Generating dimeric Fbw7 from insect cells 36
FPLC methods 38
Purified Fbw7 dimer was used for crystallography trials and a hit was identified 40
Cyclin E/CDK2 purification from insect cells 44
Use of cyclin E peptide, other protein additives to improve crystal formation 47
Attempt to visualize SCF^{Fbw7} dimer by electron microscopy 48
Conclusions and future directions 49

Chapter 4: Characterization of Fbw7 dimers and monomers *in vitro* **65**
The SCF's cognate E2s 65
Neddylation of Cullins 65
The two-degron model can be studied *in vitro* 66

Recombinant dimeric Fbw7 is active against cyclin E and c-Myc and can utilize two different E2 enzymes 66
The two-degron model can be recapitulated in vitro, both with ubiquitylation and binding assays....68
The dimeric SCF has more ubiquitin attachment sites than does the monomer 68
Cullin neddylation is not necessary *in vitro*....69
UbcH5 is a very promiscuous E2 69
Several substrate-like proteins that are not degraded in cells can be poly-ubiquitylated *in vitro*....70
Purification of Fbw7 wild-type/arginine mutant hetero-dimer....71
Using purified Fbw7 in surface plasmon resonance pilot experiments....72
Conclusions and future directions 74

Chapter 5: Conclusions 87

BIBLIOGRAPHY 90

CURRICULUM VITAE 97

LIST OF FIGURES

Figure Number		Page
1.1	The ubiquitin cascade	11
1.2	Ubiquitylation is a multi-faceted protein signal	12
1.3	The Cullin-RING ligase superfamily	13
1.4	The Fbw7 substrate network	14
1.5	Fbw7 binds a consensus degron sequence in substrate molecules	15
1.6	Dimerization represents an addition facet of Fbw7 substrate regulation	16
2.1	*FBXW7* locus and Fbw7 dimerization domain	29
2.2	Gene-targeting of Fbw7 dimerization domain	30
2.3	The ΔD mutation does not affect abundance, does interrupt dimerization *in vivo*	31
2.4	Cyclin E and c-Myc are moderately deregulated in ΔD cells	32
2.5	Cell cycle kinetics of ΔD cells	33
3.1	Fbw7 dimer purification by GST-affinity	52
3.2	Insertion of a flexible linker sequence allows TEV access to the cleavage site	53
3.3	Workflow for purification of crystallography-grade dimeric Fbw7	54
3.4	Purification of the Fbw7 dimer by anion exchange chromatography	55
3.5	Purification of the Fbw7 dimer by size exclusion chromatography	56
3.6	Fbw7 dimer protein crystals	57
3.7	The known structures of cyclin E/CDK2	58
3.8	Purification of the GST-cyclin E/CDK2 complex works, TEV cleavage is problematic	59
3.9	Reversing the tagging scheme resulted in extremely little cyclin E	60
3.10	Thrombin cleavage of GST from cyclin E is effective but very concentration-sensitive	61
3.11	Formation of the Skp1/Fbw7 dimer: cyclin E/CDK2 complex	62
3.12	Formation of the Fbw7/Skp1/Cul-1 NTD complex	63
3.13	Negative stain electron micrographs of purified Fbw7 complexes	64
4.1	Initial ubiquitylation reaction with recombinant cyclin E	75
4.2	Poly-ubiquitylation of over-expressed cyclin E in cell lysate	76
4.3	Active Cdc34 can be purified from insect cells	77
4.4	Over-expressed c-Myc is also poly-ubiquityated by Cdc34 in a CPD-dependent manner	78
4.5	Two-degron model of cyclin E degradation is recapitulated *in vitro*	79
4.6	Fbw7 monomer and dimer lysine accessibility and poly-ubiquitin chain composition	80
4.7	Neddylation of Cul-1 does not affect poly-ubiquitylation by Fbw7 *in vitro*	81
4.8	UbcH5 is an extremely promiscuous E2	82
4.9	Other purified E2s do not demonstrate significant activity with the SCF *in vitro*	83
4.10	Pseudo-substrates are poly-ubiquitylated by UbcH5 but not Cdc34	84
4.11	Fbw7 hetero-dimer is deficient in leading to poly-ubiquitylation of cyclin E	85
4.12	Qualitative comparison of Fbw7/cyclin E binding by SPR	86

ACKNOWLEDGEMENTS

Many thanks to Bruce and Ning for their guidance and support. More thanks to Markus Welcker for his firm yet excellent instruction and collaboration—and for buying me a beer on a few occasions when I really needed it.

I am also grateful to the members of the Clurman lab for teaching and helping me, especially in the early years: Jherek Swanger, Jon Grim, Bridget Hughes, Michael Davis, Asli Hizli, Amanda Hagar, Shlomo Handeli.

I am also incredibly grateful to the wonderful, warm Zheng lab. They taught me so much scientifically, and also completely took me into the fold. I wouldn't have done it without you: Xiaobo Tang, Haibin Mao, Nabiha Saifee, Jian Payandeh, Erik Zimmerman, Ken Garbutt, Ji Sun, Hui Wang, Chris Nicolaus, Weiman Ting, Jeannine Gibbons. And our dear Laura Sheard.

Thank you to the other scientists who consulted with us on various aspects of this work and helped this project along: Della Friend and Roland Strong; Matt Iadanza and Tamir Gonen; Peter Littlefield and Rachel Klevit; Brett Kaiser and Barry Stoddard; Anda Cornea and Dave Russell.

Thank you, Lisa Connell-Crowley, for the incredible mentorship. You were just what I needed—thank you for the opportunities.

Thank you to my wonderful group of classmates whose camaraderie and friendship buoyed me along through this process. I'm including Albert Lang here.

Thank you to my lay-friends for having absolutely no doubts that I could do this. Arielle Jordan, Malgorzata Bereziewicz, Emily Mangone: you're the best. Thanks also to Dana Chen and Marquise McGraw.

And thank you to my family for all of your support and empathy. I couldn't be any luckier.

And thank you, G. You're my favorite.

DEDICATION

For my mom and

for my dad,

the original Dr. Larimore

CHAPTER 1

Introduction

Elimination of short-lived proteins is a crucial aspect of various cellular processes

Intracellular communication is largely accomplished by modifications in protein structure and localization. Reversible modifications such as phosphorylation, acetylation and methylation effect changes in protein function or localization. Protein destruction, on the other hand, is an irreversible modification and represents the ultimate commitment to a cellular decision.

Vacuolar and cytoplasmic proteases digest cellular proteins in a generally non-specific manner. In contrast, the ubiquitin-proteasome system (UPS) carries out regulated destruction of short-lived and damaged proteins, rapidly eliminating its targets in response to cellular signals [1]. The UPS is a vital regulatory component of various cellular processes including signal transduction, cell cycle progression, and the induction of the inflammatory response. The UPS relies on the 26S proteasome, a ubiquitously expressed barrel-shaped complex that processively digests substrates in an ATP-dependent manner with a high degree of specificity [2]. Because the UPS is central to so many different cellular processes, proteasome inhibition by small molecules is a topic of interest in cancer treatment, and such compounds have been employed in treating myeloma.

The proteasome targets cellular proteins that are covalently modified with a chain of ubiquitin moieties. Ubiquitin is a small (approximately 8 kDa), ubiquitously expressed protein conserved in all eukaryotes. The general process of protein ubiquitylation (Figure 1.1) consists of discrete steps catalyzed by specialized enzymes [3]. The ubiquitin-activating enzyme (E1) charges the ubiquitin moiety: in an ATP-consuming reaction, a high-energy thioester bond is formed between a cysteine residue in the active site of the E1 and the carboxy-terminus of the ubiquitin molecule, thereby activating the ubiquitin C-terminus for nucleophilic attack. There is just one E1 enzyme in the yeast genome and two in the human genome. When the ubiquitin•E1 engages a ubiquitin-conjugating enzyme (E2), the thioester bond is then transferred to a cysteine residue in the E2. There are 13 E2 enzymes in the yeast genome and at least 38 in the human genome [4]. The cascade terminates with the conjugation of the carboxy-terminus of

activated ubiquitin to a lysine residue of the substrate and relies on an E3 substrate-recognition protein, termed the ubiquitin ligase. There are two classes of E3s. In the case of the approximately 60 human HECT domain-containing E3 ligases [4], substrate ubiquitylation occurs after transfer of the ubiquitin moiety to an active-site cysteine in the E3. In the case of the approximately 600 human RING domain-containing E3 ligases [4], the transfer of ubiquitin from the E2 to substrate is simply bridged by the E3, which brings the charged E2 and the substrate into close proximity. (The RING domain is the docking site for the charged E2 [5].) The reaction iterates, attaching another ubiquitin moiety to a lysine residue of the prior moiety. Because ubiquitin itself contains seven lysine residues (K6, K11, K27, K29, K33, K48, K63), the ubiquitin-ubiquitin conjugation can theoretically occur on any of seven sites and each linkage displays a different structural topology [6]. The chain formed is thought to be mainly a function of the E2 enzyme performing the conjugation [7]. (See Figure 1.2.) The originally identified and best-studied poly-ubiquitin modification is the K48-linked chain. A K48-linked poly-ubiquitin chain of at least four ubiquitin moieties is recognized as a substrate for proteolytic degradation by the 26S proteasome [8]. K63-linked chains are important in signaling protein localization information and are involved in DNA-damage [9] and NFκB signaling [10]. Some E2s perform mono-ubiquitylation of substrates, which is an important localization signal for a variety of cellular proteins [11].

As mentioned above, a subset of the UPS relies on E3 ligases, of which there are hundreds of human proteins and protein complexes. Substrates are recognized via degron motifs, primary protein sequences that attract the cognate E3. The E3 is important in bringing the targeted substrate and the E2 in proximity and, in at least some cases, precisely positions the components to promote substrate ubiquitylation. In summary, for substrates that are regulated by the UPS and whose regulation is dependent on one or more E3s, recognition by the E3 is the rate-limiting, regulated step in substrate turnover and is of intense interest in the study of regulated proteolysis [12].

The ubiquitin-proteasome system regulates cell cycle transitions

Protein destruction by the UPS is important in driving the key transitions of cell cycle progression and ensuring its unidirectionality. Two RING-containing E3s are especially important in cell cycle control,

the anaphase-promoting complex/cyclosome (APC/C) and the Skp1-Cullin-1/Cdc53-F-box protein (SCF) complex, one member of the Cullin-RING superfamily (Figure 1.3). Both are multi-subunit protein complexes and several components show an evolutionary relationship between the two [13]. However, the substrates they regulate differ and the regulation of the ligases are quite divergent [14]. The activity of the APC/C itself is regulated by the availability of activating subunits: association of these subunits induces ubiquitin ligase activity toward its substrates. The abundance of the APC/C activating subunits, Cdc20 and Cdh1, are controlled in a cell cycle-dependent manner. In contrast, SCF complexes are theoretically active toward substrates throughout the cell cycle whereas regulation is accomplished at the substrate level, namely via the modification of substrate degron sequences. I will focus below on the SCF.

Cullin-1 (Cul-1) is the elongated scaffold at the core of the SCF ligase and precisely positions the additional components required for substrate ubiquitylation [15]. The C-terminus binds a RING-domain protein Rbx1, which serves as the dock for the E2 ubiquitin-conjugating enzyme to the SCF. The N-terminus of Cul-1 binds Skp1, which serves as the adaptor to one of many F-box proteins. The F-box protein is the interchangeable component of the ligase machinery, and performs the substrate recognition and binding, thereby facilitating the transfer of ubiquitin from the E2 to the substrate [16, 17]. F-box proteins are of particular interest, namely in how they accomplish substrate recognition for the SCF. There are about 70 proteins in the human genome that contain the F-box domain that binds Skp1 [18]. Most F-box proteins remain uncharacterized, and they may not necessarily play roles in protein degradation.

Drivers of cellular proliferation must be carefully controlled in normal cells to safeguard against uncontrolled division. Thus, defective degradation of such oncoproteins is associated with cancer and other malignancies. Ubiquitin ligases that regulate proto-oncoproteins and how this regulation is subverted in cancer cells are areas of intense interest in cancer biology.

The oncoprotein cyclin E is a crucial cell cycle protein and its destruction is phosphorylation-dependent

A hallmark of cancer cells is their active proliferation, proceeding unchecked through the cell cycle. At the core of normal cell cycle progression are the cyclin-dependent kinases (CDKs) that

phosphorylate a variety of proteins to promote DNA replication, mitosis, etc. CDK activity is controlled, in part, by the availability of its activating subunits, the cyclin proteins. Cyclin E is one such protein that activates CDK2 in the G1 phase of the cell cycle. Cyclin E mRNA and protein increase in late G1/S and then rapidly decline in S phase [19]. In contrast, the levels of the CDK proteins do not fluctuate appreciably; however, their kinase activity drops without the activating cyclin.

As a positive regulator of the cell cycle, cyclin E is an oncoprotein. Indeed, over-expression of cyclin E drives S-phase entry in tissue culture experiments [20, 21] and excess cyclin E has been reported to cause chromosomal instability in cell lines [22]. Cyclin E protein levels are deregulated in a variety of human malignancies including breast, ovary, and endometrial [23, 24] and high cyclin E protein levels among breast cancer patients correlates with poor survival [25, 26]. Cyclin E expression in mouse mammary epithelia results in hyperplasia [27], reinforcing the clinical relevance of proper cyclin E regulation.

As mentioned above, in a normal cell cycle, cyclin E-CDK2 activity is kept in check by rapid elimination of the cyclin E protein after S-phase entry. The cyclin E gene locus is amplified in a few human tumors [28, 29] but in most cases deregulation is post-translational, which implicates improper protein turnover in these malignancies. Cyclin E protein is degraded by the SCF complex [23, 30], and the phosphorylation status of a degron sequence at the C-terminus of cyclin E (T380 and S384) largely dictates the stability of the protein [31, 32]. Because T380 is auto-phosphorylated by CDK2, cyclin E elegantly limits its own abundance. T380 is also a glycogen synthase kinase-3 (GSK3) target [33], indicating cyclin E is a node in several signaling pathways. The phosphorylation status at an additional site, threonine 62 (T62), also impacts protein stability, but the C-terminal degron is the dominant determinant of cyclin E stability [33, 34]. The synergistic effect of multisite phosphorylation events will be discussed in more detail below.

An alternative degradation pathway for cyclin E not complexed to CDK2 is Cul-3-dependent [35]. Deletion of the Cul-3 gene in mice causes accumulation of cyclin E and affects proper cell cycling [35, 36]. The mechanism for the Cul-3-dependent cyclin E degradation is not as well understood as the Cul-1-

dependent pathway; the Cul-3 substrate adaptor (BTB) protein that recognizes cyclin E has not been identified.

Fbw7, the ortholog of yeast Cdc4, is the F-box protein that recognizes phosphorylated cyclin E

Fbw7 is the human F-box protein that recognizes phosphorylated cyclin E and leads to its SCF-mediated degradation [23, 30, 37]. In addition to cyclin E, Fbw7 was found to also regulate the oncoproteins c-Myc [38-40], c-Jun [41, 42], and Notch [38, 40-46]. (See Figure 1.4.) Indeed, Fbw7 is frequently mutated or deleted in human cancers and is a tumor suppressor [47, 48]. More recently additional pro-growth and anti-apoptosis proteins such as SREBP [49, 50], MCL1 [51, 52], TGIF1 [53] and KLF5 [54, 55] have been identified as Fbw7 substrates, and the list continues to grow. Fbw7 was also identified as one of the driver mutations in colorectal cancer [56].

Fbw7 is the human ortholog of *Drosophila* Archipelago, *C. elegans* Sel-10, and budding yeast Cdc4 [23, 37, 57]. These proteins are highly conserved and share core functional domains. The C-terminus of Fbw7 and its orthologs contain WD repeats that fold into an eight-bladed propeller structure made of β-sheets. The WD propeller makes contact to the phosphorylated degron sequence in its substrates [58], which will be discussed at length below. The molecular interaction between Fbw7's propeller and the phospho-degron of its substrates is mediated by three conserved arginines in the WD repeats that form a phospho-binding pocket in the propeller structure. These arginine residues constitute mutational hotspots in human tumors [59, 60], accounting for nearly half of all Fbw7 mutations. The mutational spectrum of Fbw7 in cancers and the implications for its basic biology will be discussed in further below.

The human and mouse Fbw7 genes specify three protein isoforms (α, β, and γ) that display unique sub-cellular localization and tissue-specific expression patterns: α is nucleoplasmic and ubiquitously expressed; β is localized to cytoplasmic membranes and is expressed in mouse brain and skeletal muscle; γ is nucleolar and is expressed in heart and skeletal muscle [30, 43, 47, 61]. A conserved, approximately 40-amino acid dimerization domain was described in Fbw7 several years ago, located N-terminal to the F-box [62, 63]. Three distinct protein isoforms and the potential for dimerization

are features of Fbw7 that suggest additional layers of complexity in substrate regulation by the ligase. Dimerization will be discussed further below.

Multiple site recognition accounts for degradation of some SCF substrates and may demand F-box protein dimerization

In the yeast cell cycle, the SCF^{Cdc4} catalyzes the degradation of the cyclin-dependent kinase inhibitor Sic1, and substrate recognition depends on phosphorylation of Sic1 by the active yeast CDK [64, 65]. Degradation of other yeast proteins including transcription factor Gcn4 [66], mating pheromone arrest protein Far1 [67], and replication initiation factor Cdc6 [68] occurs in a similar phospho-dependent manner: Cdc4 recognizes and binds phosphorylated sequences in these substrates that conform to a consensus sequence termed a Cdc4 phospho-degron, or CPD [69]. (See Figure 1.5A.)

There are nine potential CPDs in the Cdc4 substrate Sic1, and yet not one is sufficient to lead to degradation. This is because each Sic1 CPD varies substantially from the optimal consensus sequence [69], and one can imagine that the 'mismatches' might compromise Cdc4 binding affinity. However, there appears to be *cooperativity* among these weak degrons: phosphorylation of four or more CPDs lead to Sic1 destruction [70]. This multiple site recognition serves a biologic purpose in the yeast cell cycle: Sic1 degradation does not efficiently proceed until a high threshold of CDK activity is achieved. The current model in the field to explain this phenomenon is one of allovalency [70-72]. This model supposes that these low-affinity CPDs may weakly recruit Cdc4, but that the molecules dissociate before ubiquitylation occurs. Once Sic1 reaches a threshold of multisite phosphorylation, though, it can no longer diffuse away from Cdc4. Each Sic1 CPD still only weakly attracts Cdc4, but because there is a critical number of phospho-degrons, Sic1 is trapped near Cdc4 and substrate turnover will eventually occur.

Like Cdc4, Fbw7 recognizes and binds to phospho-degrons in its substrates. The characteristics of the primary amino acid sequence that makes up a CPD elegantly defined by Nash et al. largely apply to the CPDs within substrates that Fbw7 recognizes (Figure 1.5B). In fact, the human cyclin E CPD is bound by yeast Cdc4 protein. As mentioned above, cyclin E stability is largely determined by the phosphorylation

status at T380; the amino acid sequence surrounding T380 constitutes a CPD that is recognized and bound by Fbw7.

There is also evidence of Fbw7 functioning through multi-site recognition. Cyclin E contains a second CPD sequence at T62 that, although phosphorylated by an undetermined kinase, is *not* sufficient to recruit Fbw7 and promote turnover. The affinity of this sequence to Fbw7 was undetectable by isothermal titration calorimetry (ITC) [73]. Thus, this cyclin E T62 CPD appears similar to the many CPDs of Sic1, at best a 'low-affinity' degron, and its role in cyclin E turnover was poorly understood, at least in the shadow of the potential 'high-affinity' CPD at T380.

The 'high-affinity' nature of the T380 degron can be studied by perturbation of the amino acid sequence surrounding the central threonine. Strikingly, mutation of S384 to non-phosphorylatable alanine (S384A) renders the T380 degron, alone, insufficient to promote cyclin E turnover. (The S384A mutation does not grossly affect T380 phosphorylation: S384 is strictly auto-phosphorylated by CDK2, and while it *does* prime for T380 phosphorylation by GSK3β, in the absence of S384 auto-phosphorylation T380 is auto-phosphorylated by CDK2.) The additional phosphorylation at S384 confers an approximately 1000-fold increase in affinity to the single T380 phosphorylation when measured by ITC [73], which is concordant with the observation that the wild-type, fully phosphorylatable sequence is sufficient to recruit Fbw7 while the S384A mutant is not.

And yet, more strikingly, mutant S384A cyclin E *can* be degraded; however, this turnover strictly requires phosphorylation at T62 (M Welcker, unpublished observation). Remarkably, dimerization of Fbw7 is a requirement for this degron cooperation (M Welcker, unpublished observation). A small deletion of the Fbw7 dimerization domain renders over-expressed Fbw7 non-dimerizable, ie monomeric [63] and while monomeric Fbw7 is able to efficiently degrade most substrates, including wild-type cyclin E and T62A mutant cyclin E, monomer cannot degrade S384A mutant cyclin E. (See Figure 1.6.)

Dimerization may partially explain the cancer-associated selection for point mutations at critical arginines in Fbw7

Dimerization has been previously reported in the fission yeast Fbw7 orthologs Pop1 and Pop2 [74, 75] and the budding yeast ortholog Cdc4 is also reportedly found primarily in dimers [76]. The Fbw7 dimerization domain is also conserved among other F-box proteins including human β-TrCP 1 and 2 [77]; Fbx4, the human F-box protein responsible for cyclin D1 turnover [78]; and budding yeast Met30 [76, 79]. This conservation across species and among F-box protein lineages indicates dimerization is an important functional feature of a subset of SCF-mediated ubiquitination.

As mentioned above, many cancer-associated Fbw7 mutations are point mutations of the key arginines in the WD propeller that form the CPD-binding pocket. Nearly half of mutations hit R465 or R479. In overexpression studies, these mutations abrogate substrate binding, thus rendering the ligase unable to properly regulate its substrates. What is interesting about the mutational spectrum, however, is that these mutations are typically only found in only one *FBXW7* allele and do not exhibit concomitant loss of the wild-type allele. Although it is not known whether the wild-type alleles are normally expressed in these tumors, the wild-type protein is theoretically present. How are these mutations sufficient to drive tumorigenesis in the context of wild-type protein?

Fbw7 dimerization presents a mechanism for the mutant protein to dominantly inhibit the wild-type protein. If all Fbw7 forms dimers and protein dimerization occurs randomly, we would predict 25% of dimers would be mutant/mutant, 50% would be wild-type/mutant, and only 25% would be fully functional wild-type/wild-type. If substrate-binding functionality is required in both protomers, a point mutation in one allele combined with protein dimerization would effectively cause a loss of 75% of the Fbw7 function.

However, this hypothesis is not completely satisfactory to explain the selection for arginine point mutations. If loss of substrate binding combined with protein dimerization comprised the whole story, nonsense mutations C-terminal to the dimerization domain would also be highly selected for. However, this type of selection is not observed; nonsense mutations are much more rare than R479 and R465 mutations and are found along the entire length of the coding sequence.

This evidence points to a model in which mutation of a key arginine residue in half the Fbw7 protein is advantageous for some reason to a cancer cell. Complete loss of Fbw7 function is not advantageous, perhaps because too many systems fail and the cell can sense this as a disaster. But it

might be that dialing down the system by 75% is a compromise that keeps many Fbw7 substrates largely under control while allowing escape for just one or a few critical oncoproteins. The Fbw7 isoforms may also play a role because, with their differential localization, they may regulate different substrate subsets.

A model for Fbw7 dimer function: separate contacts to separate degrons

As discussed in the section above, a mixed mutant/wild-type dimer may or may not be able to effectively regulate its target substrates. We have seen in overexpression experiments that monomeric Fbw7 can be recruited to substrates with high-affinity CPDs. Thus, we might expect that the wild-type half of a mixed mutant/wild-type dimer may well be sufficient to regulate this class of high-affinity substrates. On the other hand, there may be low-affinity substrates that require a completely functional dimer for turnover. Although we have yet to identify a natural substrate that demonstrates such dimer-dependency, we demonstrated it with our overexpression studies of cyclin E CPD mutants described above.

To explain our Fbw7 dimer-dependent cyclin E turnover data, we proposed the novel hypothesis that each Fbw7 moiety of a dimer is able to make independent contact with one of the two cyclin E CPDs. This model accounts for the observation of dimer-dependent turnover requiring two distinct degrons in the S384A background. Unlike the allovalency model discussed for Sic1, we propose that both WD propellers can simultaneously engage distinct CPDs, leading to substrate turnover. This is an important distinction, saying that F-box protein dimerization does not simply serve to indirectly increase local affinity to a single CPD signal, but suggesting a highly specific mode of dimer/substrate interaction.

Because distinct phospho-degrons are potentially generated by different signals, this model also implied additional possible layers of substrate regulation. We proposed Fbw7 dimerization also allows for discrimination among substrates based on their CPD ‘strength.’ We can speculate that for substrates with only a single low-affinity CPD, a binding partner might supply the additional degron required for turnover. Spatial separation of two degrons that are generated by different signals would allow for exquisite control of substrate abundance.

Aims of dissertation research

The experiments discussed in the following chapters aimed to understand in greater detail the phenomenon of Fbw7 dimerization. When this work was undertaken, it was not known to what extent Fbw7 dimers were formed in human cells and whether Fbw7 dimerization was a regulated cellular process. The first report of regulated F-box protein dimerization is of the SCF^{Fbx4} that regulates cyclin D1: GSK3β phosphorylation of the F-box protein Fbx4 proximal to the conserved dimerization domain promotes Fbx4 dimerization and, consequently, cyclin D1 turnover [78]. This is the first evidence of turnover regulation not at the substrate level, but rather by regulation of the SCF ligase itself. This finding sets an exciting precedent, but whether dimerization regulation is a mechanism common to Fbw7 substrate regulation or the SCF in general remains a major open question. More recently, the activity of the prolyl isomerase Pin1 was reported to structurally disrupt an Fbw7 dimer after phosphorylation of Fbw7α at T205. Our data, however, does not confirm these findings (M Welcker, unpublished data).

Chapter 2 discusses my generation of a knock-in human cell line in which Fbw7 dimerization has been perturbed. Chapter 3 discusses my purification of Fbw7 dimers and crystallography trials involving this protein. Chapter 4 discusses my *in vitro* studies using purified Fbw7 dimer and monomer.

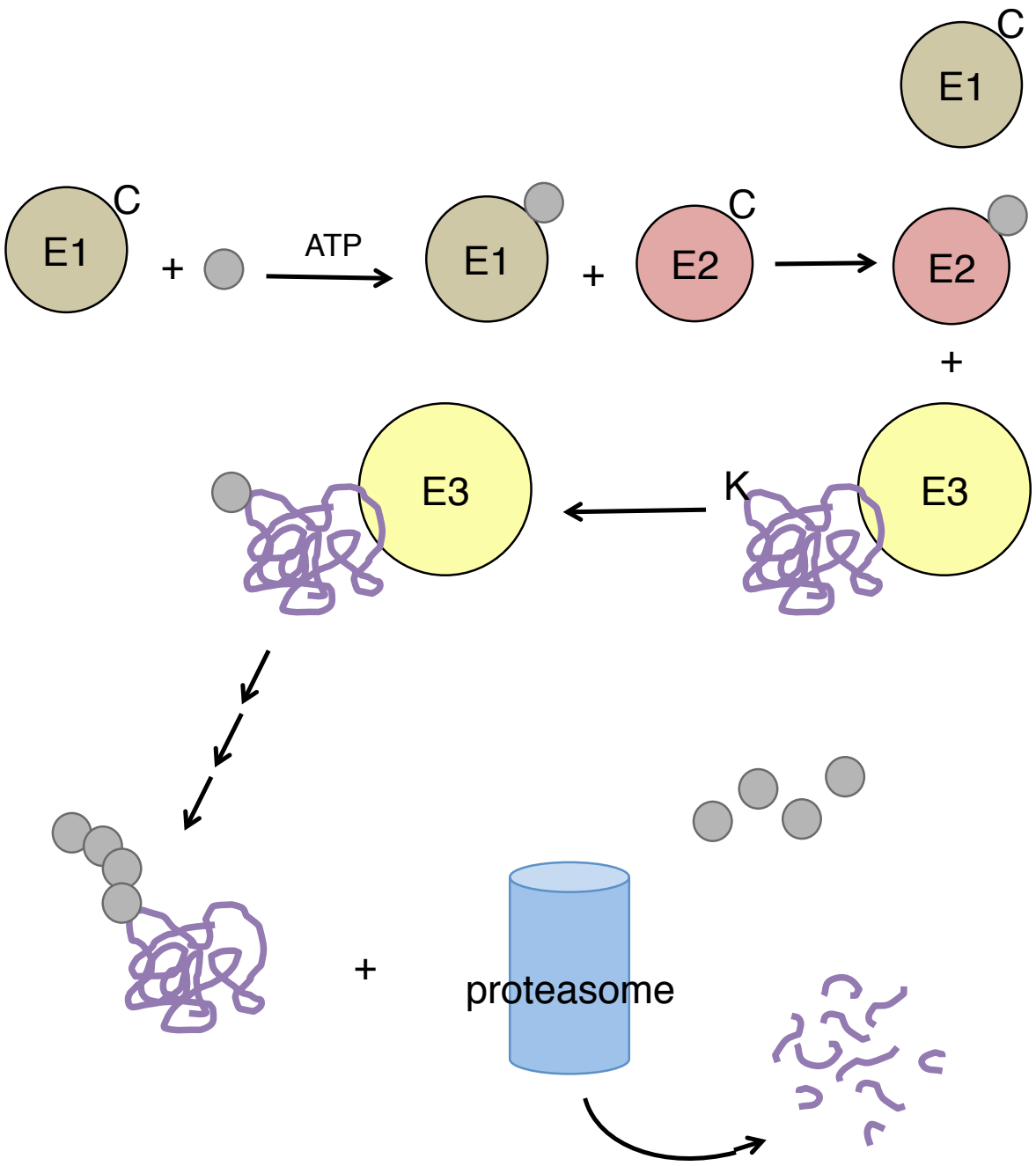

Figure 1.1: The ubiquitin cascade

In an ATP-consuming reaction, the C-terminus of a ubiquitin molecule (gray circle) forms a high-energy thiolster bond with the active site cysteine residue in the E1 ubiquitin activating enzyme. The ubiquitin is then transferred to the active site cysteine in an E2 ubiquitin-conjugating enzyme. Ubiquitylation of many substrates relies on a third protein, called the E3 ubiquitin ligase. The E3 carries out substrate recognition (the substrate is in purple) and facilitates transfer of the ubiquitin onto a lysine residue in the substrate. The reaction iterates, resulting in a poly-ubiquitin chain. Proteins with a chain of four ubiquitin moieties are substrates for proteolytic cleavage by the 26S proteasome.

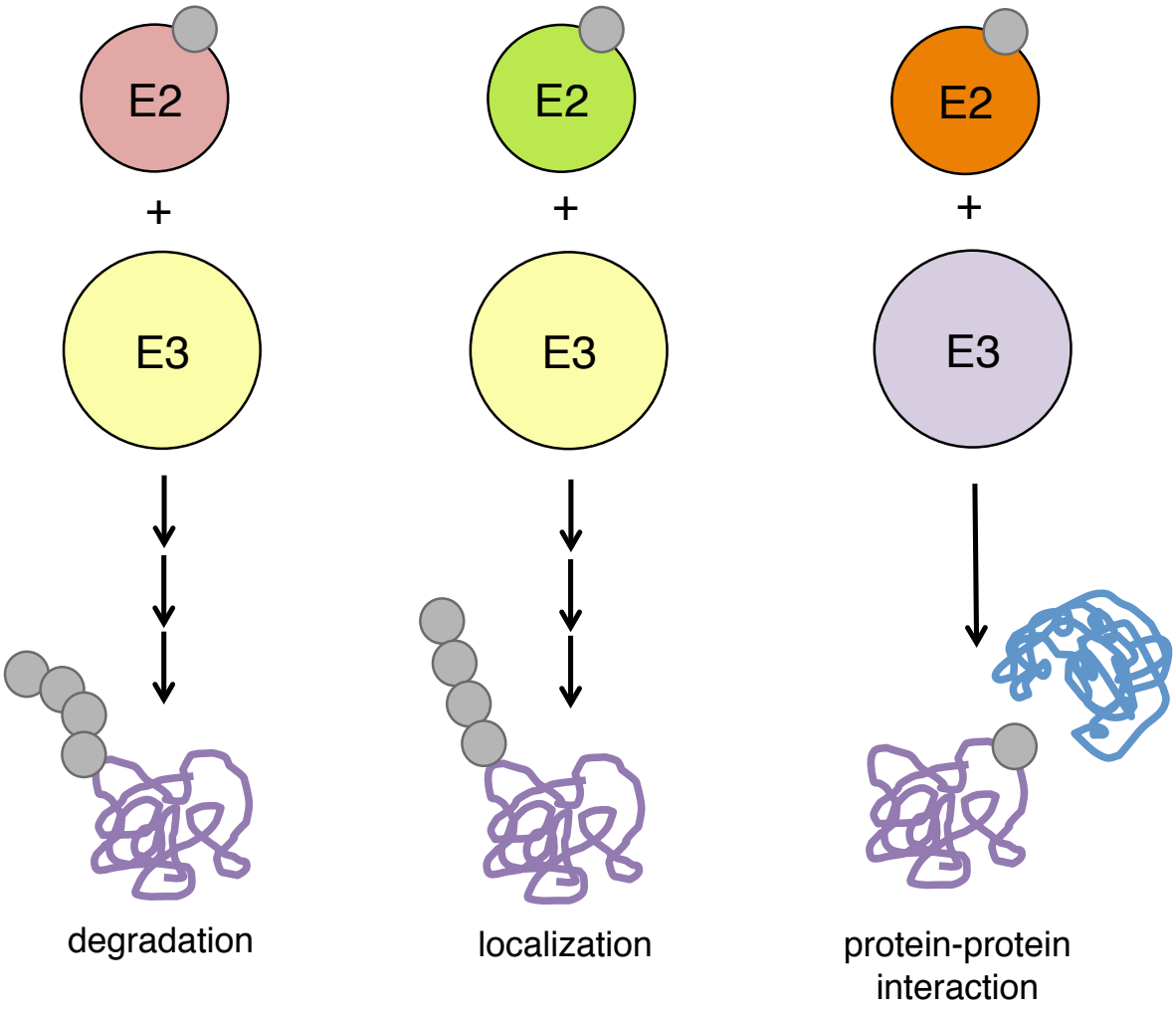

Figure 1.2: Ubiquitylation is a multi-faceted protein signal

Although protein degradation is the best-understood role of the ubiquitin-proteasome system, protein ubiquitylation can signal a variety of protein fates. A poly-ubiquitin chain linked through the K48 residue in ubiquitin signals the substrate for proteolytic degradation. A poly-ubiquitin chain linked through K63, for instance, might encode a localization signal. Conjugation of a single ubiquitin moiety is a distinct modification and often results in localization changes and/or modulates protein-protein interactions. The different chain topologies are thought to mainly be dictated by the E2 involved, although the E3 can also play a role.

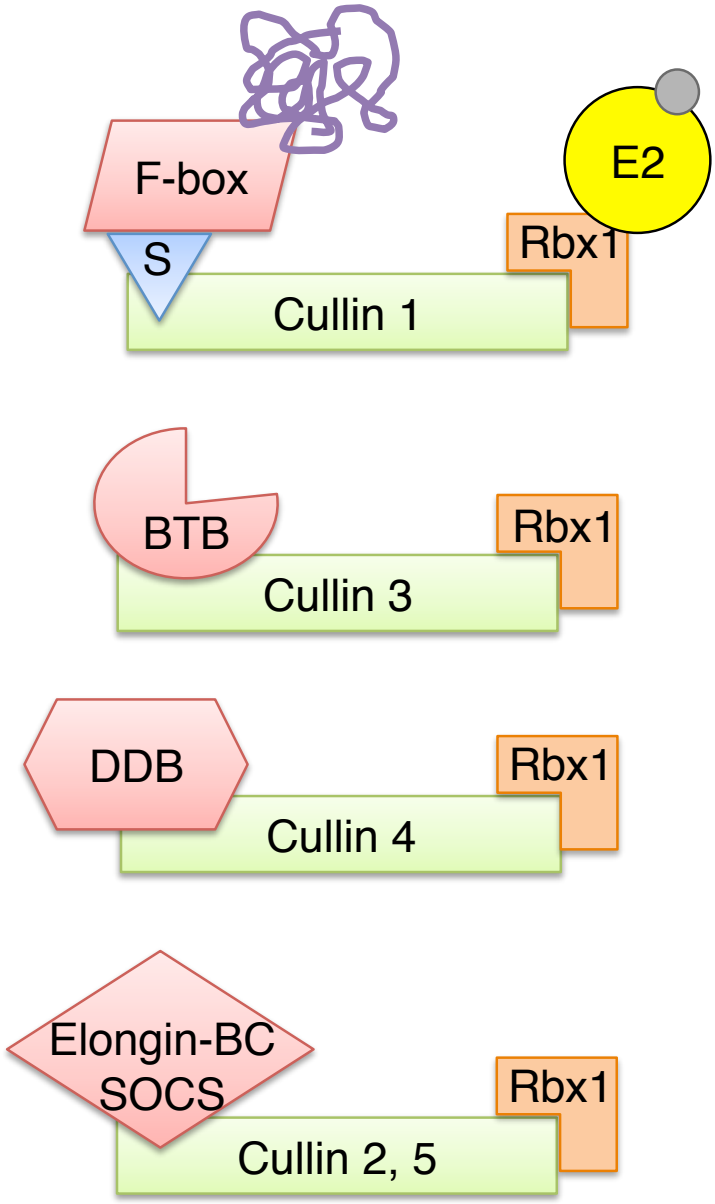

Figure 1.3: The Cullin-RING ligase superfamily

The largest family of RING E3s are the Cullin-RING ligases, multi-protein complexes that share a similar architecture. The Cullin molecule coordinates both the the RING-containing protein (Rbx1 or 2) and the relevant substrate-adaptor protein (shown in pink, the substrate is shown in purple). The substrate-adaptor protein is the interchangeable component of the system, lending exquisite specificity to this general ligase architecture. The SCF is the best-studied family of Cullin-RING ligases. The small adaptor protein Skp1 is depicted in blue.

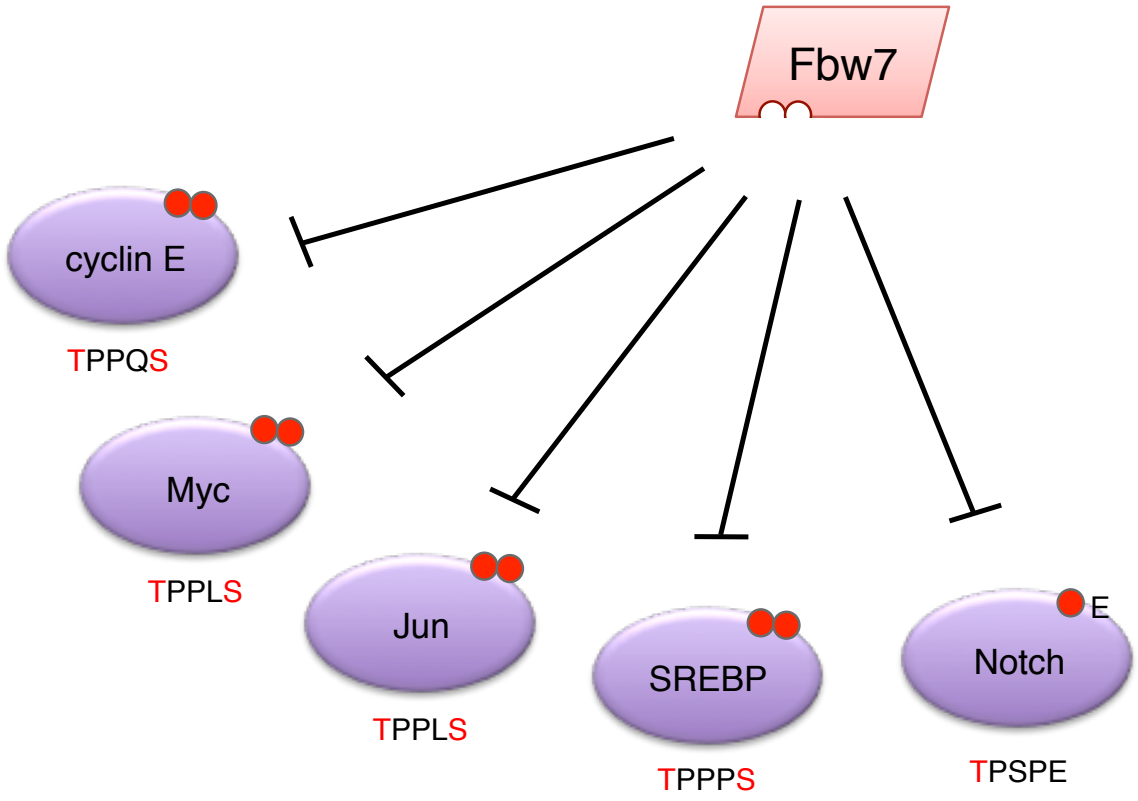

Figure 1.4: The Fbw7 substrate network

Fbw7 regulates the abundance of a network of positive regulators of cellular growth and differentiation including cyclin E, Myc, Jun, SREBP, and Notch. As such, Fbw7 is a tumor suppressor protein. Substrates are bound by Fbw7 after they are phosphorylated at consensus degron sequences as shown; many degron sequences are substrates of the glycogen synthase kinase GSK3, suggesting a coordinated regulation of Fbw7 substrates. The Fbw7 network and its significance continue to expand as additional substrates are identified.

A

-6	X
-5	X
-4	X
-3	X
-2	I/L
-1	I/L/P
0	pT
+1	P
+2	[RKY]
+3	[RKY]
+4	pT/pS/E
+5	[RKY]
+6	X

B

	-2	-1	0	1	2	3	4	
Cyclin E	L	L	T	P	P	Q	**S**	T380
	I	P	T	P	D	K	**E**	T62
Myc	L	P	T	P	P	L	**S**	
Jun	G	E	T	P	P	L	**S**	
SREBP	T	L	T	P	P	P	**S**	
Large T	P	P	T	P	P	P	**E**	
Notch	F	L	T	P	S	P	**E**	
Presenilin	I	Y	T	P	F	T	**E**	

Figure 1.5: Fbw7 binds a consensus degron sequence in substrate molecules

(A) Consensus Cdc4 phospho-degron (CPD) sequence. Reproduced from [69]. Red indicates phosphorylated residues.
(B) Degron sequence alignments of several Fbw7 substrates (the Large T protein binds Fbw7 like a substrate but is not degraded). Cyclin E is a unique substrate in that it contains two CPD sequences.

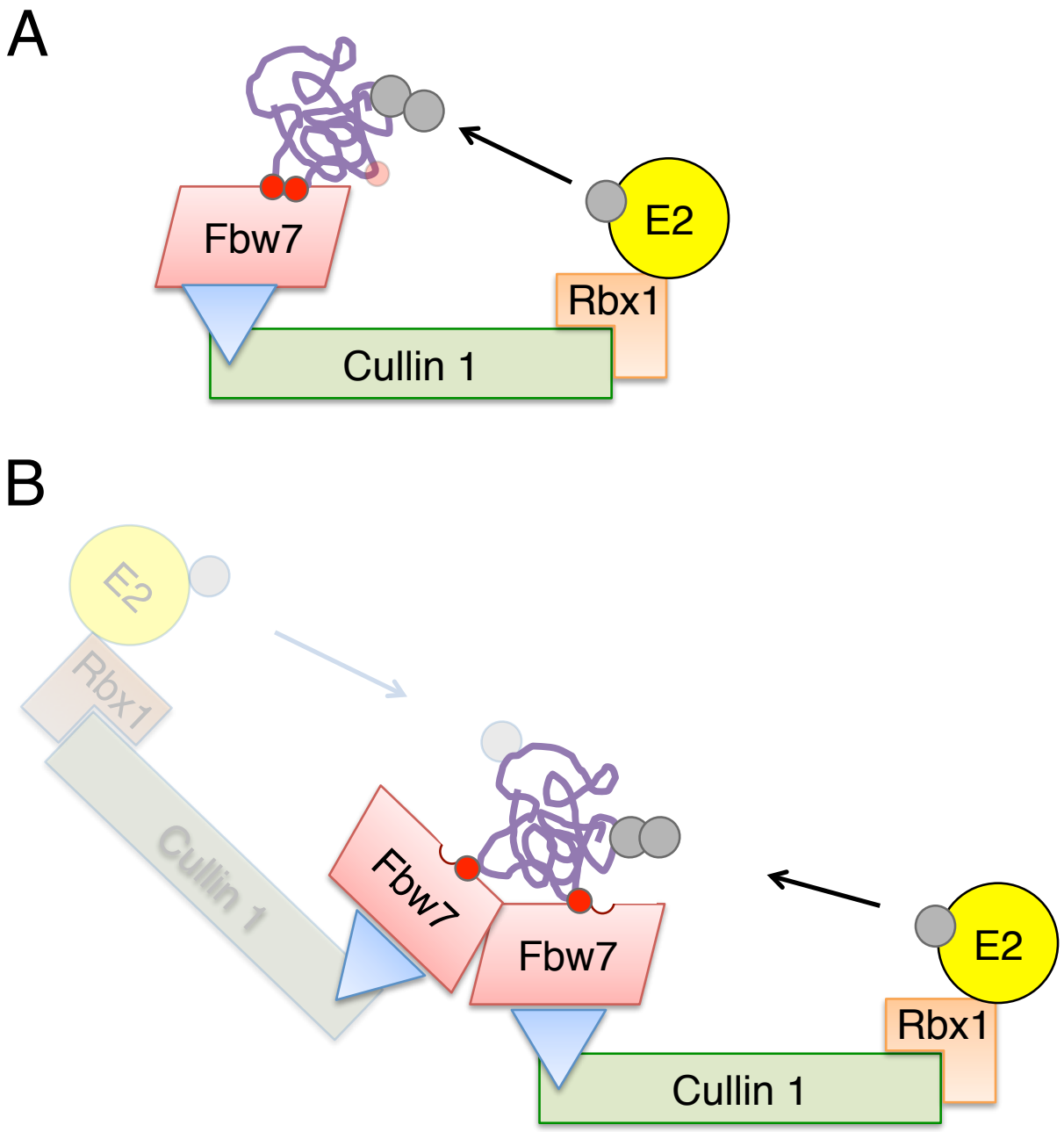

Figure 1.6: Dimerization represents an additional facet of Fbw7 substrate regulation

A) The monomeric SCF^{Fbw7} is able to regulate substrates (depicted in purple) with high-affinity degrons. Wild-type cyclin E contains a doubly-phosphorylated C-terminal degron that is sufficient to recruit Fbw7. Phosphorylation of the secondary N-terminal degron is not required for this interaction.

B) Fbw7 dimerizes through a conserved dimerization domain. In the case of cyclin E, when the C-terminal degron is weakened by mutation of the accessory phosphorylation site (S384A), the secondary degron is required for Fbw7 interaction as is the Fbw7 dimerization domain. This suggests each moiety of the dimer makes independent contact to each degron sequence.

CHAPTER 2

Disruption of Fbw7 in human cells leads to deregulation of substrates cyclin E and Myc

Rationale behind engineering a human cell line that lacks Fbw7 dimers

We have always supposed that cellular levels of Fbw7 protein are quite low because Fbw7 has always been difficult to detect in human cells using a panel of commercial as well as antibodies generated in-house. Since our data suggests that affinity between ligase and substrate is an important factor determining regulation, it is a reasonable assumption that the stoichiometry of Fbw7 to substrate is crucial for understanding substrate regulation. This subtlety is, of course, completely lost in any over-expression assay, in which we vastly overexpress tagged, detectable Fbw7 and substrate to gain an overview of regulation.

The only way to study the endogenous situation is to genetically manipulate the endogenous Fbw7 gene to disrupt dimerization. We previously characterized a small deletion in the dimerization domain that, in overexpressed protein, has such an effect [63]. Because the lab has extensive expertise in animal models, we considered generating a mouse in which Fbw7 dimerization was ablated. The lab also has recently done a significant number of gene-targeting studies in human cells in culture. This approach is cheaper, takes much less time, and is of course allows one to conduct the study in the human background instead of the model murine background.

For these reasons, we decided to use gene-targeting techniques to create a cell line in which the Fbw7 dimerization domain was disrupted. By looking for substrate regulation defects when Fbw7 is strictly monomeric, would point to endogenous substrates that are dependent on Fbw7 dimerization for their regulation.

Adeno-associated virus is an efficient method for gene-targeting in human cells

In the lab, human cells are a relatively intractable genetic system. Exogenous genes of interest can be over-expressed; expression of endogenous genes of interest can be knocked down. Unlike yeast and bacteria, in mammalian cells homologous recombination is a low-efficiency process. Designing

customized endonucleases to introduce double-strand breaks at target sites is an area of interest in the gene-targeting field and while this approach does increase the frequency of homologous recombination events, it also increases non-homologous end-joining, which lead to mutation events. Off-target cleavage is another challenge.

The use of viruses to conduct gene-targeting is attractive because viruses are evolved to enter human cells and integrate into the host genome. Adeno-associated virus (AAV) has been exploited as a gene-targeting delivery method [80-82]. It is a non-pathogenic virus; most patients will not mount an immune response to the virus or targeted cells when exposed. AAV is a small, non-enveloped parvovirus with a single-stranded DNA genome. The linear 4.7 kb virus genome contains two open reading frames, *rep* and *cap*, that produce all the proteins necessary to form the viral capsid and to copy the genome, package it and perform site-specific integration [83]. These sequences are flanked by palindromic inverted terminal repeats (ITRs), which are essential for mediating integration [84].

In the lab, to make a vector for gene-targeting, the sequence between the ITRs is replaced with the host's genomic region of interest [85]. (In order to produce functional virus, however, the *rep* and *cap* sequences must be provided by another vector in *trans*.) A disadvantage of AAV is that only a relatively small amount of host DNA can be packaged into the virus.

AAV has been shown to carry out effective gene-targeting in various animal models, and even in human trials [80]. Although the mechanism of integration is not known, something akin to homologous recombination must occur: the sequence inside the ITRs is swapped into the homologous locus of the host genome. Challenges for using AAV and other viral gene-targeting therapies in humans include getting the virus to the most critical tissue; this has been explored by exploiting different virus serotypes and by creating novel sereotypes *de novo* by protein engineering of the viral capsid. Another challenge is insertional mutagenesis, in which the integrated DNA alters critical host genes. The therapeutic gene may also be present but silenced; the host may direct an immune response against the delivery vector or the therapeutic protein itself.

Generation of AAV targeting vector

From our previous transfection-based work, we learned that deletion of amino acids in a given region of the dimerization domain of Fbw7 results in loss of dimerization as measured by co-immunoprecipitation [63]. However, our previously published deletion in Fbw7 cDNA spans two exons that are separated by about 9 kb of intronic sequence (Figure 2.1A and 2.1B). This particular deletion, then, is not suitable for introduction by a gene-targeting approach. We investigated whether a different, six-amino acid deletion (ΔEWLKMF) that lies completely in shared exon 2 would suffice to disrupt dimerization. By transfection and co-immunoprecipitation, this deletion disrupted dimerization as well as the previously characterized deletion (Figure 2.1C). This EWLKMF deletion is ideal because it leaves the final three nucleotides of the exon undisturbed, preserving any sequence information relevant to splicing at the exon terminus.

The gene-targeting vector was constructed to introduce this deletion into HCT116 cells, a human, epithelial cell line from a colorectal carcinoma. Previous Fbw7 manipulations had been performed in this background in our lab [86] as well as others [87-89]. Although it is a cancer cell line, HCT116 is considered genomically stable and, from our knock out of Fbw7 by gene-targeting [86], we know the Fbw7 locus exists in only two functional copies in these cells.

Although the exact mechanism of gene-targeting by AAV is not understood, it is helpful to imagine a situation like homologous recombination: a region of homology is used to introduce the mutation of interest. The 2 kb genomic region around the mutation to be engineered is cloned into a cloning vector convenient for manipulation (in our case pCS2+), in this case as a BglII/BglII fragment. The site where the mutation is to be introduced should be near the center of the sequence [85]. The mutation then was introduced by PCR mutagenesis and confirmed by sequencing. The drug resistance selection cassette was then inserted into intronic sequence as near to the mutation as possible. Reducing the distance between mutation and selection cassette likely reduces the chance that the selection cassette “crosses over” into the genome but the desired mutation does not; however, again, being mindful of sequence containing splicing information near the exon/intron border. In constructing this particular vector, nucleotides 78 bases into the intron were engineered to contain ClaI and NotI sites for directional ligation of a neomycin-resistance cassette as a ClaI/NotI fragment. The selection cassette in generating this cell

line was a 1.2 kb sequence denoted INpA, which is flanked by loxP sites and contains an IRES site preceding the neomycin-resistance gene [90]. Once all manipulations were complete, the integrity of the sequence was confirmed by sequencing and the entire insert was excised by BglII digest and ligated into a BglII-linearized AAV vector (serotype 2), pA2. The directionality of the ligation was confirmed by restriction enzyme digestion. See Figure 2.2A for a depiction of this targeting construct. The total insert of approximately 3.2 kb approaches the limit of the amount of DNA that can be packaged into the AAV virus particles.

Generation of AAV virus

The pA2 vector is prone to rearrangements because of its functional ITRs, but is more stable when grown in *E. coli* at 30° C. A maxi-prep of the targeting vector was thus produced at 30° C and the vector integrity confirmed by several different restriction enzyme digestions.

To generate recombinant AAV virus particles, the modified pA2 vector is co-transfected with another vector, called pDG, which supplies in *trans* the viral genes necessary for virus packaging. (These genes were excised from the pA2 genome to allow for the insertion of the engineered host DNA for targeting.) We co-transfected these two vectors by calcium phosphate into HEK293A cells. We typically use 2 10-cm dishes of cells that are approximately 60% confluent the time of transfection. The media is changed 16-20 hours after transfection, and cells are harvested 36-44 hours after transfection. The cell monolayer is scraped in PBS into eppendorf tubes and lysed by three freeze/thaw cycles in either liquid nitrogen or an ethanol/dry ice bath. After the final thaw, the lysate is spun at 15,000 rpm at 4° for at least 10 minutes to pellet cellular debris, leaving the AAV particles in the supernatant. All steps after transfection should be performed with proper virus-safety protocols, since this virus does infect human cells and is engineered to target the human Fbw7 locus.

Once virus is collected, it can be directly used to infect the parental cells of interest. At this step, virus can be concentrated by centrifugation and purified by heparin affinity column; the titer of the virus stock can also be measured. While surely informative, this protocol requires a large amount of cell lysate, as well as time and reagents for purifying and concentrating virus and measuring titer. By experience, we

have found that crude lysate from the transfected cells typically contains enough virus to yield sufficient gene-targeting events for screening.

Targeting and confirming proper engineering of Fbw7

Wild-type, parental HCT116 cells were plated 1 million cells per 6-cm dishes. The following day, virus-containing 293A lysate is added; a control plate should be treated with only PBS. I infect the cells in a low volume (2 ml media with 0.5 ml virus-containing PBS) for three hours, and then bring the volume up to a normal level with additional fresh media. The cells are trypsinized and plated at various densities two days later. The cells are plated directly into media containing 800 ug/ml G418 to select for integration events. Over the next week, most of the cells die; the dead cells can be aspirated but selection should be maintained throughout the grow-out period. Within two to three weeks, small colonies will appear if targeting events occurred. Colonies are ring-cloned to 48-well plates to expand. Once drug resistance is confirmed, colonies can be expanded and frozen back if desired; genomic DNA should be harvested and screened by PCR and Southern.

I created a PCR screen in which one primer sits within the neo cassette and one primer sits outside the targeting construct altogether. Thus, the amplified product should only appear if the correct targeting event occurred. (If the neo cassette integrated at an off-target site, the proper-sized product is unlikely to be amplified.) The weakness of screening for targeting by PCR is that a true positive control DNA is missing. One can create a “mock” vector that contains the genomic sequence representative of the targeting event; this can be used as positive control template in the PCR screening. It should be kept in mind that the concentration used as template ought to mimic the genomic concentration of the locus in the harvested genomic DNA.

Once positive clones were identified by PCR, I confirmed the genomic integration by restriction enzyme digestion and Southern blotting. See Figure 2.2B and 2.2C for the digestion maps of the locus. In this specific targeting, an EcoRI double digest was employed to indicate specific targeting. A radioactive probe was generated to hybridize to a sequence outside of the targeting vector, yet within the relevant two EcoRI sites. Whereas the parental chromosome, when digested with EcoRI, yields a 4.6 kb band using

the locus-specific probe, the neomycin cassette introduces an additional EcoRI site and so the probe hybridizes to a 2.6 kb band. Proper targeting occurred in 3 out of 35 clones that were neomycin resistant and deemed positive by PCR (clones numbered 10, 31, and 69). We chose clone number 69 to proceed. It is the WT/targeted clone shown in Figure 2.2C.

Because we were confident that both alleles of Fbw7 needed to be targeted to generate the cells of interest (in which all cellular Fbw7 is monomeric), targeting of the second allele also needed to be performed. My initial strategy had been to create two viruses with distinct selection cassettes (neomycin to select for one event and hygromycin to select for the second), but I saw no specific targeting by the hygromycin resistance-containing virus in 17 clones that were resistant to both drugs. I changed my strategy and decided to remove the neo selection cassette from the targeted allele with Cre recombinase (supplied by adenovirus, called Ad-Cre) and use the neo virus to target the second, wild-type allele. The challenge associated with this approach is that there is a propensity for the integration to occur at the first allele—possibly because the targeted allele, with the remaining loxP site after Cre recombination, contains slightly more homology to the targeting vector than does the wild-type allele.

The cells of clone 69 were plated 100,000 cells into a 6-cm dish and Ad-Cre was added at approximately 1000 PFU per cell the following day. Two days later, cells were trypsinized and plated at various low dilutions to allow for colony growth. Single colonies were picked to duplicate wells; media with G418 was used in one set. Cells that were sensitive to G418 were those of interest, indicating the neomycin cassette was successfully removed by the action of Cre. Three clones of interest were expanded and genomic DNA was harvested for analysis by Southern. Using the same probe described above, proper Cre-out results in a loss of the 2.6 kb band. A second radioactive probe was generated complementary to sequence in the neomycin cassette. This is useful for assaying the appearance and removal of the neomycin resistance cassette. Only one clone “69cre1,” showed proper Cre-out by Southern blot. It is the WT/ΔD clone shown in Figure 2.2C.

Additionally, we harvested RNA from these heterozygous cells and reverse-transcribed into cDNA, which we amplified with Fbw7-specific primers flanking the dimerization domain and restriction-digest cloned en masse into a generic cloning vector (pCS2+). Colonies were picked, miniprepped and

the DNA sequenced. Out of ten colonies analyzed, five showed wild-type sequence while five showed the expected 18 bp deletion (corresponding to amino acids EWLKMF) in the dimerization domain. Although hardly an exhaustive analysis, this was a promising indication that expression of the mutant allele was not grossly changed by the introduction of the mutation.

Cells from clone 69cre1 were infected with the targeting virus as described above. Clones were picked and analyzed by PCR and Southern. A different Southern strategy had to be employed for this second allele targeting. The screening was designed to distinguish between the wild-type locus and the successfully targeted and cred-out locus. Because the loxP sites leaves behind a HindIII site, the distinction can be made with an EcoRI/HindIII double digest, using the same probe as is used for the single EcoRI digest. As shown in Figure 2.2B and 2.2C, the 2.3 kb band indicates the wild-type allele and the 1.7 kb band indicates the targeted allele, regardless of whether or not the neomycin cassette is present. Therefore, the two digest strategies need to be employed together to definitively assay the locus. Six clones scored positive by PCR and five were confirmed by Southern (clones numbered 33, 35, 55, 71 and 73). The desired targeting event results in a loss of the 2.3 kb wild-type allele band; clone 33 is shown in Figure 2.2C as ΔD/targeted. Cells from clone 33 were subjected to Ad-Cre and neomycin-sensitive clones were again identified, as described above. Clones “33cre2” and “33cre13” were chosen for further analysis. In Figure 2.2C, “33clone2” is the ΔD/ΔD clone shown. From now on, “ΔD” will refer to 33clone2 unless otherwise stated.

Introducing the ΔD mutation does not alter total Fbw7 level, causes the endogenous protein to form monomers

A potential criticism of this approach is that the introduction of the mutation might have altered the expression or the stability of Fbw7 in the ΔD cells. To address this, I analyzed the endogenous Fbw7 protein, despite the fact that it has always proved a difficult protein to visualize. I first assessed total protein abundance, immunoprecipitating Fbw7 using a large amount of cell lysate.

I lysed three 10-cm plates of asynchronously growing cells of each genotype in Tween20-containing buffer, sonicated for completeness, and cleared the lysate by centrifugation. I normalized the

lysates and loaded 3.7 mg protein onto ProteinA beads coupled to Bethyl's anti-Fbw7 antibody A301-721A. I analyzed the immunoprecipitated protein by Western, probing with Bethyl's anti-Fbw7 antibody A301-720A. The result of this experiment, shown in Figure 2.3A, verifies that the introduction of the mutation did not alter total expression levels of Fbw7 in these cells.

Another potential critique of these cells is that, despite the transfection data, we do not know for certain that the endogenous Fbw7 is truly rendered monomeric. I realized that I could separate monomeric and dimeric protein complexes by their mobility on a non-denaturing protein gel, which does not dissociate the Fbw7 dimers. To make this approach work on endogenous protein, soluble protein complexes are necessary. These can be obtained by elution of the complexes off of the beads. To accomplish this, I immunoprecipitated endogenous Fbw7 from of normalized lysate (generated as described above), using the rabbit polyclonal antibody generated in-house against the sequence KVSEYTSTTGLVPC in the common region of the protein ("2998" antibody) coupled to ProteinA beads. (ProteinG did not work for this application.) After pull-down for 1.5-2 hours, I washed the beads with Tween-20-based lysis buffer; better results were obtained when beads were then rinsed once with RIPA buffer, then were equilibrated back into Tween-20 buffer. Bound protein was then competitively eluted from beads by incubating in Tween-20 buffer containing 200 ug/ml of the antigen peptide. Successful elution of protein was confirmed by analyzing the eluates by Western and blotting for Fbw7 with Bethyl 301-720A. Once successful elution was confirmed, the remainders of the eluates were run in native form on 7.5% gels without SDS; running buffer and sample buffer also lacked SDS.

As seen in Figure 2.3B, this protocol was also carried out using 293A cell lysate that had been transfected with FLAG-tagged Fbw7α dimer and monomer, to provide a comparison for the migration of the endogenous protein. As we see in Figure 2.3B, the Fbw7 protein from ΔD cells runs faster through the gel, as expected of a smaller protein complex. So the Fbw7 in the ΔD cells is rendered monomeric. Another insight gleaned from this work is that in wild-type HCT116 cells, it seems all Fbw7 protein is in the dimerc form, as a monomeric pool of protein is undetectable. We unfortunately may not be able to definitely prove that there is no dimeric protein in the ΔD cells, though, because of the large amount of background signal that co-migrates with the dimeric Fbw7 pool. (We attempted unsuccessfully to clear

this background in multiple ways.) But because the intensity and pattern of the background signal in the null and ΔD lanes appears identical, it suggests the absence of a dimeric pool in the ΔD cells.

Analysis of cyclin E levels in Fbw7 ΔD cells

Once the cells of interest were generated, I wanted to assess the effect of the mutation on substrate regulation. I performed all analyses by comparing the ΔD cells to parental, wild-type HCT116 cells, as well as to HCT116 cells in which there is no expression of Fbw7; both alleles were disabled by the gene-targeting introduction of stop codons into sequence shared by all three Fbw7 isoforms [86]. We denote these cells Fbw7 null or -/-.

As shown in Figure 2.4A, cyclin E in asynchronous ΔD cells is partially stabilized in asynchronously growing cells. Cyclin E levels are much higher in the null cells, but when compared to WT cells, the ΔD cells show an intermediate phenotype. Because cyclin E expression and activity is very much dependent on the cell cycle, we also analyzed cyclin E levels in cells arrested at different phases of the cell cycle: treating growing cells overnight with 5 ug/ml aphidicolin arrests cells in S-phase, and overnight arrest in 40 mg/ml nocodozole arrests cells in M-phase. In all three genotypes, cyclin E protein is most abundant in S-phase arrest. In M-phase arrest, as in the asynchronously growing cells, we see the ΔD cells have an intermediate phenotype: there is more cyclin E than in the wild-type cells but less than is found in the null cells.

The activity of cyclin E-associated CDK2 kinase was also assessed on these same cell lysates by immunoprecipiation of cyclin E and subsequent kinase assay using γ-P^{32} ATP, with histone H1 as substrate. We see in Figure 2.4A that the abundance of cyclin E protein correlates well with the associated kinase activity (the phospho-signal is quantified at the right of the figure). Thus, in the ΔD cells, cyclin E/CDK2 activity is moderately elevated when compared to wild-type cells.

Analysis of c-Myc stability in Fbw7 ΔD cells

Another very important oncogenic Fbw7 substrate is c-Myc. Myc abundance is tightly controlled in cells by a variety of feedback regulatory mechanisms. Thus, in Fbw7 null cells, the total abundance of

Myc is not grossly misregulated. However, when *stability* of c-Myc is assessed by cycloheximide, the half-life of c-Myc is significantly elongated in Fbw7 -/- cells.

When we analyzed c-Myc in Fbw7 ΔD cells, we found that the protein half-life is elongated in comparison to wild-type cells (Figure 2.4B). In fact, the stability of Myc is comparable between the ΔD cells and the null cells. This was initially a somewhat surprising finding because, in transfection-based experiments, we had determined that the phospho-degron in Myc is highly phosphorylated and so appears to makes a high-affinity interaction with Fbw7 that is not dependent on Fbw7 dimerization. However, the endogenous protein stability reconciles with data in the field that suggests that the accessory phosphorylation site in the degron of c-Myc (S62) is dephosphorylated after it primes for GSK3β phosphorylation of the CPD's central residue, T58 [91]. This may explain why endogenous c-Myc regulation appears to be dimer-dependent.

Cell cycle analysis of ΔD cells

The cell cycle kinetics of cells can be analyzed without using drugs like aphidicolin and nocodozole. When work in the lab showed that drug-induced arrests induce checkpoint effects on cell cycle proteins of interest, the technique of arresting cells in G1 by amino acid deprivation came into use. For these experiments, we put asynchronously growing cells into media that lacks the essential amino acid leucine. After 48 hours of leucine starvation (44-50 hour arrests were used in these experiments), the cells that survive the starvation (many die and are aspirated off) are released into normal, serum-containing media and time points are taken while the cells progress through the cell cycle. (Because we are curious how the population progresses out of the arrest and through one cell cycle, we typically release the cells into 40 ug/ml nocodozole, thus preventing the cells from entering the following cell cycle.) At each time point, the harvested cells are typically divided: a fraction is fixed for flow cytometry to analyze the cell cycle profiles and the rest are frozen for biochemical analysis.

Strikingly, ΔD cells proceed through the cell cycle faster than the wild-type parental cells. Looking at cell cycle profiles, the ΔD cells appear to be about 3 hours faster than the wild-type cells (Figure 2.5A). The Fbw7 null cells typically proceed through the cell cycle at the same rate as the wild-type cells; in the

experiment shown in Figure 2.5A, the null cells released from the starve slightly slower than the WT cells, but this was the only instance in which this was observed. The phenotype of the ΔD cells is surprising: how can a mutation in Fbw7 elicit a more drastic phenotype than its complete deletion?

Because the cell cycle kinetics seemed to be showing a premature S-phase entry of the ΔD cells, we repeated the experiment, taking earlier time points after release. When we examined total cyclin E levels, we did not see a significant difference between the wild-type and the ΔD cells (Figure 2.5B). As published, the Fbw7 null cells noticeably accumulate cyclin E, but we thought early activation of cyclin E might explain the ΔD cells' quicker progression through the cell cycle. Indeed, when we analyzed cyclin E-associated CDK2 activity at these early time points, we saw a large difference: the ΔD cells show early and persistent cyclin E activity (Figure 2.5B shows the phosphorylation signals, Figure 2.5C shows the quantified autoradiography signal corresponding to kinase activity against histone H1). In the null cells, although cyclin E/CDK2 activity eventually skyrockets at 17 hours post-release and beyond, at early time points the cyclin E-associated CDK2 activity is equal to that in WT cells.

The observation presented above that the cell cycle of the ΔD cells proceeds more quickly than either wild-type or Fbw7 -/- cells was tantalizing but confusing. The phenotype was confirmed using a second clone of the ΔD cells (33cre13), but it is unfortunately not a completely independent clone since only one heterozygous clone was obtained after cre-out of the first targeted allele. Because the cell cycle phenotype was potentially significant but puzzling, we repeated the gene-targeting protocol to generate two additional completely independent clones (called A6 and B7). The cyclin E and Myc stabilization phenotypes were reproduced in all three clones, but the cell cycle phenotype and the early activation of cyclin E/CDK2 were not reproduced.

Conclusions and future directions

There are two major avenues of future work with this line of human cells. First, these cells will be useful in determining whether other Fbw7 substrates are dimer-dependent. As of yet, other validated substrates (Jun, Notch, SREBP) have not been easily studied in these HCT116 cells with our current

antibodies and techniques. As the Fbw7 substrate network continues to expand, however, these cells will continue to serve as a tool to explore the role of ligase dimerization in substrate regulation.

Second, our interest in substrate/Fbw7 interaction and the notion that a dimer serves to increase binding affinity/avidity to substrates begs the question: if we perturbed the binding surface of a substrate in the ΔD background, would we see larger effects on regulation? Cyclin E is the substrate we understand best and we would be interested in introducing an S384A or S384E mutation: in transfection studies, perturbation of this site causes regulation by Fbw7 to become dimer-dependent. This seems like a straightforward gene-targeting, as it is a single codon mutation, versus the 6-amino acid deletion created in this chapter. I designed and created the gene-targeting vector for this purpose, but presumably due to the fact that the sequence sits much further from intronic sequence, I observed no positive targeting events in the neomycin-resistant clones examined by PCR. This may be worth trying again with a more efficient gene-trap vector, or by simply examining more colonies. What would be gained from this avenue would be genetic support for our model that the dimer can simultaneously contact two (presumably) distinct degron sequences. If this has been convincingly shown by our transfection and *in vitro* data in the following chapters, however, the knowledge gained from this experiment may be minimal and confirmatory.

To those interested in ubiquitin ligase dimerization in general rather than Fbw7 specifically, this work could be extended by performing gene-targeting to create similar mutations in other dimerizing F-box proteins (such as β-TrCP) or in dimerizing substrate adaptor proteins of other Cullin-RING ligases (such as the Cul-3 BTB proteins Keap1 or SPOP). Perhaps a higher-throughput proteomics analysis would be a more comprehensive approach to study the effects of abrogating dimerization on various ligase networks.

A

exon	exon end	exon start	exon nucleotides	subsequent intron nucleotides	amino acids
α	153332455	153332955	501	61180	167
Y	153303341	153303487	147	32066	49
β	153273622	153273882	261	2347	87
1	153271194	153271276	83	2972	541
2	153268082	153268223	142	8995	
3	153258954	153259088	135	5084	
4	153253748	153253871	124	1729	
5	153251884	153252020	137	948	
6	153250824	153250937	114	1284	
7	153249360	153249541	182	1978	
8	153247158	153247383	226	1613	
9	153245336	153245546	211	1036	
10	153244033	153244301	269		

B

C

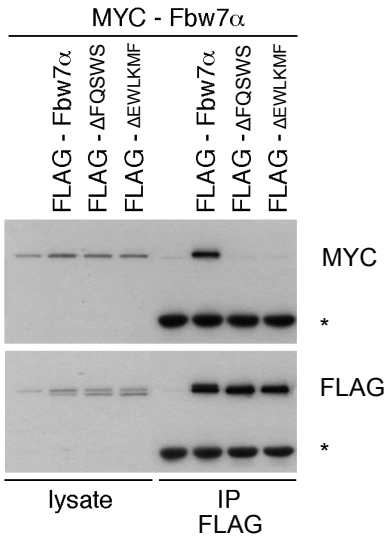

Figure 2.1: *FBXW7* locus and Fbw7 dimerization domain

(A) Chart depiction of the linear relationship of the isoform-specific and shared exons of *FBXW7* gene on chromosome 14.
(B) Linear schematic of the Fbw7 protein and its domains. Below, the amino acid sequence of the dimerization domain. In yellow are the amino acids deleted in [63]. In red is the deletion pursued for gene-targeting.
(C) Confirmation that this deletion abrogates protein dimerization as well as the originally described deletion. 293A cells were transfected with various Fbw7 combinations, and cleared lysate was IPed with M2 FLAG antibody. * denotes heavy chain.

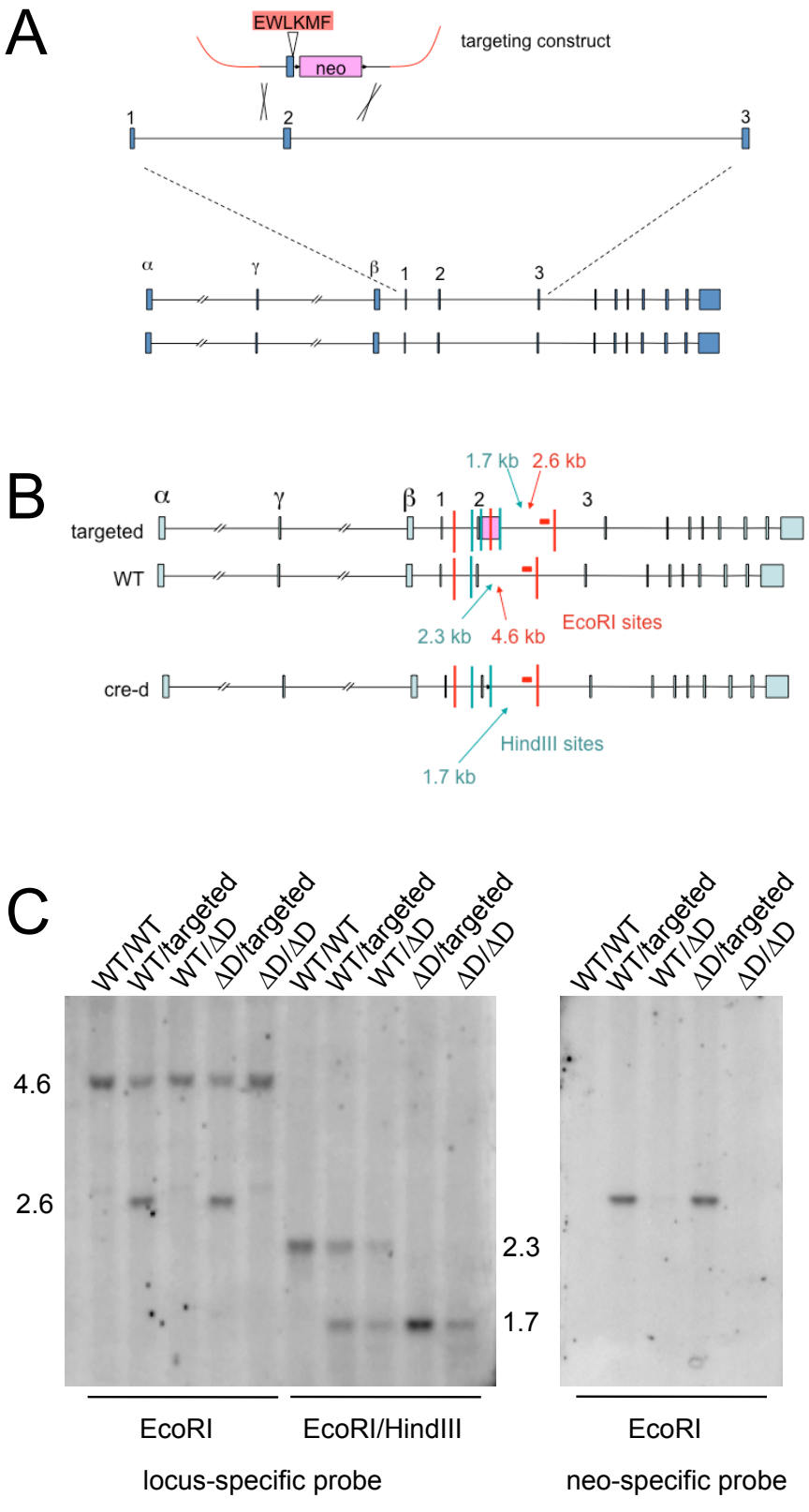

Figure 2.2: Gene-targeting of Fbw7 dimerization domain

(A) Schematic of AAV targeting construct.
(B) Southern blot restriction enzyme map. EcoRI digest distinguishes the WT and the targeted allele. EcoRI/HindIII double digest distinguishes WT and the targeted allele after cre-out, which is crucial for the second round of targeting. The location of the probe is shown by the red box near the EcoRI site.
(C) Southern blots of digested genomic DNA from HCT116 cells. Genotypes are listed above each lane. The blot on the right used a probe complementary to sequence in the neomycin-resistance cassette that picks up the 2.6 kb fragment.

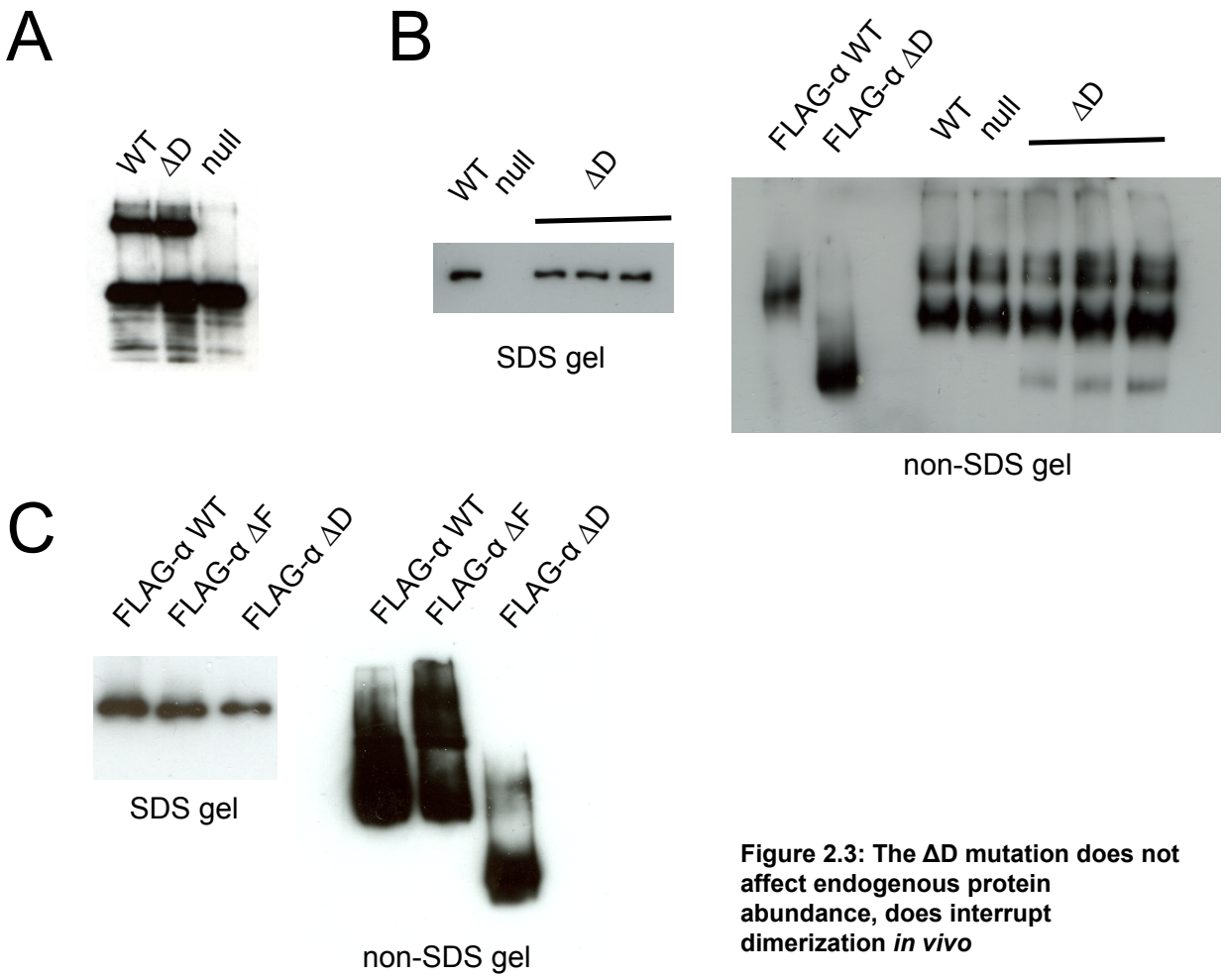

Figure 2.3: The ΔD mutation does not affect endogenous protein abundance, does interrupt dimerization *in vivo*

(A) Endogenous Fbw7 was immunoprecipitated from HCT116 cells of the three genotypes. Introduction of the mutation does not affect protein abundance.
(B) From the same experiment, some IPed Fbw7 was eluted from beads with the competing peptide. A small fraction was run on an SDS gel. Eluates were also run on a non-reducing, non-denaturing gel; 293A cells transfected with FLAG-tagged Fbw7 were used as controls. Monomer and dimer are separable.
(C) The smeary migration of the WT Fbw7 is not due to the formation of high-molecular weight SCF complexes, as the F-box mutant also migrates with a similar pattern.
(D) Both characterized dimerization mutations show the same migration pattern, quite different from the WT.

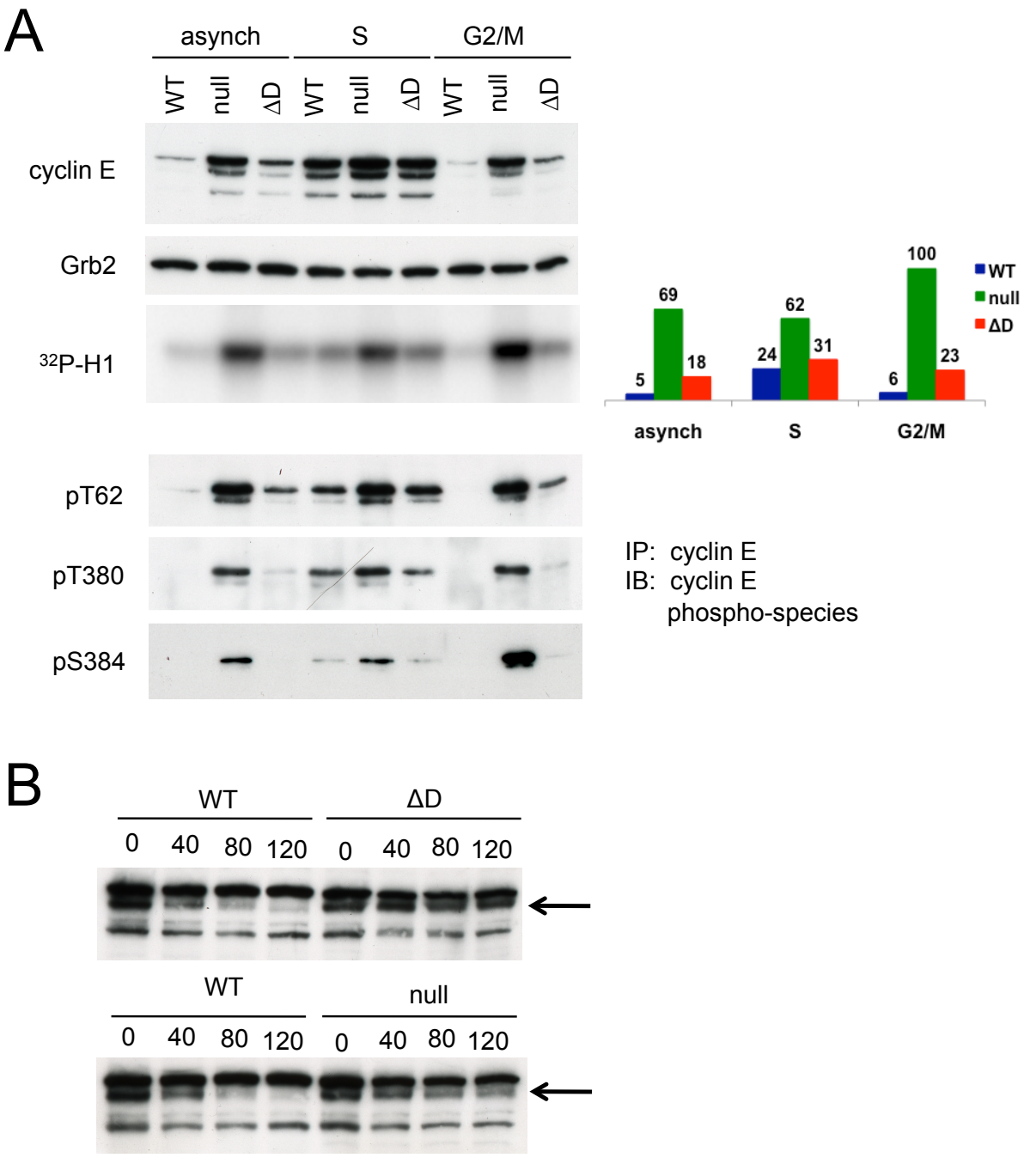

Figure 2.4: Cyclin E and c-Myc are moderately deregulated in ΔD cells

(A) Analysis of total cyclin E abundance and phosphorylation status in the three HCT116 Fbw7 genotypes, in asynchronous cells, cells arrested in aphidicoloin, and cells arrested in nocodozle. Also shown is a quantification of relative cyclin E-associated CDK2 activity on histone H1. Detection of endogenous cyclin E always results in multiple lower-molecular weight bands, which may represent breakdown products.
(B) Myc stability analyzed by cyclohexamide time course. Arrows indicate the labile Myc protein.

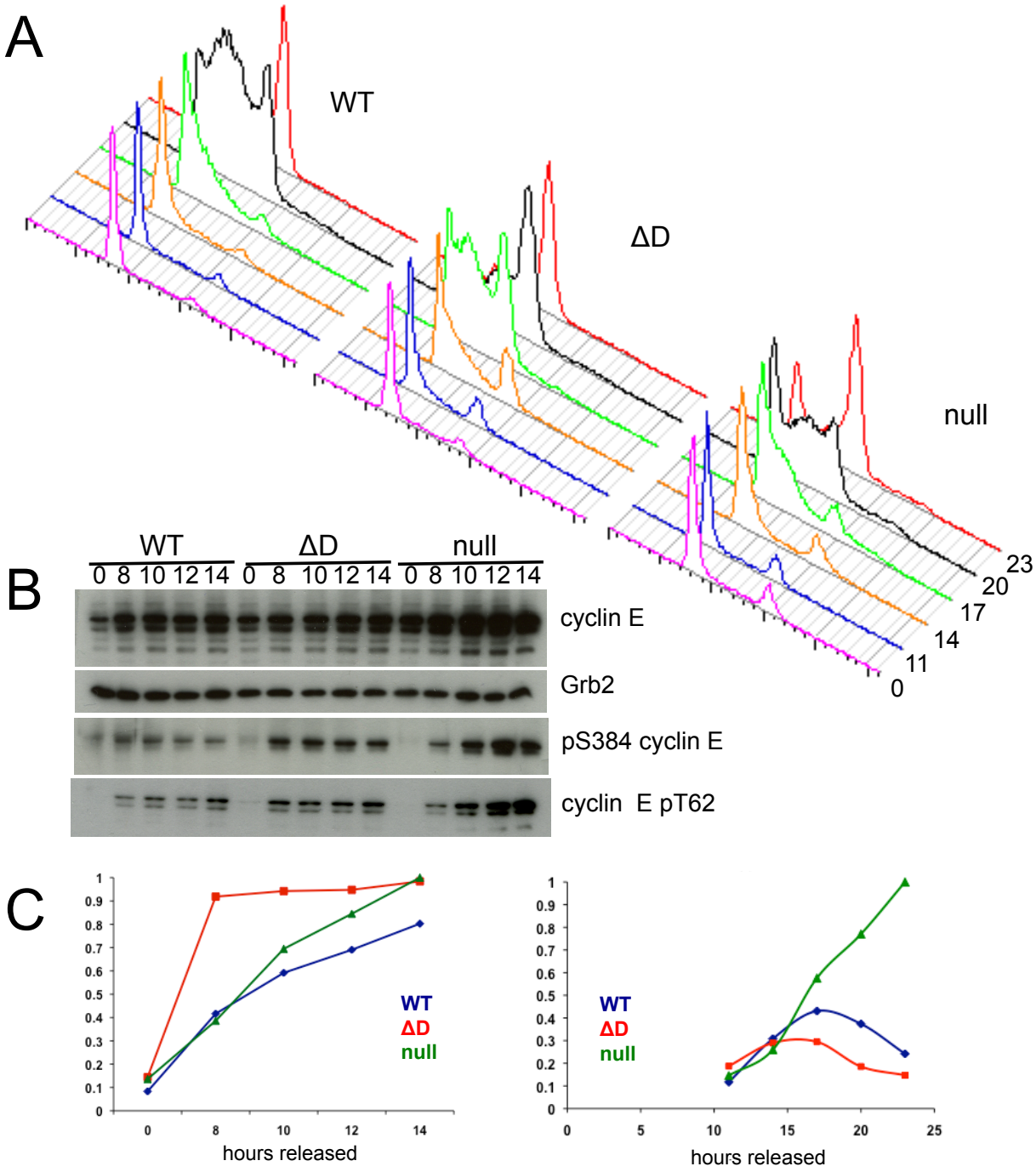

Figure 2.5: Cell cycle kinetics of ΔD cells

(A) Cell cycle kinetics of the three Fbw7 genotypes after release from amino acid starvation. Cells were released into serum-containing DMEM and nocodozole.
(B) Total and S384-phosphorylated cyclin E levels of cells starved and released as in (A) but harvested at earlier time points. Grb2 is a loading control.
(C) Quantification of relative cyclin E-associated CDK2 activity on histone H1 at early and late times points after release.

CHAPTER 3

Purification of recombinant Fbw7 dimer and crystallography efforts

Fbw7 has been largely studied as a monomer

In 2007, the crystal structure of the monomer of human Fbw7 bound to Skp1 was solved [73], both alone and bound to peptides consisting of the T380 and the T62 CPDs. This work built upon the prior structure of the eight-bladed Cdc4 WD propeller [92]. (Previous to [92], the structure of the Cdc4 propeller was only hypothesized by superimposition onto the seven-bladed β-transducin propeller, as seen in [30].) In the 2007 Fbw7 structure, twelve residues of the C-terminal degron visibly make contact to the propeller, including both the phosphorylated residues T380 and S384. However, the N-terminal degron makes far fewer contacts, and only eight residues of that peptide are ordered. These observations are concordant with our model in which the C-terminal degron is a higher-affinity interaction than that of the N-terminal degron.

A second study in 2007 published the crystal structures of the 45-amino acid interlocked dimerization domain of yeast Cdc4 as well as that of human β-TrCP [93]. Both dimerization domains are composed of clustered hydrophobic α-helices. The authors conclude that, because of 1) the very short distance between the dimerization domain and the structurally rigid F-box domains and 2) the similar architecture of the two interlocked D-domain structures, the two F-box protein dimers probably adopt fairly similar overall conformations. These structures also argue against higher order oligomer formation. The authors also collected SAXS data on Cdc4 dimer and used the known crystal structures of the interlocked D-domain, the Cdc4 monomer with Skp1, as well as Cul-1 and Rbx1 and Cdc34 to project the hypothetical structure of the entire dimeric complex. They conclude, however, that the two WD propellers are facing in the same general direction, with a distance of 65 Å between. These findings do not conflict with our hypothesis of simultaneous engagement of both propellers; however, the data collected for this structure was at a resolution of 46 Å, which is not nearly high enough to make definitive conclusions on the dimer architecture.

The two studies from 2007 state the difficulty of including the D-domain in their protein for crystallography. Although the domain itself is clearly not unstructured (because of its successful crystallization), its inclusion apparently hinders protein production.

The structural knowledge of cyclin E is incomplete

One structure of the cyclin E/CDK2 complex exists, but it only contains the core of the cyclin E protein; the CPD sequences at both the N- and C-termini are truncated (they used residues 81-363, the major product of a limited proteolysis reaction) because the authors report that the complex containing full-length cyclin E yielded no crystals [94]. Unfortunately this study does not provide information regarding the domains that interact with Fbw7. The CPD sequences may well be disordered, which is how the Fbw7 propeller is able to interact with them on the level of the primary amino acid sequence. However, the structures of Cdc4 or Fbw7 with cyclin E peptide indicate that the interaction between the CPD and the propeller is stringent and well structured. Therefore, unstructured CPDs hanging off of a structured cyclin E/CDK2 core may not pose a challenge to crystallization so long as they are engaged by the ligase.

An F-box protein dimer structure (with or without substrate) would greatly inform our understanding of substrate interaction

Athough we are interested in the simultaneous engagement of two substrate degrons, the crystal structure of a dimerized F-box protein alone would be quite novel. As described above, we currently have only the structure of the interlocked 45 amino acids of the Fbw7 dimerization domain and the very low-resolution SAXS structure predicted by superimposition of the various structures of SCF components obtained by crystallization over the past decade. A true picture of the relative orientations of the two WD propellers and the (presumably) two Skp1 molecules would still be quite a high-impact finding with implications for the other dimerizable Cullin-RING ligases. While trouble-shooting cyclin E/CDK2 purification, I worked on the more simple aim, crystallization of the Fbw7 dimer.

Generating dimeric Fbw7 from insect cells

First we considered the monomeric Fbw7 construct used for crystallography by the Pavletich group. Their construct began at the threonine 96 amino acids into the common region of Fbw7, which is immediately before the start of the F-box domain. We decided to reproduce this construct as a control for expression and purification purposes.

To generate dimeric protein, we needed to start the construct more N-terminal in the common region. Looking at output from a structure-prediction algorithm, we selected two positions for the start site: P63 and L67 of the common region. Primers were generated to amplify and clone these fragments as BamHI/EcoRI fragments into the pFastBac-GST-TEV vector. (The expression scheme is depicted in Figure 3.1A.) Positive constructs sequenced, and then were transformed into DH10Bac *E. coli* for recombination into bacmid vectors. Bacmids were harvested and used to transfect Sf9 insect cells. Virus was amplified using Sf9 cells and expression was tested using adherent Hi5 cells. Purification was carried out by sonicating cell pellets in 20 mM Tris pH 8.0, 200 mM NaCl, 5 mM DTT in the presence of protease inhibitors. Lysate was cleared by centrifugation and passed over a GST column. The resin was washed and protein was eluted with buffer including 10 mM glutathione. The resulting protein was analyzed by SDS-PAGE and Coomassie staining.

All three constructs were expressed, and the monomer and dimer protein were easily distinguishable by size (not shown). Co-infection of Hi5 cells with Skp1 virus resulted in co-purification of the Fbw7/Skp1 complex, which is likely more amenable to crystallography because the F-box exposed surface is bound by the small, 19 kDa protein Skp1. Yield of the Fbw7 dimer was also improved by Skp1 co-infection, likely an effect of improved solubility, as shown in Figure 3.1B. (In all remaining work, Skp1 is untagged and the "ΔΔ" version in which two disordered loops are deleted as previously described [95], unless otherwise noted.)

Unfortunately, addition of commercial or in-house purified His-tagged TEV was not able to lead to efficient cleavage in either of the dimeric versions of Fbw7, although the tag was cleaved from the monomer quite well (Figure 3.1C and not shown). Additional enzyme, additional time, and addition of EDTA did not lead to complete tag cleavage (Figure 3.1C and not shown), but we did observe more

cleavage of the P63 form over the L67 form. This suggested that the interlocked dimer interface was preventing entry of the TEV enzyme to access the site between the dimer interface and the GST tag.

I addressed this issue in several ways: 1) I swapped the tagging scheme, generating untagged (and 6His-tagged) Fbw7 constructs and GST-TEV-Skp1 constructs to attempt to purify the complex via the binding partner instead of the protein of interest, 2) I mutated the TEV site to a thrombin cleavage site and cleaving with that enzyme instead of TEV, and 3) I inserted a linker sequence between the dimerization domain and the TEV cut site. The first avenue was not terribly fruitful: although the 6His-Fbw7 fusions were visibly co-purified with GST-Skp1, cleavage of the GST tag from Skp1 was not efficient (not shown). The second avenue was interesting because I changed the TEV site in the vector to a thrombin site by site-directed mutagenesis. On-bead cleavage of the GST-bound Fbw7 by thrombin resulted in liberated Fbw7, but the amount of protease is a crucial step because too little results in incomplete cleavage and loss of yield whereas too much enzyme results in off-target cleavage of Fbw7 and loss of yield (not shown). In my experience, TEV is the preferable enzyme for tag cleavage of low-yield proteins.

The addition of a linker sequence ended up markedly improving TEV cleavage of the GST tag from the Fbw7 dimer. I recloned the P63 and L67 inserts into the pFB-GST-TEV vector, each with an N-terminal linker sequence of GAGS (Figure 3.2A and 3.2B). After virus was generated to test expression, I found that the P63 version with the linker was expressed and successfully cleaved by TEV (Figure 3.2C). I decided to proceed with this construct over the L67 construct; it seemed that the more sequence between the core dimerization amino acids and the TEV site, the better. In parallel I also made the R505L mutant (R338 in the common region numbering scheme) in both the monomeric and dimeric backgrounds that abrogates substrate binding.

Of course, at this point, I could not yet assess whether or not the purified protein effectively formed dimers. The only analysis at this point was by SDS-PAGE, so any higher-order protein complexes were denatured. In order to assess the size of the complex and to prepare sample for crystallography, I scaled up production for further purification by FPLC.

FPLC methods

Chromatographic methods are necessary to further purify the protein sample of interest for crystallography. (See Figure 3.3 for a workflow schematic for purifying crystallography-grade dimeric Fbw7.) Column purifications are able to remove contaminating cellular proteins including endogenous insect cell GST-resin binding protein, as well as aggregated protein of interest. A typical method is to use ion exchange chromatography followed by size exclusion chromatography. Ion exchange is an amenable first column because the resin is cheap and can be packed in the lab. It also has a high binding capacity. SourceS and SourceQ resins (GE) are the resins were used for cation and anion exchange chromatography, respectively. The goal is to load the sample in conditions that allow the protein of interest to bind (this condition will probably allow most contaminants to also bind), and then to competitively elute bound proteins by increasing the ion concentration in a gradient fashion, thereby differentially eluting bound proteins. Thus, the user hopes to separate the protein of interest from other bound proteins during the elution.

The user must first determine whether the protein of interest binds to S or Q resin. The predicted pI of the Fbw7 complex is quite neutral (7.6), but I tested Q resin first, since its use is more common and preferable. The sample after TEV cleavage is diluted four-fold, to lower the NaCl concentration from 20 mM to around 5 mM, an ionic strength where most proteins will bind. (Once production was scaled up, the elution volumes from GST were quite large, so a three-fold instead of a four-fold dilution was preferred to decrease the sample loading time. From experience, I learned that 7.5 mM NaCl was adequate to allow the Fbw7 complex to bind the resin. Dialysis was also used once on a 500 ml sample and was successful; however, the time that dialysis requires is not optimal since the protein of interest may undergo degradation or aggregation over time while at 4 °C.)

The Q column size is chosen based on protein content in the sample (the options were 1 ml, 2 ml, 8 ml resin where each ml of resin can bind at least 10 mg of protein), and is equilibrated in 5 mM NaCl. Sample was generally loaded using repeated injections from a 50 ml “super loop.” Once the entire sample is loaded, the unbound protein is rinsed from the column using equilibration buffer. The elution phase ramps up the ionic strength from, for instance, 5 mM NaCl to 30 mM NaCl. The Fbw7 complex typically

elutes around 17 mM NaCl, but in my experience it may vary between 15-25 mM NaCl depending on the column, the specific chromatography system used, the rate of elution, etc. Fractions are collected during the elution phase for analysis by SDS-PAGE. The user will often save the flow-through from the loading phase as well, in case the protein of interest did not bind the column.

A typical anion exchange chromatograph is shown in Figure 3.4 and resulting SDS-PAGE analysis. We see Fbw7 is eluted midway through the gradient, and the gradient partially separates the major contaminants of TEV and endogenous insect cell protein. Fortunately, size exclusion chromatography (SEC) will separate the proteins in the sample by size and the ~150 kDa Fbw7/Skp1 dimer complex is much larger than the major contaminants seen on this gel (TEV, insect cell GST-binding protein, liberated GST), which are all in the 30 kDa range.

The first chromatography step also partially concentrates the sample: the user may have loaded 200 ml of sample onto the column, but once fractions are combined, could end up with less than 20 ml of sample after Q. The first column also has the effect of buffer exchange. After TEV cleavage the sample still contained the glutathione from elution from GST. But after Q, this chemical is removed, or at least hugely diluted. The pooled fractions after Q can be loaded onto a small volume of fresh GST beads. This has the effect of binding any uncleaved GST-Fbw7 as well as remaining insect cell proteins that bind GST beads. This step is very effective in further purifying the sample (not shown). The downside is that the column should be washed well with buffer so that as much Fbw7 as possible can be recovered. For the SEC, the sample volume to be loaded preferably should not exceed 1 ml. So the sample must be concentrated before SEC. I used Amicon Ultra-4 or Ultra-15 concentrators (depending on sample volume), either 30 kDa or 50 kDa molecular weight cut-off, and concentrated by spinning in a bench-top refrigerated centrifuge and mixing the sample every 5 or 10 minutes to reduce stratification of the sample and protein aggregation. However, this step always resulted in a significant reduction of yield.

The SEC column (Superdex200 25 ml, GE) is much more delicate than those used for ion exchange. The sample to be loaded should be cleared of aggregated debris by centrifuging at top speed for 5 minutes. A filter at the top of the column protects the resin, but this becomes clogged by dirty sample. Injecting air bubbles should be avoided, and the protein sample ought to be fairly clean (i.e. used

after a first column). The column loses resolution with use and they are expensive and cannot be repacked in-house.

As mentioned above, we could not tell whether the Fbw7 I generated from insect cells was truly dimerized until its size could be analyzed. Approximately 10-14 mg of protein can be loaded onto the Superdex column, but as mentioned above, this should be loaded in a volume less than 1 ml if possible. (Sometimes 1.5 ml could not be avoided.) This is because the resolution suffers as the injection volume increases – the peaks widen appreciably. A typical Fbw7 SEC trace is shown in Figure 3.5 with accompanying SDS-PAGE gel. We see the sample is highly purified, with good separation of the Fbw7 peak and the TEV/endogenous GST-like protein peak. Also, by comparing traces like this one to protein standards run on the same column, I was confident that the Fbw7 was running as a dimer, around ~150 kDa. Production of monomeric protein (using the GST-TEV-T96 construct) was also scaled up and subjected to the same chromatographic methods; and that complex came off the column later, corresponding to the expected 75 kDa of the complex.

Purified Fbw7 dimer was used for crystallography trials and a hit was identified

As mentioned in the introduction to this chapter, the ultimate goal of this effort was to crystallize the Fbw7 dimer bound to cyclin E substrate. However, the structure of an F-box protein dimer would also be quite impressive and novel. So while I worked on generating crystallographic-grade cyclin E/CDK2, which is described below, I pursued crystallizing the Fbw7/Skp1 dimeric complex generated above.

Protein after SEC was concentrated as much as possible (preferably 8-10 mg/ml), and various crystal screens were set up using the Mosquito robot pipettor, which is able to accurately and quickly dispense a very small amount of protein sample. Using this tool, we can screen a larger number of conditions (and thus a large swath of chemical space) with a limited amount of protein sample.

To make hanging drops over the wells of a 96-well plate, the drops are prepared on a plastic adhesive sheet that is inverted and sealed over each corresponding condition. The user must aliquot 100 ul of each condition to be tested into a 96-well plate. The user must also place 5 ul of protein sample into each well of the plastic sample tray used by the Mosquito. The needle pipette tips dispense the protein

sample and each condition. The user determines the way in which this occurs: it can be done either by overlaying one onto the other, or by sequential uptake. The user may prefer the overlay method because within the drop there is inherently a gradient of the protein sample and the diluent. However, in rare instances, the Mosquito does not perfectly overlap the two drops and the sample does not mix with the diluent at all. The user can also program the robot to make up to three drops for one condition. The user can use different protein samples, different concentrations of the sample protein, etc. Generally, Fbw7 protein sample was in such low abundance that a single drop of 100 nl protein + 100 nl diluent was used. The drops are carefully placed atop the corresponding wells and sealed well. The plates can be stored at 4 degrees, 'room temperature,' or any other temperature desired (say, 16 ºC). For the most part, since Fbw7 dimer yields were quite low, I was unable to generate replicate plates to use at different temperatures so I chose the gentlest treatment of 4 ºC.

Drops are viewed using a light microscope over time. Crystal formation is by rites slower at 4 ºC than at room temperature, so typically nothing was visible the day after setting up the drops. After two or three days, I found drops worth looking at. Brown drops indicated a denatured protein, and the condition in that drop was not amenable to crystallography. Clear drops were plentiful: in these drops, we can assume the protein is too highly soluble in this condition for crystallography. Drops containing speckled precipitant were also plentiful: in these conditions, the protein was precipitated, but not wholly denatured like in the brown drops.

The most interesting drops from the initial crystal screening efforts were those with uniform phase separation, which looks like oil droplets in water. We can think of these drops as conditions where the protein is between soluble and precipitated: it could be close to forming a crystal lattice, and thus the condition may be tweaked to promote crystal formation. Another promising finding is spherulites or micro-crystals. In my experience, these drops show precipitant, but it is not uniformly distributed; instead it may show nuclei of precipitated protein that look somewhat like cells on a dish. Again, we could imagine that the protein was close to forming a lattice, but it happened too quickly due to temperature or the harshness of one component. Again, one may have luck troubleshooting a condition like this to yield protein crystals.

Specifically, the Fbw7/Skp1 dimer protein sample was used in the following crystal screens: Hampton Research Index HT (HR2-134), Crystal Screen HT (HR2-130), PEG/Ion HT (HR2-139), PEGRx 1 (HR2-082) and 2 (HR2-084); and Emerald BioSystems Wizard I and II random sparse matrix crystallization screens. Two drops, both from the Index screen, were the most interesting: 1) 0.5 M zinc acetate dihydrate and 20% PEG 3350 and 2) 1 M ammonium sulfate, 0.1 M BIS-TRIS pH 5.5 and 1% PEG 3350. The zinc acetate condition showed clusters of rough micro-crystals, whereas the ammonium sulfate condition showed regular phase separation. I then screened around these conditions in the larger, handmade format (1.4 ul protein sample, 1.4 ul diluent on a glass cover slip, inverted over the well of a 24-well greased plate, each well containing 1 ml of diluent). In these 24 wells, I aimed to vary the concentration of zinc acetate in one dimension and the PEG 3350 concentration in the other. The zinc acetate condition was not pursued because every condition resulted in brown drops of denatured protein.

The ammonium sulfate/BIS-TRIS/PEG 3350 condition was more fruitful. Several other ammonium sulfate conditions (containing buffer of different pH and larger percentages of different varieties of PEG) from the Hampton Crystal Screen yielded irregular phase separation in the first pass of screening. When I set up a screen varying the pH of 100 mM BIS-TRIS (5.0, 5.5, 6.0, 6.5) and the concentration of ammonium sulfate (0.4, 0.6, 0.8, 1, 1.2, 1.4 M), keeping the PEG 3350 concentration constant at 1% in each condition and 5 mM DTT in each condition (the protein sample contains 5 mM DTT), I saw crystals formed among heavy precipitate in two conditions: pH 6.0 with 1.2 M ammonium sulfate; and pH 6.5 with 1.4 M ammonium sulfate. (See Figure 3.5A for an image of these crystals.) We determined the crystals in this condition were proteinaceous by harvesting and freezing, shipping them to the Advanced Light Source (ALS) synchrotron at Berkeley, California for analysis of x-ray scattering. These crystals yielded spots in a lattice formation that is indicative of a protein lattice, but no spots were found below around 7-8 A. (A salt crystal will yield very low resolution spots.)

Next I used the protein sample in a Hampton Ammonium Sulfate grid screen to quickly screen more extreme pHs and ammonium sulfate concentrations. This was not terribly informative because only spherulites were observed at pH 5, 6 and 7 and at the midlevel concentrations of ammonium sulfate (1.6 M and 2.4 M).

I performed additional screens, more finely varying the ammonium sulfate concentration, the BIS-TRIS pH and the PEG 3350 concentration (as well as the PEG mass), to attempt to optimize crystal formation. Because the PEZ-shaped crystals always sat in heavy precipitate, only a fraction of the Fbw7 protein was making it into the crystal lattice, while the rest precipitated. Also, the conditions that hit tended to contain multiple (6-12) crystals. The optimal situation would be a clear drop containing one huge crystal; the lack of precipitation would indicate that nearly all the protein is being formed into the crystal and bigger is typically better in terms of generating more spots.

Unfortunately, crystal growth was not incredibly reproducible. If I set up the same six conditions in quadruplicate, crystals form in unpredictable and different conditions. It seemed that something was limiting, i.e. nucleation events. When conditions were just right for nucleation, it occurred 6-12 times in a drop but in most attempts, the conditions were not quite right. I attempted to improve the condition by screening additives, but nothing useful came out of it (I pursued a calcium chloride additive for some time, but it ended up I was forming calcium crystals). As mentioned, the crystal formation was not predictable; this could be improved by streak seeding crystals using a cat whisker (Figure 3.5B), but crystals harvested from this effort did not show an improved resolution. Improvement efforts of the rare large crystals were also frustrated by troubles with ice accumulation during shipment of crystals to ALS for remote collection. Despite very focused efforts to avoid ice build-up during crystal harvest, puck loading and dry dewar shipment, the loops containing these crystals always ended up with huge ice crystals caking the loops. I ended up not trusting my methods and asked other more experienced users to do the harvest and transfer steps, but still my loops always ended up icy. Thus, if no diffraction was seen, it could not even be determined whether a crystal remained in the loop after shipping.

I also performed methylation of the surface lysine resides on the protein complex to try to alter the physico-chemical surface of the protein complex, in hopes of attaining additional conditions that result in crystal formation [96, 97]. Methylation did not affect the dimerization of the Fbw7 as assessed by SEC; a small upward shift in size was observed, indicative that methylation was successful (data not shown). Separate screens (Hampton PEG/Ion and Crystal Lite, PEGRx, Index and Crystal Screen) were performed with this protein sample, but no hits were obtained.

The challenges associated with my attempt to solve the structure of this complex can be summarized as follows:

1. The yield of protein of interest is quite low, and so many liters (>20 L) of suspension insect cells must be accumulated before efficient FPLC can be performed. Further purification always results in a significant loss of yield, especially at the concentration step before SEC and after SEC to attain a high concentration for crystallography.
2. Because the protein yield is low, relatively few avenues can be pursued in crystallography. Indeed, only one condition was attained from screening, and there were not even crystals visible from that screen, they were optimized in. Crystal formation in this condition was unpredictable at best.
3. Crystal optimization was frustrated by shipment troubles in the switch to remote data collection.

I was able to elicit valuable advice from experienced colleagues, but the above challenges made it difficult to properly pursue multiple lines of optimizing.

Cyclin E/CDK2 purification from insect cells

As mentioned above, the known structure of cyclin E only encompasses the core of the protein (Figure 3.7), truncating off both the N- and C-terminal degrons, which are presumed to be unstructured. However, because we wanted to look at substrate/Fbw7 binding, we needed to include both degron sequences in cyclin E. We did not know how expression or solubility would be affected.

The main cyclin E degron sequence centered at T380 is very near the C-terminus of the protein (A395 is the last residue of cyclin E1, short version) so we proposed including the entire C-terminus in the construct. As for the N-terminal degron, centered at T62, we decided to truncate away much of the sequence preceding the degron. We created a cyclin E construct in the pFB-GST-TEV vector that starts at residue P56, which was chosen by analyzing a sequence prediction software output (Figure 3.8A). In parallel, all the relevant degron mutants were also produced: T62A, T380A, S384A, T62A/S384A. We also prepared constructs to co-infect cells with CDK2 virus. We decided to use full-length CDK2, since

this was successfully crystallized. Virus was prepared and expression tested. Soluble protein complex was obtained (Figure 3.8B), but yield was not significantly better than seen with recombinant Fbw7. Note that CDK2 is purified as a doublet. The doublet represents different phospho-species of CDK2 [98, 99], which represents an added complication to the aim of generating homogenous protein sample for crystallography. We hoped that 1) the two species would be resolved by ion exchange chromatography and/or 2) they would not pose a problem to high-quality crystal formation.

Unfortunately, as was seen with the Fbw7 protein discussed above, cleavage of the GST purification tag was incredibly weak with TEV (Figure 3.8C). Because of my experience with Fbw7 as described above, I re-cloned the panel of cyclin E mutants with a GAGS linker sequence; and into the thrombin site-containing vector (pFB-GST-Thr); and into the 6His-tagging vector and the untagged vector (pFB-Dual) both to be used with CDK2 that I cloned into the GST-TEV vector.

Surprisingly, the insertion of the linker sequence did not improve TEV cleavage (not shown). The tag reversal scheme did not appear to be a viable option, as cyclin E that was not GST-tagged (untagged cyclin E, as in Figure 3.9A and 3.9B, and even 6His-fused cyclin E, not shown) was not appreciably expressed/soluble/bound to CDK2: when CDK2 was GST-fused, it was incredibly highly expressed, but it co-purified very little cyclin E (Figure 3.9B). (Cyclin E could be detected by Western in the corresponding lanes of Figure 3.9B, not shown. But the fact that the amount of cyclin E could not be seen by eye on Coomassie meant this was not a viable option for purification of the E/K2 complex.)

Cleavage of the GST tag from cyclin E by thrombin (Figure 3.10A) appears to be the best option, but off-target cleavage events are a risk. The experiment in Figure 3.10B demonstrates that the concentration of thrombin added to the substrate is the critical factor.

In sum, in my experience, the only way to pursue purified cyclin E/CDK2 is through the GST-Thr scheme (Figure 3.10C shows the optimal scenario), but the propensity of thrombin to cleave off-target is especially troubling when trying to generate homogenous sample for crystallography. Any uncleaved GST-cyclin E or non-specifically cleaved cyclin E negatively impacted yield and sample homogeneity. Thrombin must be added at limiting amounts dependent on sample concentration and volume, but because these vary fairly widely from prep to prep, thrombin addition is always a risky step. In my

experience, TEV the a preferable protease because it is much more faithful to its cleavage site over a wide range of protease:substrate ratios and substrate protein concentrations.

We do not know the extent to which the endogenous insect cell kinases are able to phosphorylate the overexpressed protein. Because cyclin E/Fbw7 binding is phosphorylation dependent, this is not a trivial concern. We have antibodies to the relevant cyclin E phospho-sites, and when I probed the panel of recombinant cyclin E mutants with each of these antibodies, I saw abundant signal when expected (not shown). However, that does not provide any information about the stoichiometry of phosphorylation. We could, in effect, perform another 'purification' by selecting for crystallography only the cyclin E protein that binds Fbw7. An additional selection step will likely cause a decrease in yield.

The recombinant Fbw7 and recombinant cyclin E do associate *in vitro* (Figure 3.11). We could not tell by Coomassie staining whether binding was 2 Fbw7:1 cyclin E or 2:2. We had no way of knowing if the cyclin E was saturated by Fbw7, or if some fraction of the cyclin E is simply not fully phosphorylated and so is unable to bind Fbw7. If incomplete phosphorylation by endogenous insect cell kinase cascades is an issue, one might be able to increase cyclin E phosphorylation *in vitro*. Cyclin E is auto-phosphorylated by CDK2 at S384, which primes for GSK3 phosphorylation at T380. I attempted to perform an *in vitro* kinase assay on the recombinant cyclin E/CDK2 protein complex, but this did not have any discernable effects on the cyclin E phosphorylation status (as determined by Westerns with phospho-antibodies) or on Fbw7 binding (data not shown). I also produced a T160E mutant of CDK2, to mimic a constitutive activating phosphorylation by the CDK activating kinase (CAK). This mutation did not have a discernable effect on the CDK2 doublet. I also purified a recombinant Cak1p, the *S. cerevisae* CAK, which is reportedly active against human cyclin-bound-CDKs [100], but I did not observe any effect on the purified CDK2. An alternative approach would be to infect the GST-cyclin E/CDK2-infected cells with additional viruses to over-express CAK, GSK3β, and/or MAP kinases, which should result in a downstream increase in cyclin E phosphorylation (and might resolve the CDK2 doublet).

When soluble Fbw7/Skp1 and cyclin E/CDK2 samples were generated (similar to the experiment shown in Figure 3.11; complex was assembled on beads but instead of liberating the complex by glutathione elution, the complex was liberated by thrombin cleavage) and subjected to chromatography,

the cyclin E/CDK2 and Fbw7 dimer did not remain bound during either Q or SEC (not shown). This is apparently not uncommon for proteins that are known to interact. We assumed an FPLC step could remove unbound cyclin E/CDK2 and create a homogenous sample of F-box protein dimer bound to substrate, but it could not be utilized at this step. I never set up crystallization trials with the thrombin-liberated complex, but it seemed unlikely that sample would be pure enough to result in protein crystals. Due to the heterogeneity of the sample combined with the low yield of the soluble cyclin E/CDK2 complex, we deemed (nearly) full-length cyclin E not viable in crystallization of the Fbw7 dimer.

Use of cyclin E peptide, other protein additives to improve crystal formation

Although using the nearly full-length cyclin E protein for crystallography is the only way we know of to visualize both degrons and their relationship to the dimeric F-box protein, as mentioned above, the structure of dimerized F-box protein alone would be highly significant as well. We currently do not know whether an F-box protein dimer is able to recruit two whole, active SCF complexes or if steric hindrance prevents the simultaneous association of two Cul-1 scaffolds. We also do not confidently know the relation of the two WD propellers. Shedding more light on an F-box protein dimer would facilitate extrapolation of more information than we currently have regarding substrate binding to a dimerized SCF.

As in previous studies, we can use phosphorylated cyclin E peptide to bind the substrate-binding pockets in the propellers. We purchased doubly phosphorylated cyclin E peptide from New England Peptide. Crystal screens were performed after mixing Fbw7/Skp1 with the peptide in a 1:3 molar ratio. No hits were obtained.

Any unengaged protein-protein interaction surfaces might negatively impact crystal formation. In the Fbw7 dimer, the two dimerization domains are bound to one another. The substrate binding pockets in the WD propellers can be occupied by mixing the complex with an excess of cyclin E peptide. The two F-boxes are bound to Skp1 molecules. But the Skp1 molecule itself contains an interface for binding to the N-terminus of Cul-1. Thus, as another additive for crystal screening, I purified the N-terminus of human Cul-1 (NTD) and then the full-length protein as well. Cul-1 vectors for purification from *E. coli* were available from the Zheng lab. The N-terminus was purified as a GST-fusion from 12 L of BL21 *E. coli*.

Yield is incredibly high compared to insect cell yields of Fbw7 and cyclin E. Because the pI of the NTD was predicted to be neutral, I tested for binding to SourceS and SourceQ resins. The NTD bound well to SourceQ resin so I further purified the protein on a Q column. After this point I tested for binding to Fbw7. The proteins bound and remained bound during SEC (Figure 3.12). This was encouraging and crystal screens were set up with and without cyclin E peptide. No hits were found.

As mentioned, I also purified full-length Cul-1 from *E. coli*. In this case, the vector also provides untagged yeast Rbx1. Because the implications of Cullin neddylation on SCF function and structure are not completely understood, I created and purified the neddylation site mutant, K720R. This protein cannot be neddylated in *E. coli*, but I wanted to remove all possibility of any structural heterogeneity when mixed with proteins purified from insect cells. As a full-length protein, the yield of Cul-1 from *E. coli* is lower than the NTD truncation or the 'split form' (in which the two halves of the protein are co-expressed and self-associate), but yield was still quite high. Anion exchange does result in a yield loss, but not as much as oral tradition had warned. The full-length protein also bound to the Fbw7 complex and was stable over SEC. Again, we could not determine by Coomassie staining whether Cul-1:Fbw7 binding was 2:2 or 1:2. Crystal screens were also pursued with this protein complex, which may be as large as 350 kDa. No hits were obtained.

Another avenue I explored was the addition of the human protein Sgt1. Sgt1 (Suppressor of G2 allele of *skp1*) was identified in yeast as a novel binding protein of the SCF required for the G1/S and G2/M phase transitions [101]. I cloned human Sgt1 and found it to be easily purified at a high yield from *E. coli*. However, recombinant hSgt1 did not stably associate with my recombinant SCF^{Fbw7}. Also, in transfection assays, I could not co-immunoprecipitate tagged hSgt1 and tagged Fbw7 in human cells (not shown), despite the finding in the literature that yeast Sgt1 associates with Skp1/Cdc4 complexes.

Attempt to visualize SCF^{Fbw7} dimer by electron microscopy

The entire dimerized SCF complex (perhaps 350 kDa, or 250 kDa, depending on whether two or one Cul-1 molecules are bound) may be approaching the limit of the size of protein complex that can comfortably be used for crystallography. Because of this concern, and the low yields of protein complex

obtained, electron microscopy (EM) seemed an appropriate alternate approach that could illuminate whether the machinery for one or two SCFs simultaneously associates with an F-box protein dimer. This question is of interest because it is directly related to elucidating the fuction of an SCF dimer: does it simply lead to more rapid substrate turnover because two activated E2s can access substrates at once?

In negative stain EM, the native protein sample of interest subjected to staining by an electron-opaque solution (in our case, uranyl formate), applied to a protein-adsorbant surface, dried and imaged by transmission electron microscopy. The native protein adopts a variety of three-dimensional orientations on the surface, and so thousands of shapes identified by the user as protein are averaged to obtain an overall protein structure. Although the method *can* be used to obtain higher resolution structures, we were expecting a much lower-resolution picture of the SCF dimer architecture than can be gained by crystallography. However, because full-length Cul-1 is such an elongated scaffold, this method ought to be sufficient to identify whether one or two Cul-1 molecules bind the dimer. The other main advantage of this approach is that very little protein is used when compared to crystallography trials and trouble-shooting.

It initially appeared we might obtain usable data from this approach (Figure 3.13 shows images of the Fbw7/Skp1 dimer alone and the Fbw7/Skp1/Cul-1 NTD complex), but frustratingly, images of the complex containing the full-length Cul-1 showed protein aggregates (not shown). Even when freshly prepared protein was used immediately after SEC, the microscopy showed aggregated protein. The images also showed contamination by very large particles, which may indicate that the Fbw7/Skp1/full length hCul-1 complex (perhaps 350 kDa if two molecules of Cul-1 are indeed bound) is eluting in the void volume of the SEC column. Judging by the trace and the protein standards and the quality of the peak fractions when analyzed by Coomassie, it did not seem to be the case. However, without an SEC column meant to resolve higher molecular weight complexes, the possibility is difficult to rule out.

Conclusions and future directions

In this chapter, I discussed my work in purifying dimerized Fbw7 form insect cells, which had not previously been done. This is an important reagent in the field to be able to study this critical ubiquitin ligase in its physiologically relevant form.

The limited yield of Fbw7 makes this scope of work difficult to pursue. Around the time I was wrapping up crystallography efforts, the lab generated a small fusion sequence that dramatically increased the solubility and yield of several tricky proteins in the lab [102]. I cloned Fbw7 into this fusion vector but did not have the chance to assess whether yield was improved.

The various additives discussed above make for interesting complexes for crystallography. Although I do not think nearly full-length cyclin E/CDK2 is a tractable lead for learning more information on substrate binding, perhaps other Fbw7 substrates should be examined for their potential in crystallography. Cyclin E, of course, is the 'most interesting' substrate because of its two degrons, but Myc may also have a second contact site. I attempted to purify recombinant c-Myc using various truncations but failed to generate any appreciable yield. It is possible other substrates have second contact sites we do not currently appreciate and would be able to bind an Fbw7 dimer in a homogenous manner. Another thing to consider is that even if both propellers of a dimer are not simultaneously engaged as we suppose they are on cyclin E, the relation of a single-degron containing substrate to the two propellers is still an interesting proposition and could occur in a homogenous manner amenable to crystallography. A really novel finding would be the dimer simultaneously engaging two substrate molecules (i.e. the T58 CPDs of two Myc molecules), which would argue against dimer-specific enzyme function, at least in the case of substrate studied and with the usual caveats of crystallography.

Returning to the simplest crystal, that of the Fbw7/Skp1 dimer alone, an approach to improve the diffraction is to carry out protein engineering on surface residues of Fbw7. The structure of the monomer is solved, and so we can pick surface-exposed charged residues that may be acting to repel or destabilize lattice formation and mutate those to neutral amino acids. This is a common procedure in crystallography trouble-shooting.

As far as the simultaneous engagement of two degron sequences by an F-box protein dimer goes, a last idea is one based on protein cross-linking. One could take the Fbw7/Skp1 dimer and

monomer, mix with the recombinant cyclin E/CDK2, crosslink to trap the protein-protein interactions, trypsinize the protein and analyze by mass spectrometry. The difficulty in this procedure is on the mass spectrometry and computational side, since every peptide that flies needs to be analyzed for all tryptic combinations of Fbw7/Skp1/cyclin E/CDK2 and include possible phosphorylations and other protein modifications. However, this analysis would surely be informed by the known structures of Fbw7/Skp1 and of cyclin E/CDK2 and of the interactions between the two complexes that we would expect and hope to find. We could imagine that the monomeric Fbw7 is only found cross-linked to the cyclin E T380 degron whereas in the dimeric sample the propeller is found cross-linked to both degron sequences.

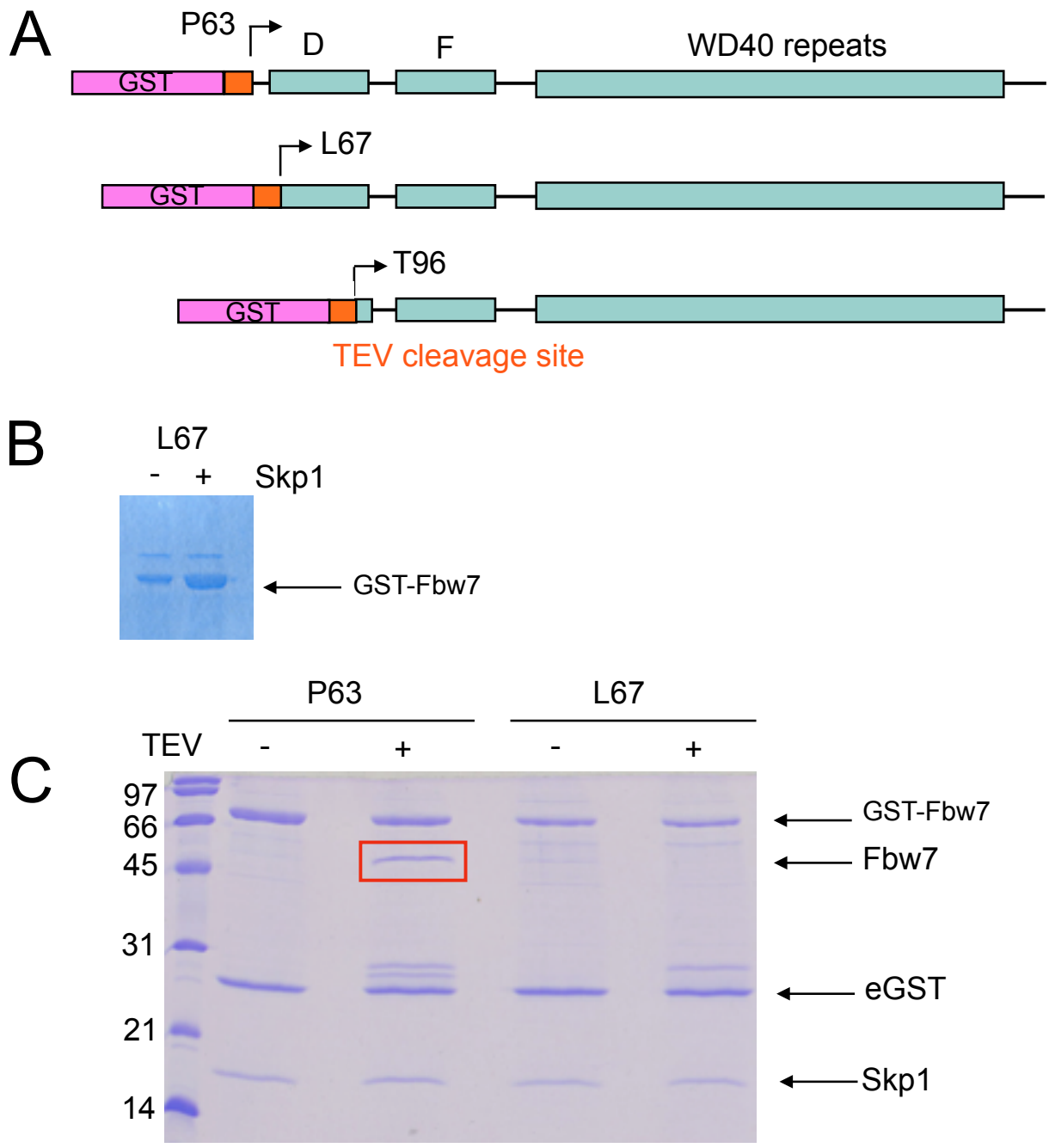

Figure 3.1: Fbw7 dimer purification by GST affinity

(A) Graphical depiction of the GST-fusion constructs for Fbw7 purification. P63 and L67 are two start sites containing the functional dimerization domain. T96 is the monomer crystalloized in [62].
(B) A Coomassie stained protein gel of material GST-affinity purified and eluted. This experiment compared two small-scale infections, with and without co-infection of untagged Skp1 virus. Co-infection with Skp1 appears to increase Fbw7 solubility.
(C) A protein gel showing the minimal TEV-cleavage of the GST tag using these constructs. This gel was run after additional TEV was added to the reactions, 4 °C at least 72 hours. TEV and liberated GST can be seen as faint bands above the endogenous insect cell GST-like protein (eGST).

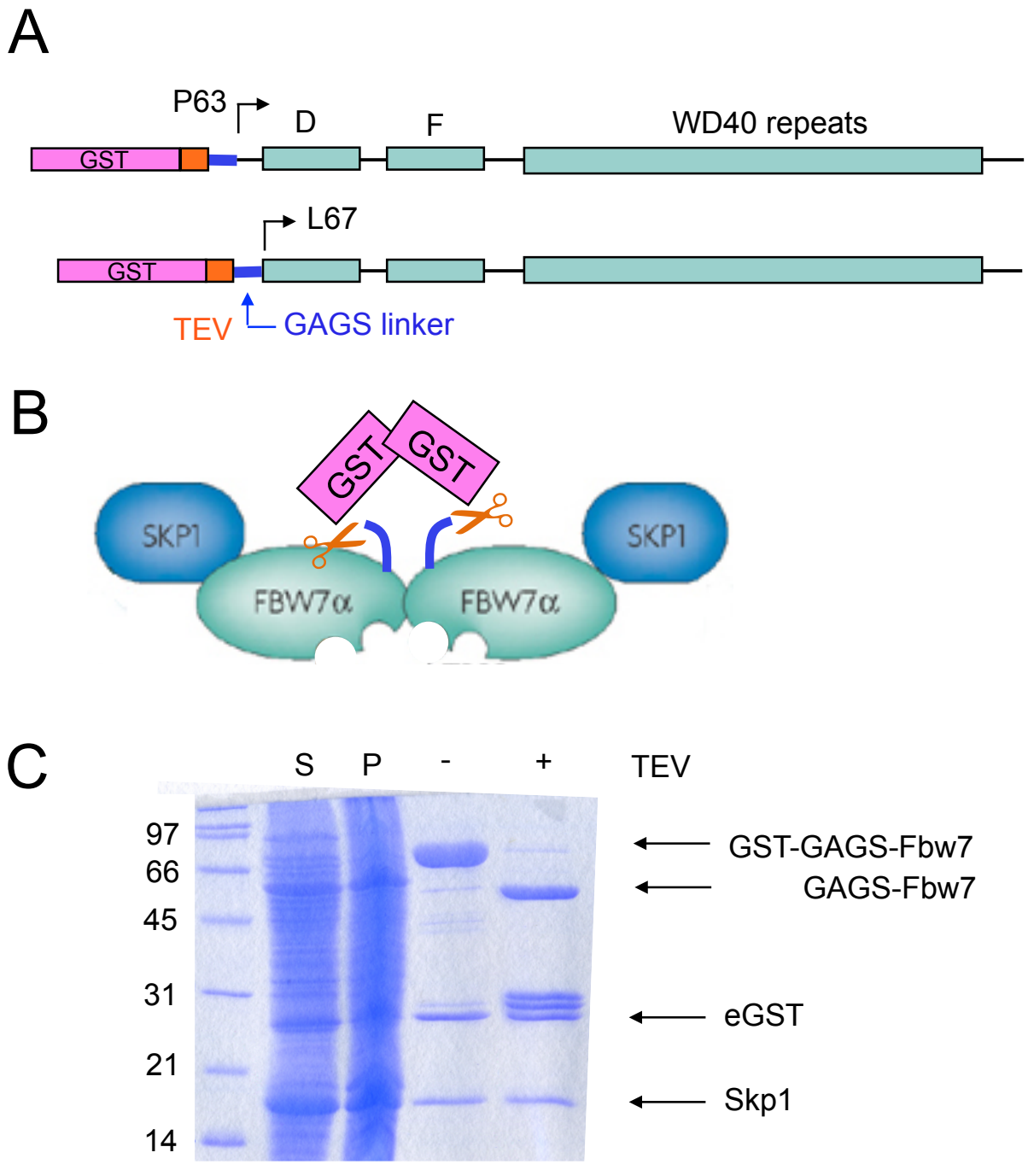

Figure 3.2: Insertion of a flexible linker sequence allows TEV access to the cleavage site

(A) Graphical depiction of the insertion of a flexible linker sequence (GAGS) into both dimeric constructs.
(B) Cartoon depiction of the utility of the linker sequence. Without it, the TEV site was apparently too closely associated with the dimer interface to allow enzyme access. GST is also known to dimerize.
(C) A Coomassie stained protein gel showing the much improved TEV cleavage of the P63 construct. S indicates lysate supernant, P is pelleted material. (Not shown: even with the linker addition, L67 did not show complete cleavage. P63 was exclusively used from this point onward.)

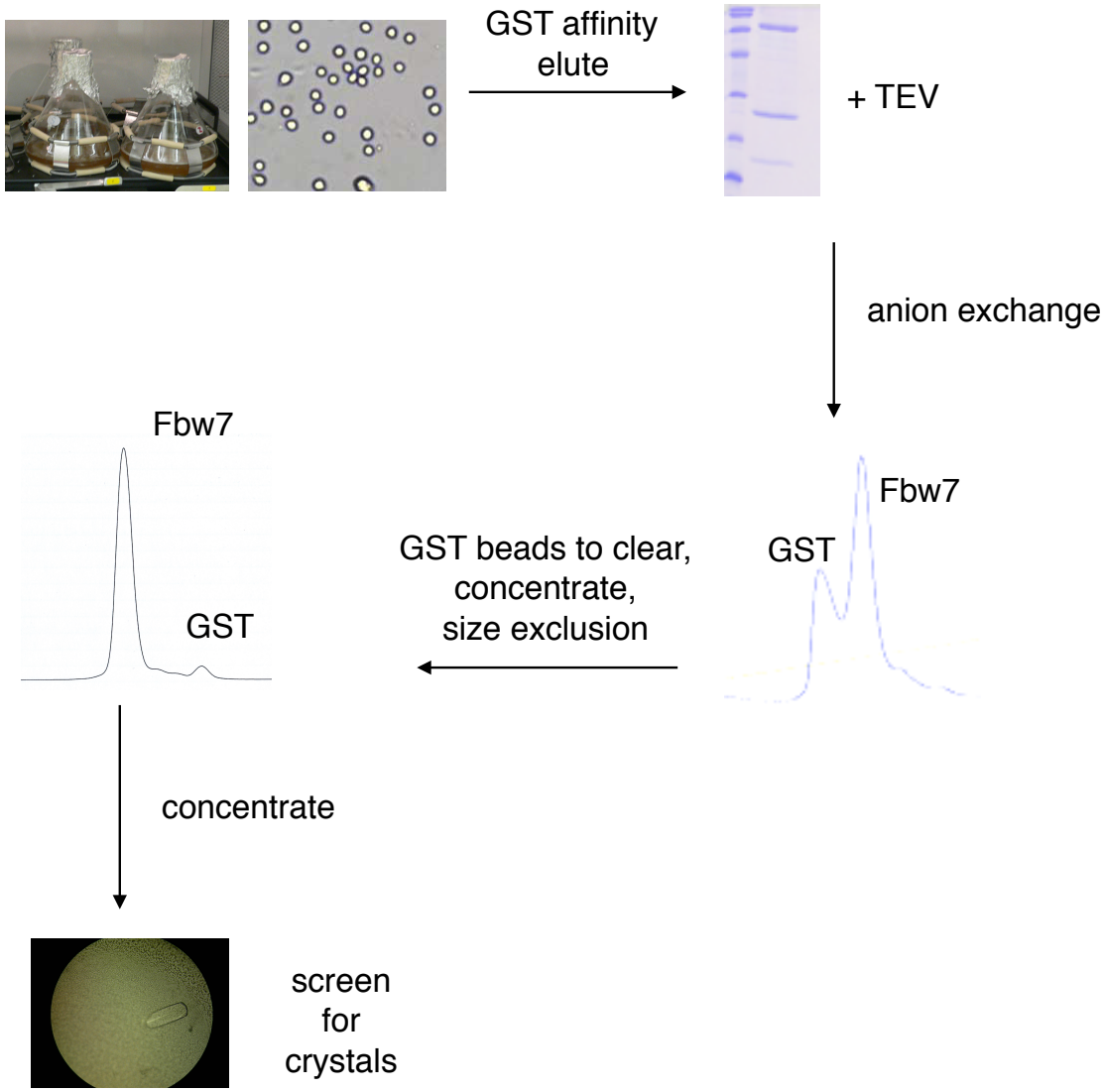

Figure 3.3: Workflow for purification of crystallography-grade dimeric Fbw7

Fbw7 and Skp1 virus are used to co-infect Hi5 cells in suspension. The complex is purified by Fbw7's GST-affinity tag and eluted into solution; the tag is then removed by TEV cleavage in solution. The protein mixture is first subjected to anion exchange chromatography. The pooled fractions can be passed over fresh GST resin to remove most contaminants; the flow-through is concentrated for size exclusion chromatography to further separate free GST and any aggregated species from the Fbw7 dimer. Peak fractions are then concentrated and used for crystallography.

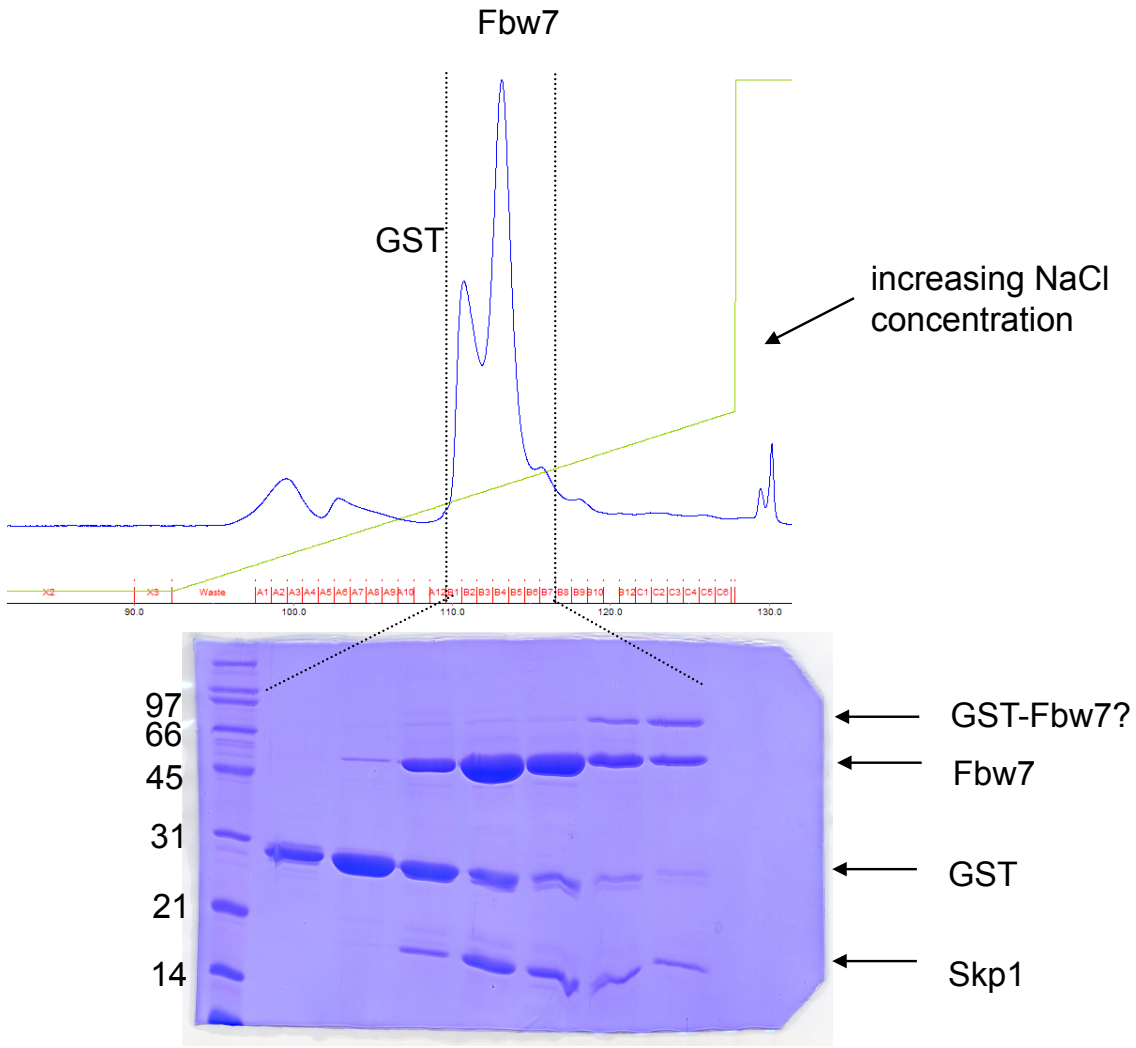

Figure 3.4: Purification of the Fbw7 dimer by anion exchange chromatography

A representative trace showing the behavior of the Fbw7 dimer on anion exchange using a 1 ml SourceQ column. The gradient elution varied the concentrations of two 20 mM Tris pH 8.0, 5 mM DTT buffers of different ionic strength: buffer A contained 0 mM NaCl; buffer B contained 1 M NaCl.

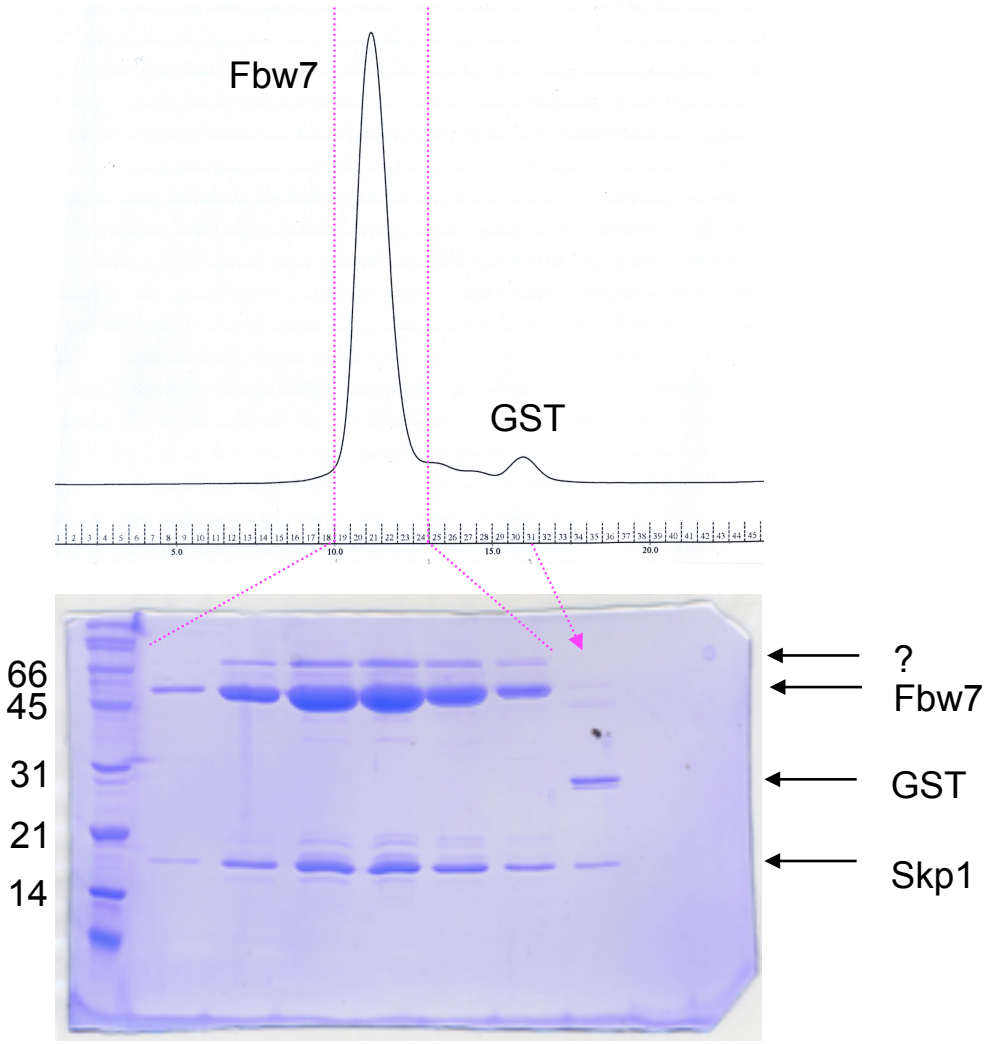

Figure 3.5: Purification of the Fbw7 dimer by size exclusion chromatography

A representative trace showing the behavior of the Fbw7 dimer on a 25 ml Superdex200 column. According to protein standards run on the same column (not shown), the Fbw7 peak corresponds to about 170 kDa, indicating that the protein complex indeed forms a dimer. SEC was performed in 20 mM Tris pH 8.0, 200 mM NaCl, 5 mM DTT at 4 °C. Because the contaminant band was not removed by running the Q fractions from Figure 3.4 over GST resin, we no longer believe it is uncleaved GST-Fbw7 contaminant; perhaps it is Hsp70.

A

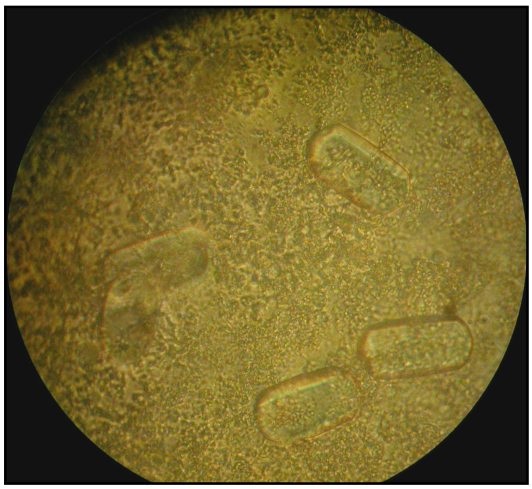

B

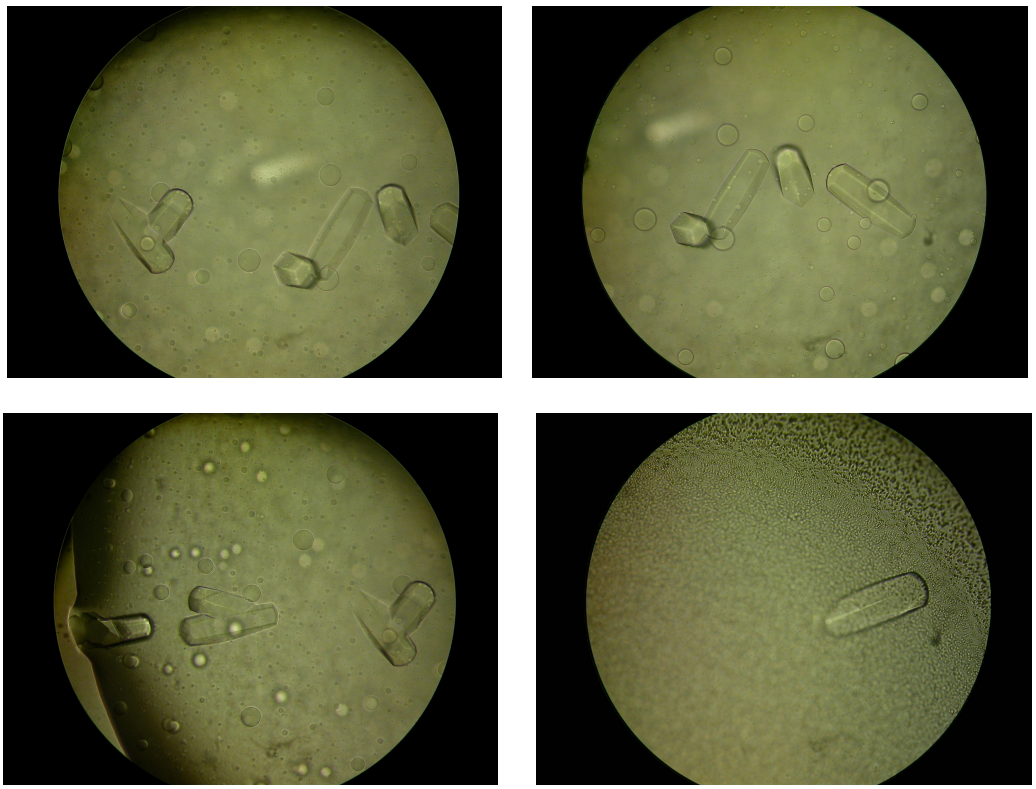

Figure 3.6: Fbw7 dimer protein crystals

(A) Initial hit from 1.4 M ammonium sulfate, 100 mM BIS-TRIS pH 6.5, 1% PEG 3350, 5 mM DTT.
(B) Crystals generated by streak-seeding for nucleation events through drops screening around the conditions describe in (A). A parent crystal was harvested from (A), physically smashed with a plastic pestle and vortexed. The thin end of a cat whisker was dipped into this solution and streaked through hanging drops equilibrated at least 16 hours at 4 °C. These crystals were observed several days later.

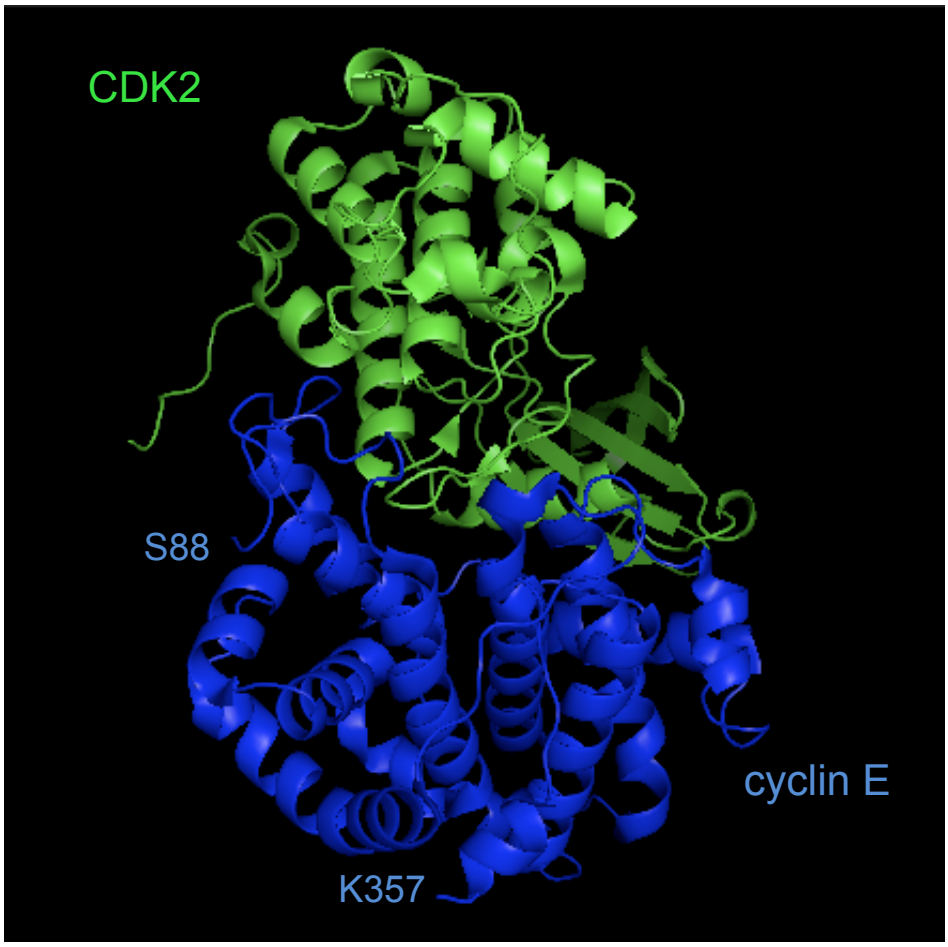

Figure 3.7: The known structure of cyclin E/CDK2

A depiction of the solved structure (1W98) of the core of cyclin E bound to full-length CDK2. Both cyclin E degron sequences are truncated.

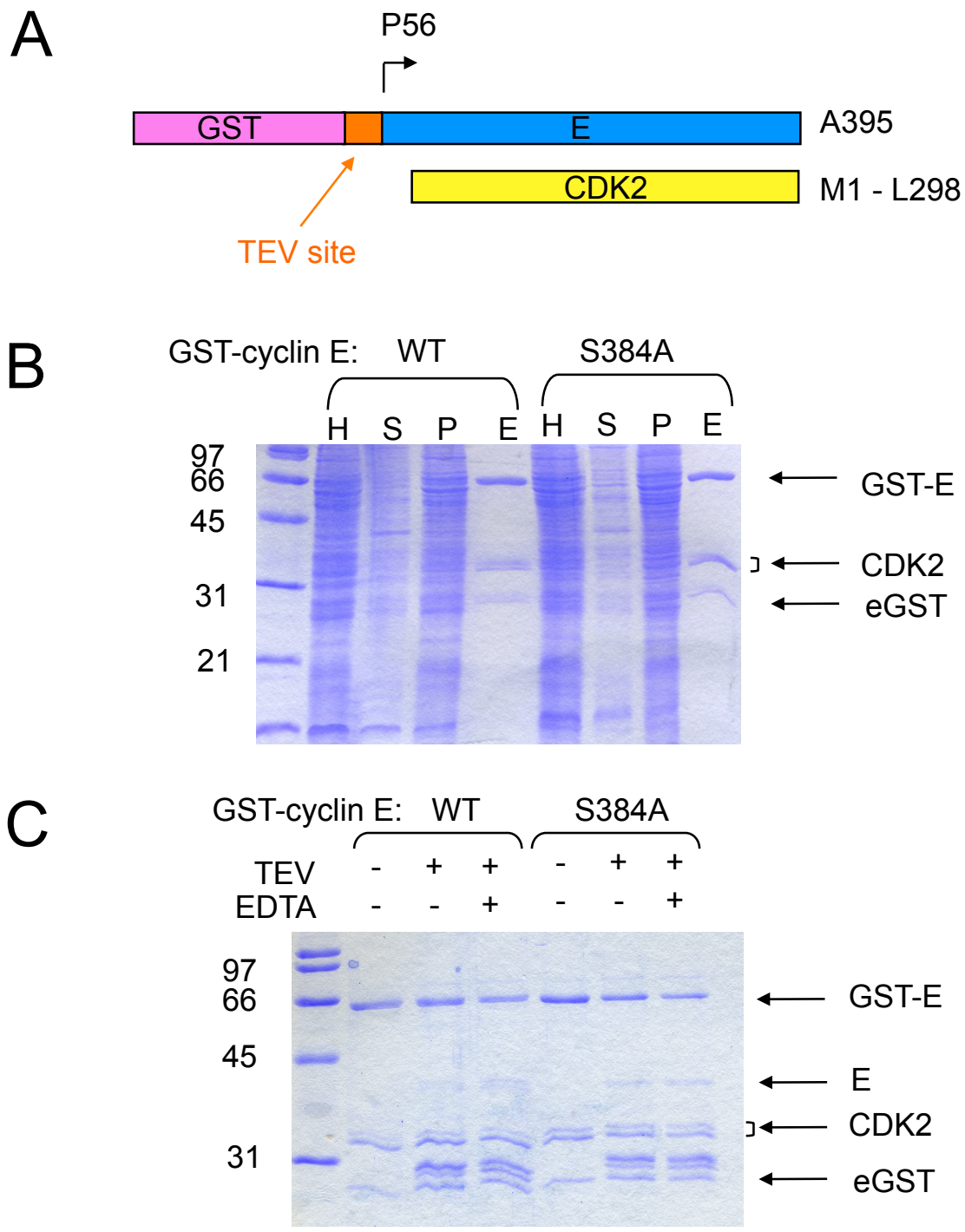

Figure 3.8: Affinity purification of the GST-cyclin E/CDK2 complex works, but TEV cleavage is again problematic

(A) Graphical depiction of the constructs used to make virus for these experiments.
(B) GST-affinity purification of the cyclin E/CDK2 complex. (H = cell homogenate, S = supernatant, P = pelleted material, E = elution.)
(C) As with the initial GST-Fbw7 construct, TEV cleavage was also not efficient for GST-fused cyclin E.

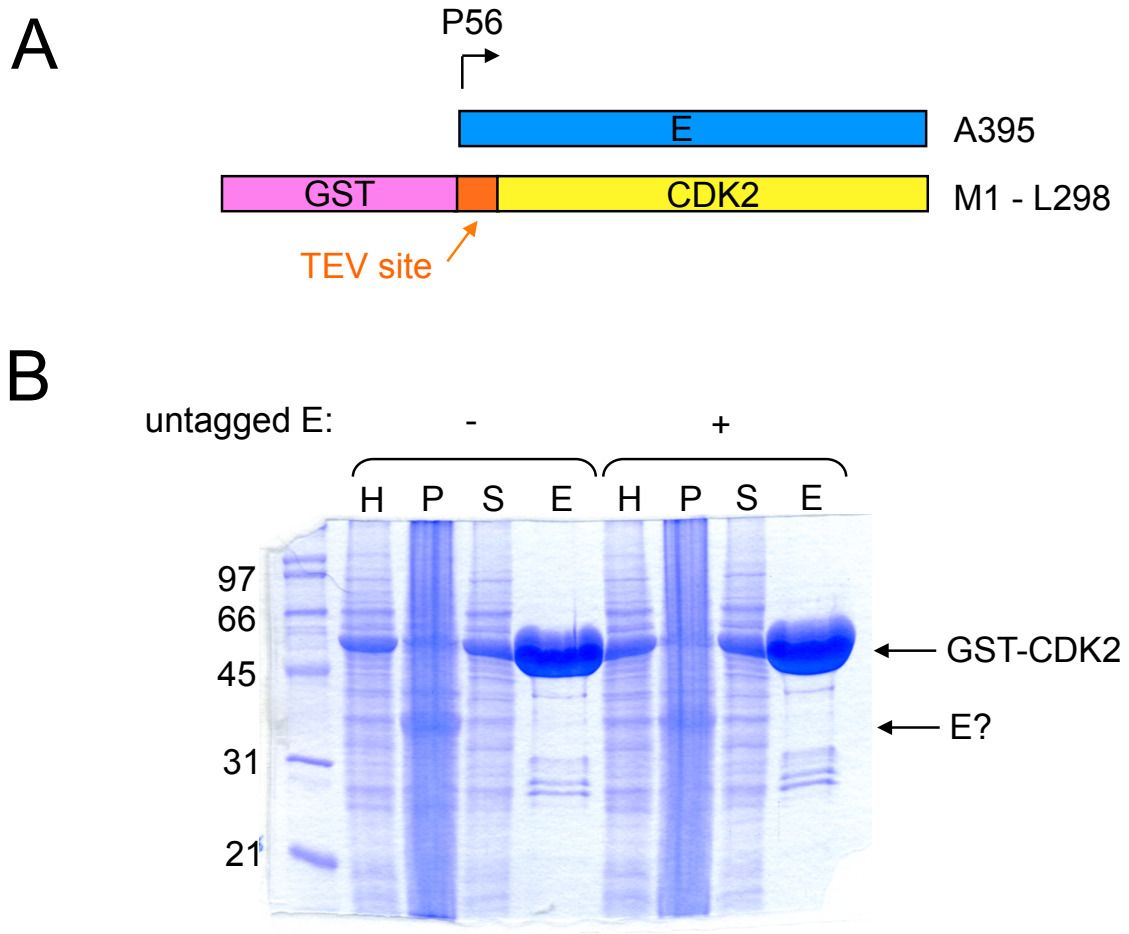

Figure 3.9: Reversing the tagging scheme resulted in extremely little cyclin E

(A) Graphical depiction of the constructs used to make virus for these experiments.
(B) GST-affinity purification of the complex. Cyclin E is detectable by Western. (H = cell homogenate, P = pelleted material, S = supernatant, E = elution.)
(C) Cleavage of the GST tag from CDK2 was not observed.

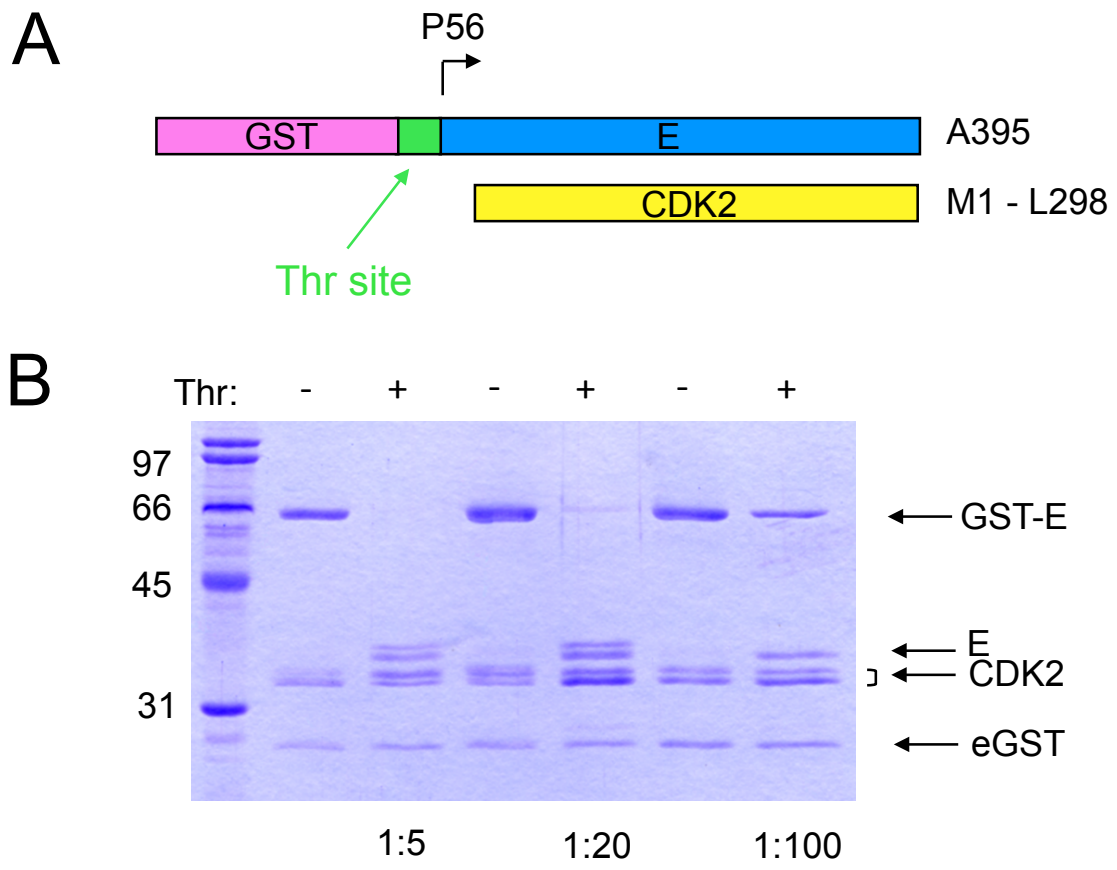

Figure 3.10: Thrombin cleavage of the GST tag from cyclin E is effective but very concentration-sensitive

(A) Graphical depiction of the constructs used to make virus for these experiments. The TEV site was mutated to a thromibn site.
(B) Overnight thrombin cleavage in solution of GST-cyclin E/CDK2 complexes eluted with glutathione. Protein concentration was estimated by Bradford and thrombin was added at various concentrations..
(C) Thrombin cleavage of GST-cyclin E/ CDK2 complex while immobilized on GST beads. Protein concentration was estimated by running a fraction of the resin on a protein gel; thrombin was mixed with the remaining resin, attempting to attain a 1:100 dilution. The liberated cyclin E/CDK2 complex was collected as flow-through.

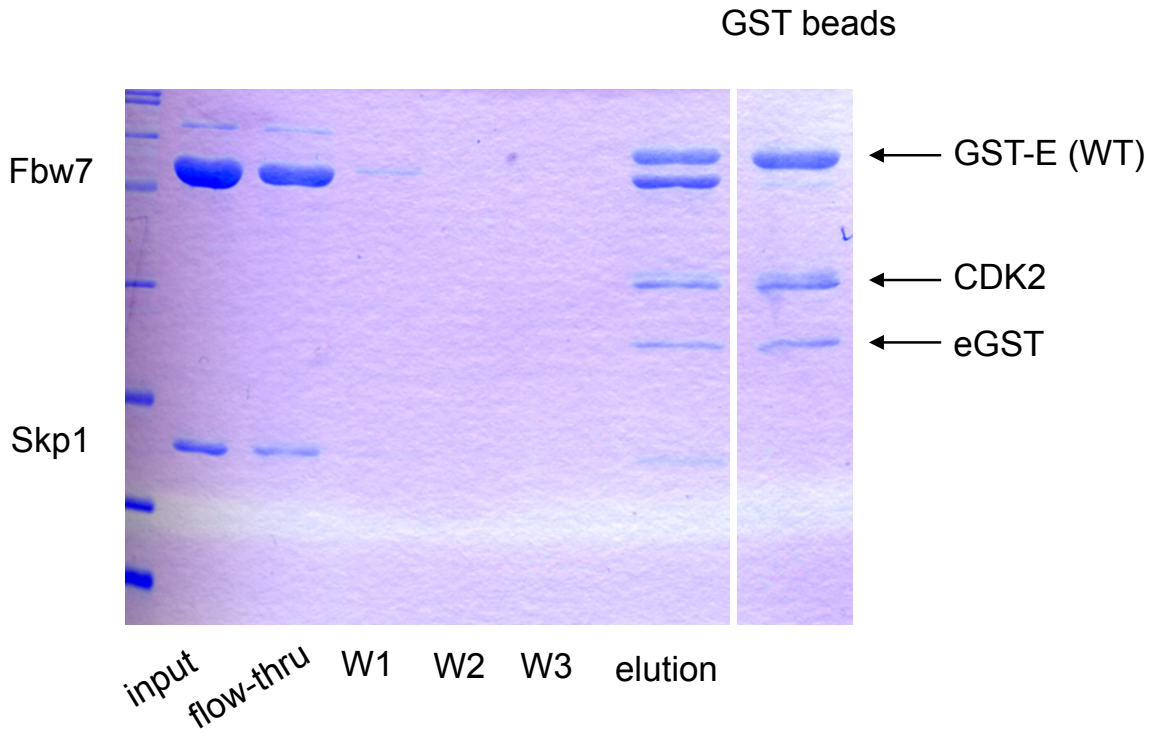

Figure 3.11: Formation of the Skp1/Fbw7 dimer:cyclin E/CDK2 complex

GST-cyclin E/CDK2 complex was affinity purified using GST beads. While immobilized on the resin, soluble Fbw7/Skp1 dimer complex was added in excess and allowed to incubate at 4 °C for 30 minutes. The flow-through was collected and the beads were washed with five sequential column volumes of buffer (the first three wash fractions are shown here). Remaining bound protein was eluted with glutathione and examined by Coommassie staining. The eluted protein shows that successful cyclin E and Fbw7 binding occurred. The final lane shows the GST resin before Fbw7 loading as a comparison.

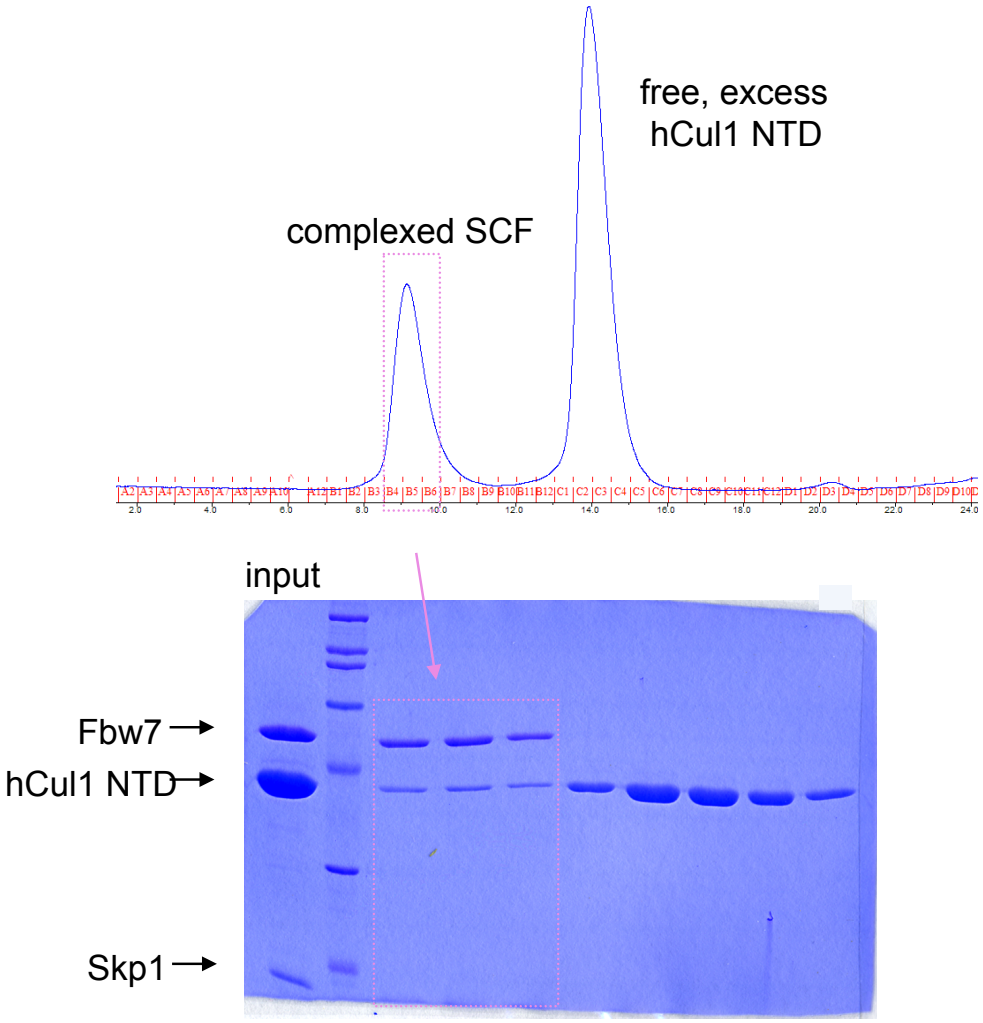

Figure 3.12: Formation of the Fbw7/Skp1/Cul-1 NTD complex

Cul-1 NTD was mixed in a 5:1 molar ratio with Fbw7, incubated 30 minutes on ice and subjected to SEC (Superdex200 25 ml). Chromatography was performed in 20 mM Tris pH 8.0, 200 mM NaCl, 5 mM DTT.

A

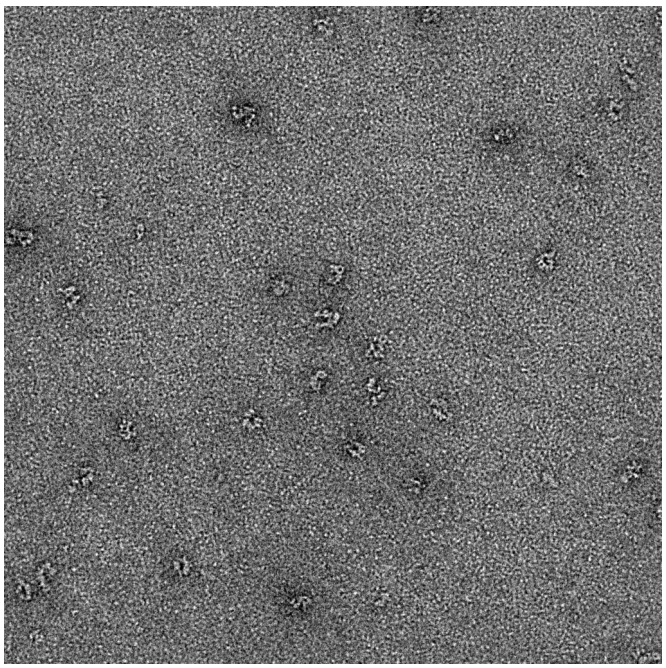

B

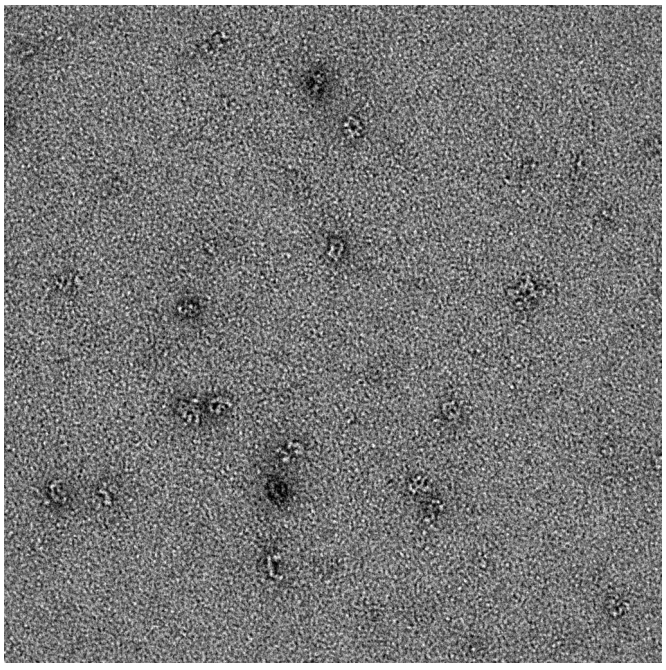

Figure 3.13: Negative stain electron micrographs of purified Fbw7 complexes

(A) Dimeric Fbw7/Skp1 complex. Images courtesy of M Iadanza, T Gonen.
(B) Dimeric Fbw7/Skp1/hCul-1 NTD complex.

CHAPTER 4

Characterization of Fbw7 dimers and monomers *in vitro*

The SCF's cognate E2s

Cdc34 is the only E2 that is genetically linked to Cdc53/Skp1 (the SCF) in yeast, indicating it is a non-redundant E2 for the ligase. However, whether or not this is the situation in human cells is not known. In fact, the pairing of E2s with ubiquitin ligases is not an active area of research in the ubiquitin field. Because E2s are quite abundant and often come in multiple isoforms, they are difficult to study by knockdown or over-expression experiments in human cells.

In vitro, E2 proteins can be purified and studied, but it is difficult to directly compare the activities of different enzymes. Also, if multiple E2s are compatible with the ubiquitin ligase of interest, it does not mean that these are physiologic pairings made in a cell. Sub-cellular localization or cell type specificity can always be a factor in elucidating physiologic E2 and E3 combinations. The E2 enzyme UbcH5 works with the SCF (and practically any ubiquitin ligase) *in vitro*, but we do not know if this is a physiologic scenario. (The promiscuity of UbcH5 will be discussed below.)

Neddylation of Cullins

Ubiquitin is one member of a family of small proteins that are attached to other proteins as modifications. Small Ubiquitin-like Modifier (SUMO) is another such protein, as is the protein Nedd-8. Nedd-8 is an interesting molecule because its only known substrates are the Cullin family of proteins. Nedd-8 conjugation occurs through a cascade analogous to the ubiquitin-conjugating cascade described in Chapter 1, and results in Nedd-8 conjugated to a specific, conserved lysine on the Cullin proteins.

Neddylation of Cullins is reported to be essential for the functioning of the many ubiquitin ligases they form. In 2008, the structure of a neddylated Cul-5 was solved [103]. In this structure, they saw the Rbx1 molecule bound at the C-terminus of the Cul-5 had popped up and away from the scaffold. This result suggests a possible solution for something that had long been nagging the field. In the landmark structure of the F-box of Skp2/Skp1/Cul1/Rbx1, the projected distance between the substrate-binding

interface of Skp2 and the active site of an E2 bound to Rbx1 was approximately 50 Å [15]. It seems this gap would need to be bridged before a charged ubiquitin would attack a substrate lysine. (However, note that F-box protein structures to date have only been solved with peptides representing substrates. A full-length substrate molecule would likely fill a significant portion of the gap.) The liberation of the Rbx1/E2 portion of the ligase by Cullin neddylation, as suggested by the authors, seems to allow the charged ubiquitin the flexibility to swing around and collide with bound substrate.

The two-degron model can be studied *in vitro*

In the absence of crystallographic data on our model of simultaneous engagement of the two degrons of cyclin E by an Fbw7 dimer, we could still study the interaction *in vitro* using purified components. As described in the previous chapter, Fbw7 can be purified from insect cells as a monomer and as a dimer, excluding and including the dimerization domain in the recombinant protein expression vector. As for Fbw7 substrates, recombinant cyclin E phosphorylation site mutants were purified as GST-fusion proteins from insect cells (also discussed in the previous chapter), and tagged full-length substrates can also be purified from transfected human lysate (where they are more likely to be properly modified) by immunoprecipitation. We can assay both protein interactions as well as substrate ubiquitylation, discussed below.

Recombinant dimeric Fbw7 is active against cyclin E and c-Myc and can utilize two different E2 enzymes

Because, for crystallography purposes, I purified recombinant Fbw7, Skp1, and Cullin1/Rbx1, I wanted to try to reconstitute SCF ubiquitylation *in vitro*. My first attempt used recombinant cyclin E/CDK2 as substrate and I attempted to see ubiquitylation by Coomassie. To the S384A cyclin E/CDK2 I added Fbw7/Skp1, Cul1/Rb1x1, recombinant E1 (*S. cerevisae* GST-E1 purified from *E. coli*), recombinant E2 (UbcH5b purified from *E. coli* in this case), ubiquitin (purchased from Boston Biochem), magnesium chloride and ATP. Some ubiquitylation was seen with UbcH5 (Figure 4.1), but not an impressive amount and certainly not complete conversion of the substrate band to higher-molecular weight species. No

changes were seen with Cdc34 as the E2. *In vitro* auto-ubiquitylation of other reaction components also masks the cyclin E-specific ubiquitylation. By Western against cyclin E, we can specifically see distinct ubiquitylation conjugates.

Because we have many cyclin E reagents, I captured transfected cyclin E on beads, performed on-bead ubiquitylation assays, and visualized all cyclin E species by probing for it in a Western (unless otherwise noted, I probe for its Myc-tag). This approach worked quite nicely, and because I use cell lysates in which cyclin E had been over-expressed, I can easily use any cyclin E mutant we desire to examine. The only downside to this approach is a slight technical one: when taking time points in an on-bead assay, it is difficult to attain equal amounts of beads in each time point. This results in unequally loaded lanes and this can confound ubiquitylation analysis (example not shown).

I observed excellent ubiquitylation of over-expressed cyclin E simply using straight cell lysate (Figure 4.2). The reaction is dependent on the added components, even though the endogenous forms of all of the added components (i.e. ubiquitin) are expected to be fairly abundant in the human cell lysate (HEK293A) harvested for these experiments.

As mentioned above, the yeast SCF uses the E2 Cdc34 exclusively. The preference of E2 for human SCF is not entirely clear in human cells [104]. The Zheng group, however, has had inconsistent results for SCF E3 activities using recombinant Cdc34 purified from *E. coli* (Figure 4.1 is an excellent example). As an alternate approach, I created baculovirus for expressing Cdc34 in insect cells. The protein purified from insect cells appears, upon Coomassie staining, the same as the protein purified from *E. coli*, i.e. both run as a doublets and exhibit the same behavior on an anion exchange column (Figure 4.3A). However, strikingly, the Cdc34 protein purified from insect cells leads to robust poly-ubiquitylation by the SCF, whereas the Cdc34 sample purified from *E. coli* does not (Figure 4.3B). What led to this drastic difference in activity is unknown. One possibility is that a novel E2 protein modification (missing in bacteria) may regulate activity. To pursue this question further, it will be worthwhile to test the two E2 samples in an additional SCF-substrate system.

Once active Cdc34 was obtained, it was used as E2 when possible because I demonstrated the extremely promiscuity of UbcH5 as E2 in our system. This will be discussed more below.

c-Myc is also poly-ubiquitylated by Fbw7 using Cdc34, and it is dependent on the c-Myc degron sequence (Figure 4.4). Unfortunately, other Fbw7 substrates (SREBP1a, Jun, Notch, MCL1) were not able to be poly-ubiquitylated in this type of *in vitro* reaction. The reasons for these failures are not known, but it seems likely that over-expressed substrates could be lacking adequate degron phosphorylation; the endogenous kinase(s) may not adequately phosphorylate the over-expressed substrate, or degron phosphorylation may be dependent on signals that are not adequately found in this cell type or context. The over-expressed protein may also out-titrate an endogenous binding partner or some other type of modification of structure that is required for Fbw7-mediated poly-ubiquitylation.

The two-degron model can be recapitulated *in vitro* in ubiquitylation and binding assays

Using over-expression of our panel of cyclin E degron phosphorylation mutants, I recapitulated our two-degron model described in Chapter 1 *in vitro*. Poly-ubiquitylation of cyclin E by an Fbw7 monomer requires a fully intact, doubly phosphorylated C-terminal degron whereas the dimer can tolerate loss of S384 phosphorylation but the N-terminal degron (T62) is required (Figure 4.5A). This can also be demonstrated with binding assays (Figure 4.5B). These results support our model that the Fbw7 dimer can simultaneously engage two distinct degron sequences.

The dimeric SCF has more ubiquitin attachment sites than does the monomer

Using commercially available ubiquitin mutants, we can dissect the nature of the poly-ubiquitin chains formed by Fbw7 dimers and monomers. Interestingly, the Fbw7 dimer may form non-K48 linkages when we use K48R mutant Fbw7 (Figure 4.6A and 4.6B) whereas the monomer does not. The reason for this is not understood; if two E2s are recruited to the dimeric SCF, perhaps they are able to extend the growing ubiquitin chains in novel ways. Cdc34 is not known to form linear ubiquitin chains. As described in Chapter 1, it has been hypothesized that a dimeric ligase may have access to more substrate lysine residues than a monomeric ligase, therefore leading to more efficient poly-ubiquitylation [93]. When we use ‘K0’ ubiquitin, ubiquitin in which all seven lysines have been mutated to arginine, we see clearly that the monomer is able to conjugate only one moiety of ubiquitin onto cyclin E whereas the dimer is able to

conjugate several (Figure 4.6B). This indicates that the dimeric SCF, indeed, is able to access additional substrate lysines than the SCF monomer.

Cullin neddylation is not necessary *in vitro*

As mentioned in the previous chapter, I generated recombinant full-length Cul-1 with the neddylation site mutation, K720R. Nedd8 cannot be conjugated to this site even if all the enzymes are present in the lysate portion of the ubiquitylation assay. Interestingly, I was never able to see any difference in substrate poly-ubiquitylation between full-length (or split-form) Nedd8-Cul-1 and the K720R mutant (Figure 4.7A and 4.7B). There are a few caveats to this statement, though. It is possible that the net effect of the substrate lysate is to de-neddylate any added Cullin. Thus, we would not see any difference between the two purified forms in the reaction conditions. Another possibility is that Cul-1 is present in such abundance in the reaction that any suboptimal character of the K720R mutant is overridden by its sheer abundance. Nevertheless, it is an observation that warrants further exploration.

UbcH5 is a very promiscuous E2

Ubiquitin E2 selection by E3 ligases is a not well-understood facet of ubiquitin biology. From genetic studies in yeast, the human Cdc34 homologs are presumed to be the cognate E2 enzymes for the SCF ubiquitin ligase. However, many *in vitro* ubiquitin studies in the literature utilize the E2 enzyme UbcH5. Because we had both E2s at our disposal, we were able to conduct comparisons of these two E2s in our purified SCF system. Both UbcH5 and human Cdc34 both promote efficient poly-ubiquitylation of cyclin E and c-Myc in our system.

Because we also had at our disposal ubiquitin lysine mutants, we were able to investigate the promiscuity of UbcH5 (Figure 4.8). We compared wild-type ubiquitin with ubiquitin in which the major lysine of destructive chain elongation, K48, was mutated to arginine; we also compared these to a ubiquitin in which all seven lysine residues were mutated to arginine. As shown, when fewer lysines are available in ubiquitin, the chains that UbcH5 builds are smaller or less branched and thus less retarded in the gel. However, even when there are no lysines in ubiquitin with which to build chains, UbcH5 is still

able to form high-molecular weight species. This suggests that UbcH5 is a highly promiscuous E2 and, in this case, is affixing a single ubiquitin moiety to every lysine residue present in the substrate molecule.

We also obtained additional recombinant E2s from the Klevit lab and tested their ability to lead to poly-ubiquitylation of cyclin E (Figure 4.9). We see that two were not active on cyclin E, although it appears UbcH6 can catalyze mono-ubiquitylation *in vitro*.

This work is interesting and significant because it suggests that the *in vitro* system we have reconstituted is specific and relevant. Addition of the purified E2 is required and the identity of the E2 is also crucial for substrate ubiquitylation. It would be interesting to test the compatibility of the SCF with the entire panel of active E2s, as is now commercially available.

Several substrate-like proteins that are not degraded in cells can be poly-ubiquitylated *in vitro*

Ebp2 is a nucleolar protein that binds to Fbw7 through a phosphodegron-like sequence and brings Fbw7 to the nucleolus. Despite binding to Fbw7, Ebp2 is not destroyed by the SCF *in vivo* in any condition we can identify. However, we see Fbw7 can lead to poly-ubiquitylation of Ebp2 *in vitro* by UbcH5 (Figure 3.10A). This is a very interesting result because it means there in fact is nothing 'wrong' with Ebp2 as a substrate. It is not the fact that the CPD is at the extreme N-terminus, or it is too low-affinity for a stable interaction, or there is steric hindrance blocking association of the SCF components, or any other internal fault that can be imagined. Perhaps in cells, something is preventing a ubiquitin chain from forming on Ebp2 or preventing access by the proteasome. It may be a de-ubiquitylation enzyme (DUB), but we have not been able to identify a DUB that when knocked-down, results in Ebp2 turnover. It could be that the nucleolus excludes a component that is required for the ubiquitin cascade, such as the E2 enzyme.

Moreover, the poly-ubiquitylation only occurs with UbcH5 as the E2, not with Cdc34. This implies that the E2 has a say in substrate turnover. One could imagine that perhaps Cdc34 has a more transient association with Rbx1 than does UbcH5, and so there are substrates (and lysines) that Cdc34 is never able to conjugate the first ubiquitin moiety. If E2 expression and/or activity are at all regulated with regard to sub-cellular localization, this may represent a mechanism for differentially regulating substrate stability.

The same results are seen with another substrate-like protein, Etv6 (M Welcker, unpublished observation). The fact that UbcH5 but not Cdc34 leads to poly-ubiquitylation of these proteins indicates that the E2 is playing a role in *in vivo* substrate regulation.

Purification of Fbw7 wild-type/arginine mutant hetero-dimer

As described in Chapter 1, the idea of Fbw7 dimerization is an attractive mechanism to at least partially explain the Fbw7 mutational spectrum seen tumors, i.e. the selection for point mutations in the context of the retention of the wild-type allele. As described in Chapter 1, this selection suggests that the wild-type/mutant dimer, which makes up as much as 50% of the cellular Fbw7 pool in this genetic situation, may be the key to truly understanding Fbw7's role in tumorigenesis.

This single-allele mutation has been reproduced in our lab by gene-targeting of human cells and also in a murine model (J Grim, unpublished at time of writing), but the effects on substrates can only be indirectly extrapolated. Also, in these models, the effects of the mutant/mutant dimer (perhaps as much as 25% of the Fbw7 pool) cannot be parsed from any effects of the wild-type/mutant dimer.

Toward this end, we leveraged the Fbw7 purification techniques developed in Chapter 3 as well as all of the various Fbw7 tagging schemes explored to exclusively purify the wild-type/mutant hetero-dimer. Insect cells were co-infected with Skp1 virus as well as differentially tagged Fbw7 viruses (6His-Thr-Fbw7 R338L and GST-TEV-Fbw7 wild-type). Hetero-dimer purification was accomplished by sequential purification of the 6His-tag, liberation by thrombin cleavage, GST-purification and liberation by TEV cleavage. (The protein generated by this method was put over SEC to confirm its size and also so that it was prepared in the same manner comparable to that of the other dimer complexes generated in this work.) The activity of this hetero-dimer then can be assayed against various substrates to see whether abrogation of the binding ability of one of the protomers is sufficient to dominantly inhibit substrate regulation, and which substrates are sensitive.

Unfortunately, we cannot tell to what extent this purified hetero-dimer reshuffles to form wild-type/wild-type and mutant/mutant dimers. If it reshuffled to equilibrium, we would obtain the 25%-50%-25% distribution we suspect are found in tumor cells displaying a single-allele arginine mutation.

Therefore, when I performed *in vitro* ubiquitylation assays using the hetero-dimer, I always compared its activity to a reaction in which I used only 25% of that amount of wild-type/wild-type dimer. I also had to perform titration experiments of the substrate:ligase ratio to make sure that I was operating in the range where I could discern a difference between 100% and 25% of the chosen amount of wild-type/wild-type dimer.

We saw that the hetero-dimer is impaired in its ability to lead to poly-ubiquitylation of wild-type cyclin E (Figure 4.11A) as well as S384A cyclin E (Figure 4.11B). We did not see any differences in poly-ubiquitylation of c-Myc, although I may not have titrated the amount of ligase low enough to detect a difference.

Using purified Fbw7 in surface plasmon resonance pilot experiments

Because we hypothesize that the affinity of the substrate/Fbw7 interaction is so critical to predicting regulation, we attempted to use our purified Fbw7 in surface plasmon resonance (SPR) experiments. In this system, one component of the interaction (the ligand) is coupled to a surface and the other component (the analyte) is flowed over the surface. Any binding interaction alters the extremely sensitive optics of the surface, and so is recorded by the machine and from this response an on-rate can be calculated. When the user stops the ligand flow (switching to buffer), the interaction dissociates, and an off-rate can be calculated. These types of experiments require much less protein than is needed for isothermal titration calorimetry (ITC), which is another approach to measuring the affinity of interactions.

We were able to use the Biacore 100 and 3000 systems in the Strong lab to do pilot experiments with our components. The Zheng lab had prior experience attempting to use Biacore to study an interaction, and they recommended against using a GST-binding surface to couple the ligand. Because of the difficulties in removing the GST tag from the recombinant cyclin E described in Chapter 3, we could not use full-length cyclin E/CDK2 in this system. However, we did obtain biotinylated peptide corresponding to the cyclin E C-terminal degron, phosphorylated at T380 and S384 (as well as the un-phosphorylated peptide). Biotinylated peptide was coupled to a streptavidin surface and Fbw7 dimers were flowed over the surface. We were interested in comparing the affinities of the wild-type dimer to both

peptides. Indeed, as expected, binding of the wild-type dimer to the phosphorylated peptide was very robust. Unfortunately, the Fbw7 did not dissociate much over time. As is common practice in Biacore experiments, we attempted to strip the interaction with a pulse of NaOH, but this appeared to damage the peptide ligand, as repetition of the Fbw7 association followed by strip resulted in continual dampening of the interaction. This is a problem because, in order to obtain any affinity values, an iterative concentration series of the analyte pulse needs to be performed. It may help to place much less phosphorylated peptide on the surface used to assay the wild-type dimer.

As expected, the wild-type dimer interacted much less with the un-phosphorylated peptide. Again, we would need to perform a concentration series to calculate any affinity values. Because the interaction was so weak, we would need to massively increase the amount of peptide bound to the surface or use a lot of Fbw7 protein in the experiment (or both). Although we did not try the arginine mutant dimer in this pilot experiments, because it presumably interacts much less with both peptides, we would again need much more densely coated surfaces and/or need to use a lot of mutant Fbw7 to attain association curves.

Because the gold-plated surfaces of the chips used for Biacore are quite expensive, it did not seem to make sense to troubleshoot these experiments by creating a series of varying concentrations of surface-coupled peptide. Instead, we attempted to reverse the setup, and couple the Fbw7 to the surface and flow the peptide as ligand. Protein coupling can be done nonspecifically by surface amine chemistry or can be done specifically via antibody binding. We attempted amine chemistry coupling first, but did not see appreciable binding of the phosphorylated peptide to the amine-coupled wild-type Fbw7 dimer. We also attempted to bind Fbw7 to the surface by first attaching a mouse monoclonal antibody that works well in detecting my purified protein. We attached the antibody by amine chemistry in our first attempt and, in our second attempt, amine-coupling a mouse anti-IgG and then flowing the anti-Fbw7 antibody over that surface. Unfortunately, neither of these strategies resulted in enough Fbw7 bound to see any peptide binding.

In fact, that appeared to be the main challenge of this approach: the Fbw7 dimer is so massive (approximately 150 kDa) that a lot of peptide (approximately 3 kDa) needs to bind the surface to significantly shift the optics of the surface above background fluctuations.

An alternative idea is to leverage the mass of the *full-length* cyclin E/CDK2 complex and the fact that binding of materials to the Biacore surface can be used as a purification step. I attempted to capture on the surface tagged cyclin E/CDK2 over-expressed in human cells. Because we already had the anti-mouse IgG surface, I flowed 9E10 (anti-Myc tag) hybridoma supernatant over the cell and attempted to capture the cyclin E/CDK2 complex by the Myc tag on the cyclin E. The antibody in the hybridoma lysate is unpurified, so I also attempted to inject commercial anti-cyclin E mouse monoclonal antibody (HE111) that we use for immunoprecipitation of the native complex. This approach worked enough that we were able to qualitatively see the differential binding of the wild-type dimer and the mutant dimer to both wild-type cyclin E and CPD mutant cyclin E (Figure 4.12). Unfortunately, the response curves do not fit well to a 1:1 binding curve and so accurate affinity values cannot be calculated. (This may not be terribly surprising, since our two-degron hypothesis states that Fbw7:cyclin E binding is 2:1.) These data can only be used for qualitative comparison, which is simply confirmatory to our observations made by *in vivo* turnover assays and *in vitro* binding and ubiquitylation assays.

Conclusions and future directions

Despite the unsuccessful efforts to elucidate the structure of an Fbw7 dimer described in Chapter 3, the protein produced for that aim are incredibly useful in a variety of biochemical assays. We can study the properties of Fbw7 itself or the properties of its substrates. The *in vitro* results can inform *in vivo* experiments, or vice versa. Omitted from this chapter are our ongoing efforts to use this purified Fbw7 dimer in screening small molecules that rescue the Fbw7/substrate interaction when either Fbw7 or the CPD is mutated (both situations are seen in cancer). Our collaborators also have used this purified Fbw7 in quench-flow experiments to analyze poly-ubiquitylation and have learned that complexing of Cul-1 to Fbw7, and addition of my recombinant GST-cyclin E both act to inhibit the deneddylation of Cul-1 [105].

These reagents will continue to be useful in studying Fbw7 regulation. However, because the purified protein only contains the dimerization, F-box and WD domains, we cannot use this tool to learn any isoform-specific information.

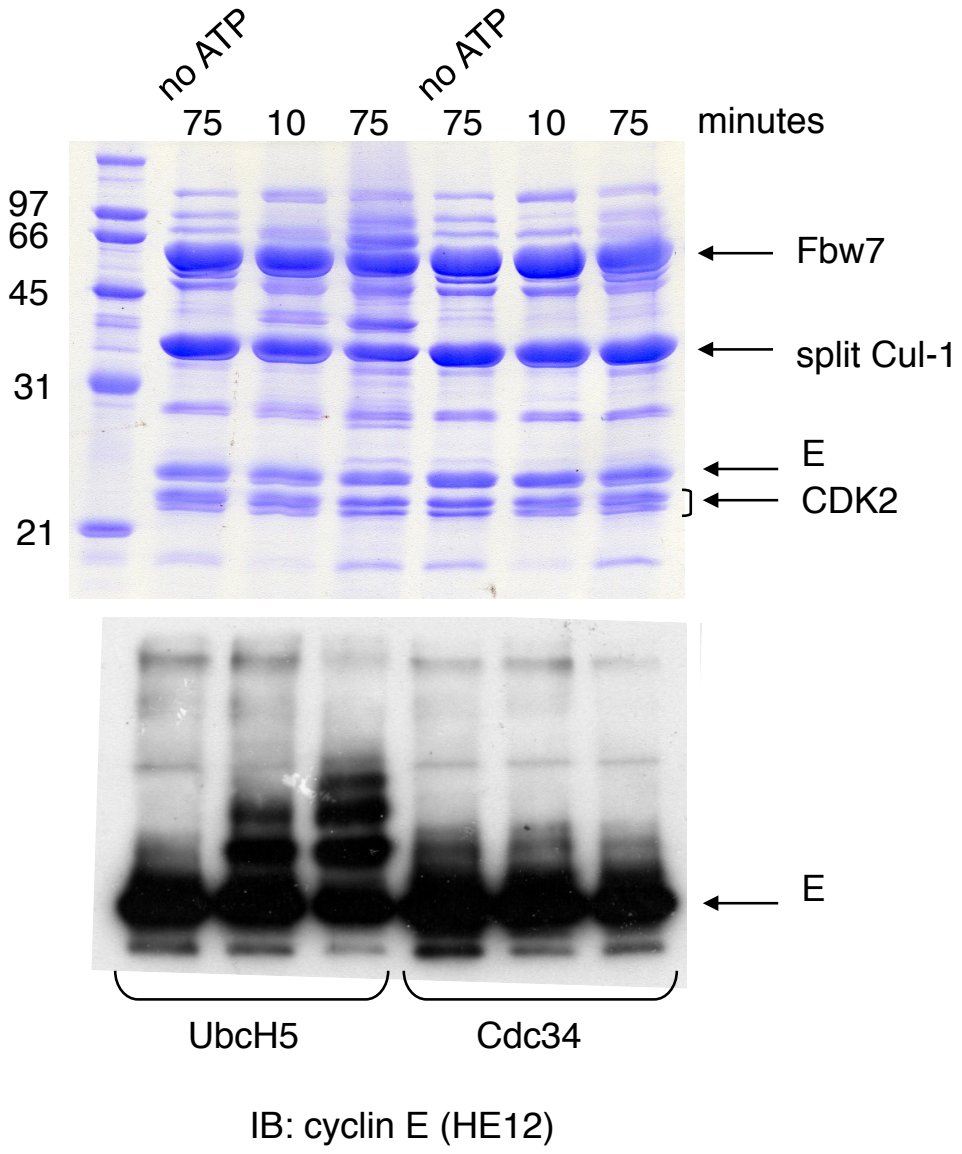

Figure 4.1: Initial ubiquitylation reaction with recombinant cyclin E

Dimeric Fbw7/Skp1, Cul-1/Rbx1, E1, magnesium chloride, and either UbcH5 or Cdc34 were added as the E2. Soluble recombinant cyclin E/CDK2 (purified as in Figure 3.10C; cyclin E in this reaction contained the degron mutation S384A) was used as substrate. ATP was added to or excluded from the reactions as indicated; aliquots were taken at the given time points.

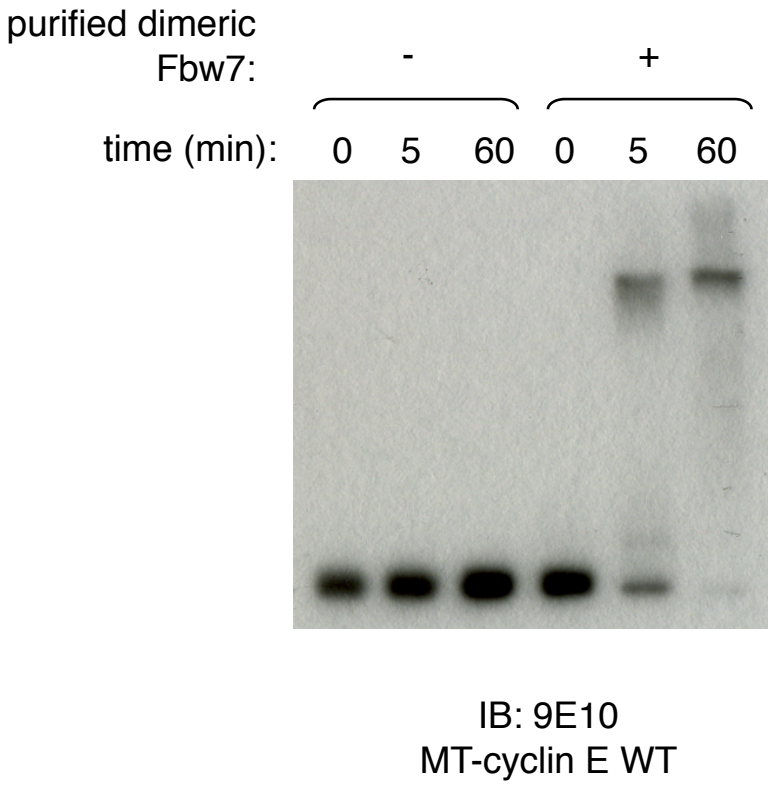

Figure 4.2: Poly-ubiquitylation of over-expressed cyclin E in cell lysate

Dimeric Fbw7/Skp1, Cul-1/Rbx1, E1,UbcH5, magnesium chloride, and ATP were added to the reactions. Poly-ubiquitylation is dependent on the added components and on the cyclin E CPD.

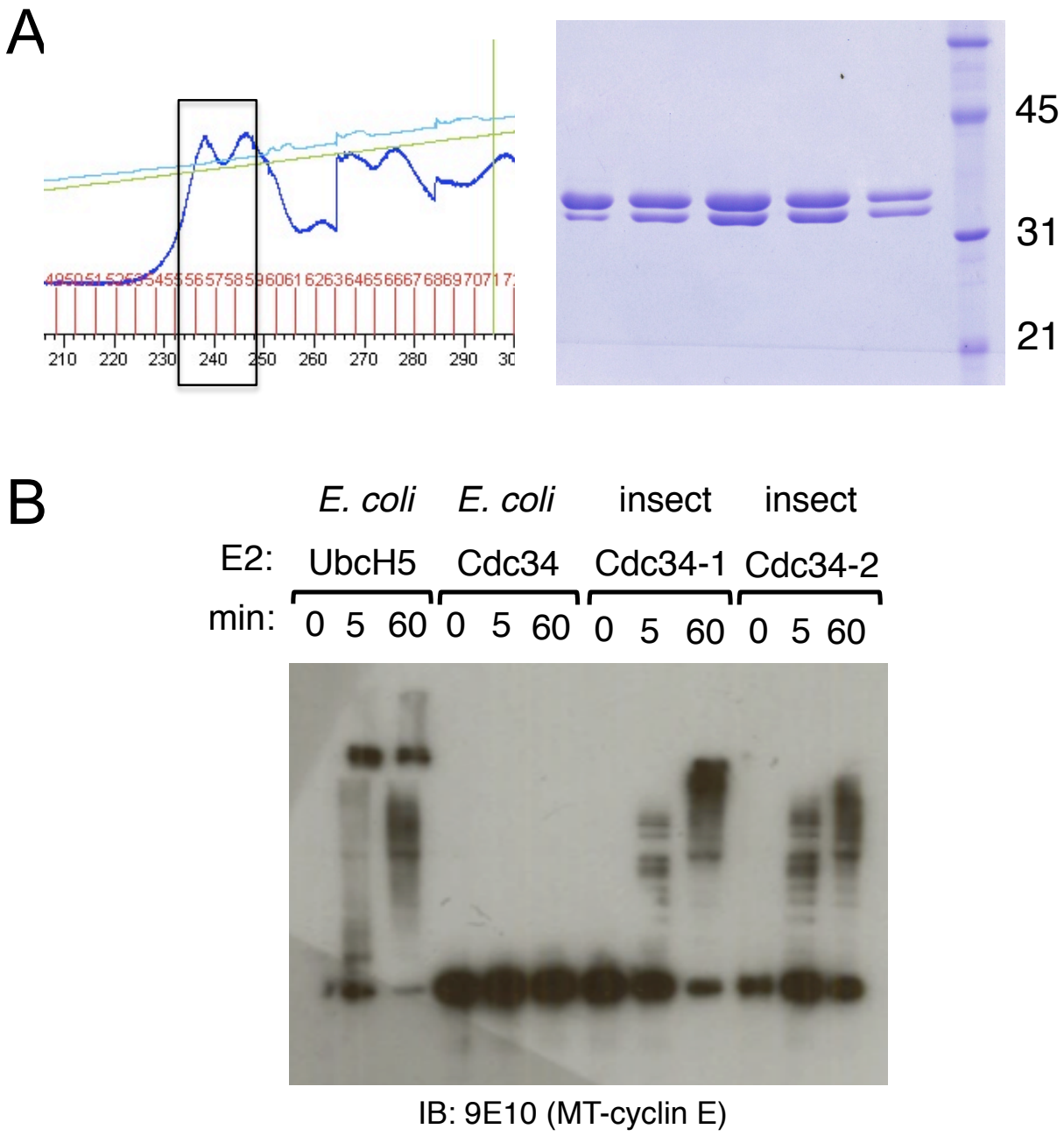

Figure 4.3: Active Cdc34 can be purified from insect cells

A) On the left, a partial trace of Cdc34 from insect cells eluted from 8 ml Source Q column. A very gradual elution was used, in an attempt to separate the two species of the doublet. On the right, a Coomassie-stained gel of purified Cdc34. The first lane is enzyme from *E. coli*; the other four lanes are Q fractions corresponding to the two peaks seen at left.

B) Cdc34 purified from insect cells is active, whereas enzyme purified from *E. coli* is not. Cdc34-1 and Cdc34-2 indicate the two sub-peaks from the anion exchange, as seen in A.

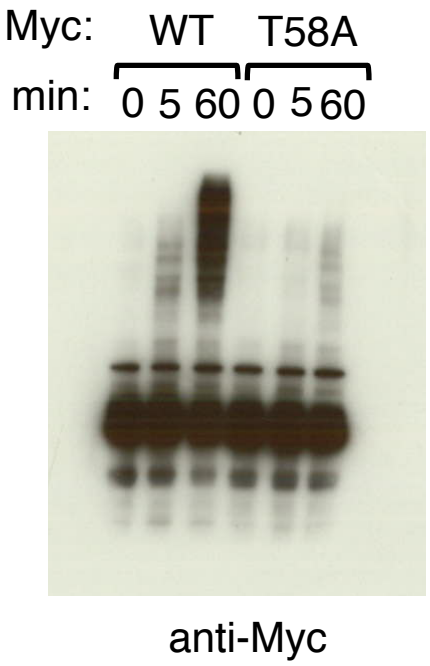

Figure 4.4: Over-expressed c-Myc is also poly-ubiquitylated by Cdc34 in a CPD-dependent manner

Cell lysate containing over-expressed c-Myc or its CPD mutant were used in ubiquitylation reactions with purified dimeric Fbw7.

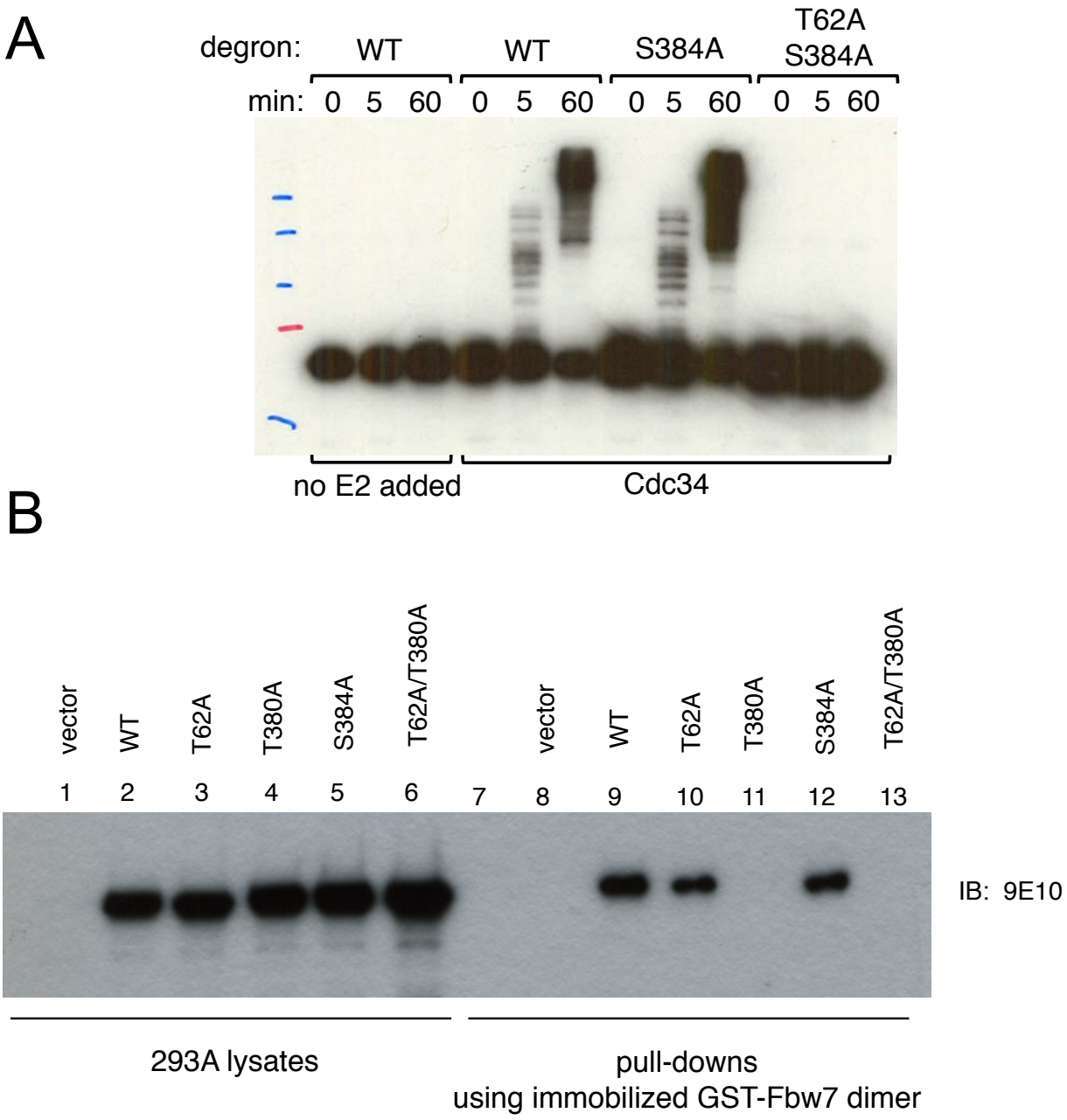

Figure 4.5: Two-degron model of cyclin E degradation is recapitulated *in vitro*

A) Ubiquitylation assays on various cyclin E mutants using purified Fbw7 dimer.
B) Binding assay using purified Fbw7 dimers also confirms that neither T62 nor S384 are required for binding in the context of T380.

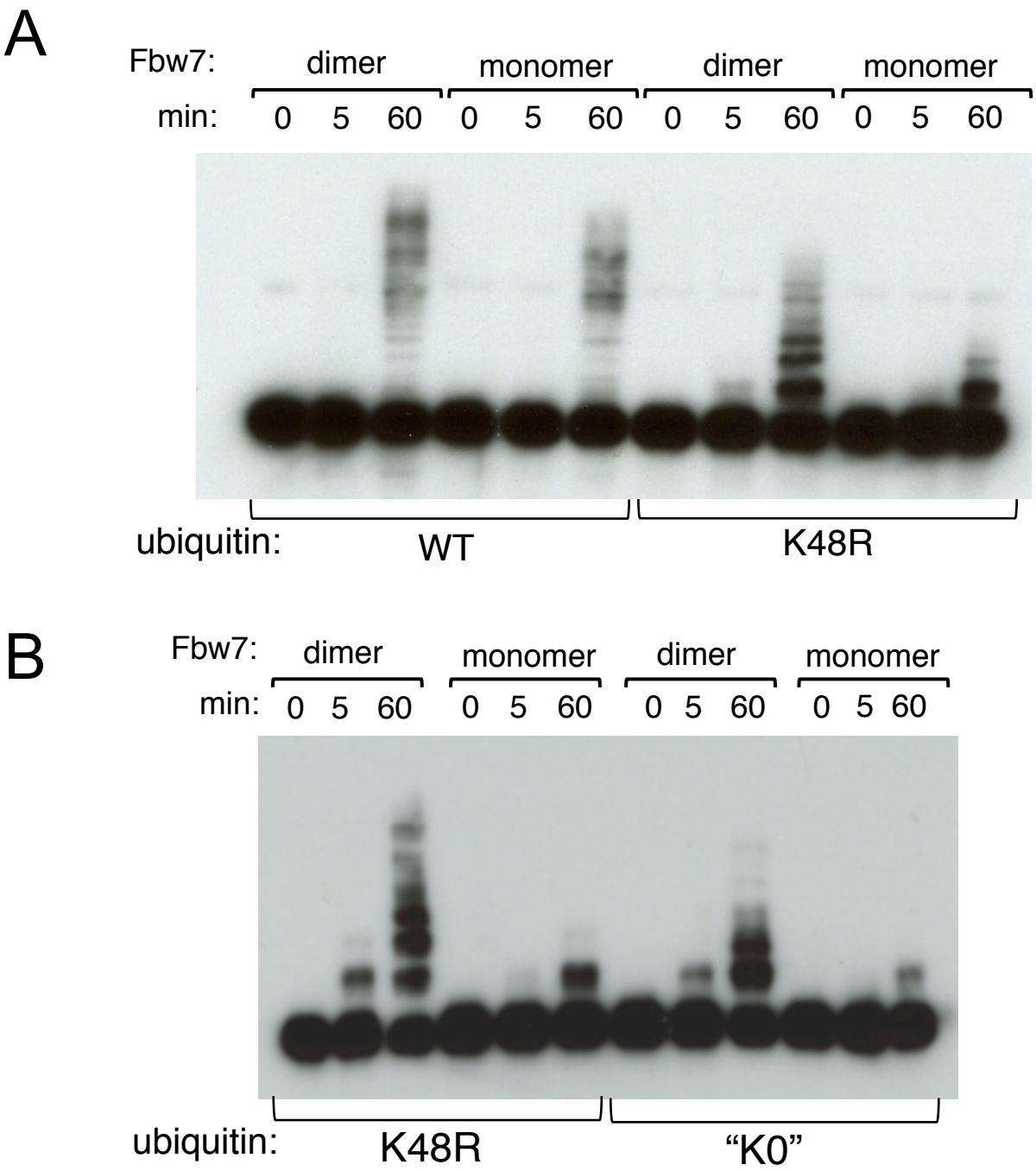

Figure 4.6: Comparison of Fbw7 monomer and dimer lysine accessibility and poly-ubiquitin chain composition

A) The activity of Fbw7 dimer and monomer on wild-type over-expressed cyclin E, utilizing WT and K48R mutant ubiquitin.
B) The activity of Fbw7 dimer and monomer on wild-type over-expressed cyclin E, utilizing K48R mutant ubiquitin and ubiquitin in which all seven lysines are mutated to arginines (K0).

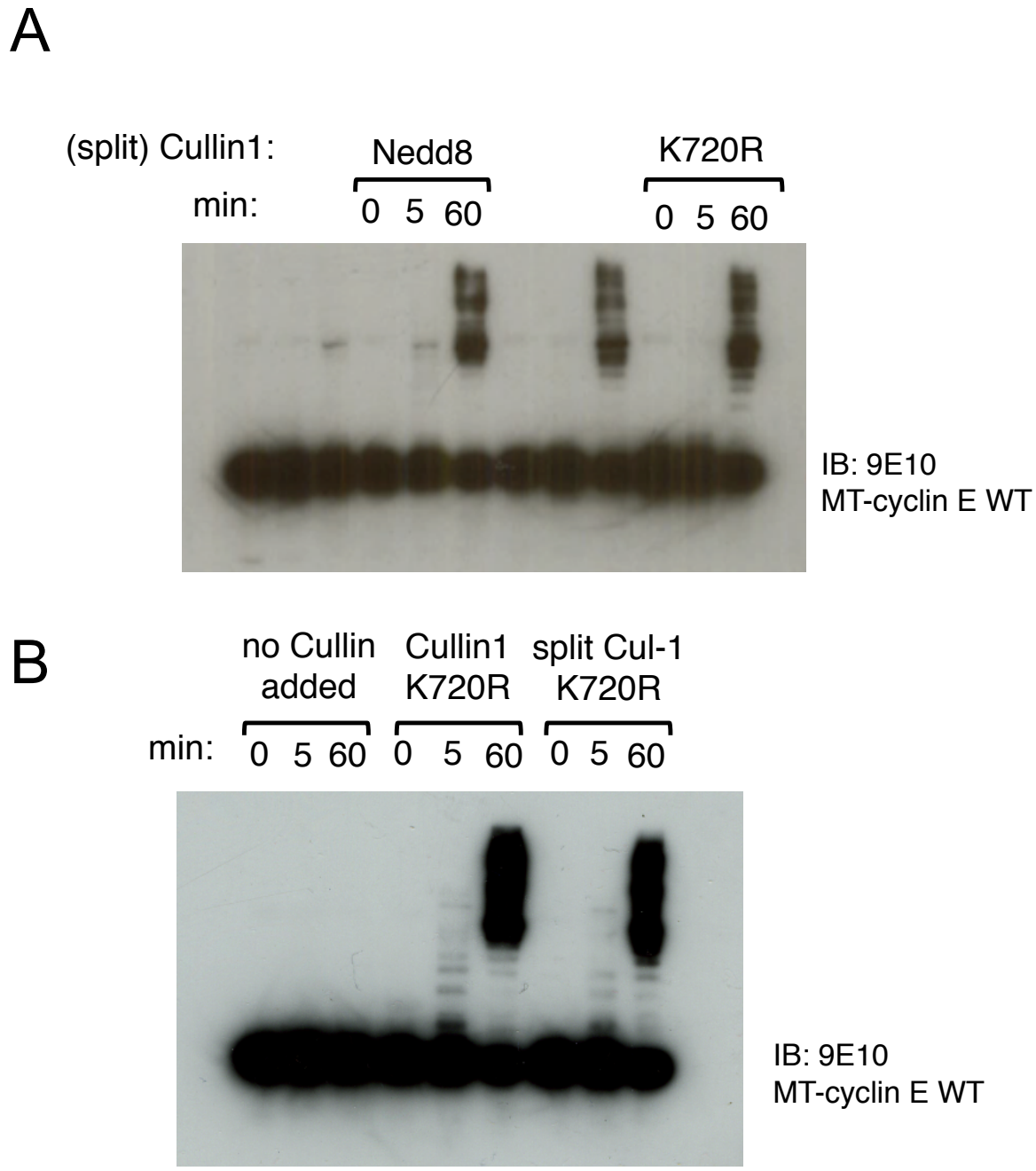

Figure 4.7: Neddylation of Cul-1 does not affect poly-ubiquitylation by Fbw7 *in vitro*

A) Comparison of the purified neddylated split-form Cul-1 (courtesy of H Mao) and neddylation site mutant split-form.
B) Comparison of the split-form and full-length Cul-1 neddylation site mutants.

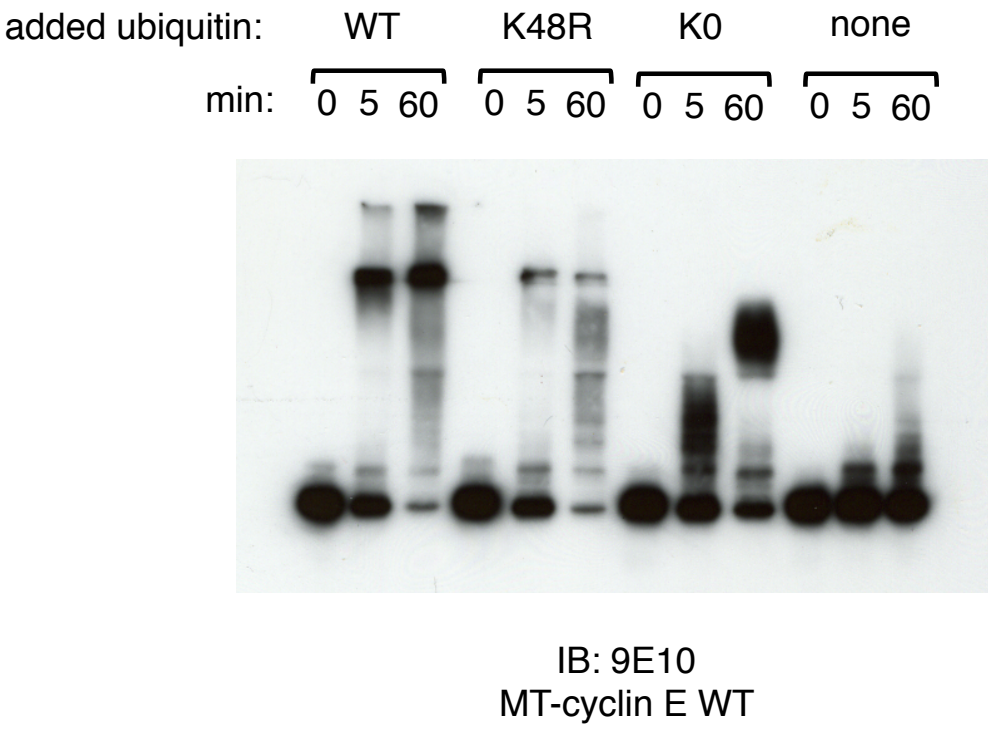

Figure 4.8: UbcH5 is an extremely promiscuous E2

Unlike the Cdc34 data in Figure 4.6, UbcH5 appears much more promiscuous in its chain-building. Even with lysine-less ubiquitin (K0), a large size shift is obvious on much of the cyclin E substrate. Whether this corresponds to many mono-ubiquitin events or N-terminal chain elongation is not known.

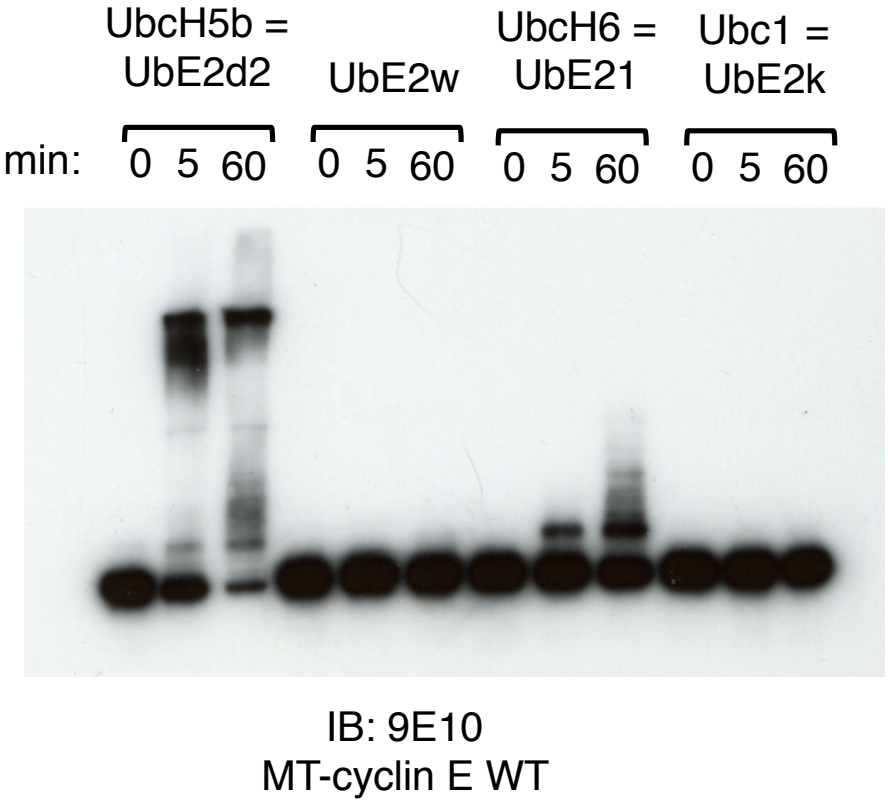

Figure 4.9: Other purified E2s do not demonstrate significant activity with the SCF *in vitro*

A panel of purified E2s was obtained courtesy of P Littlefield and R Klevit, and used in ubiquitylation reactions with over-expressed MT-cyclin E and Fbw7 dimer.

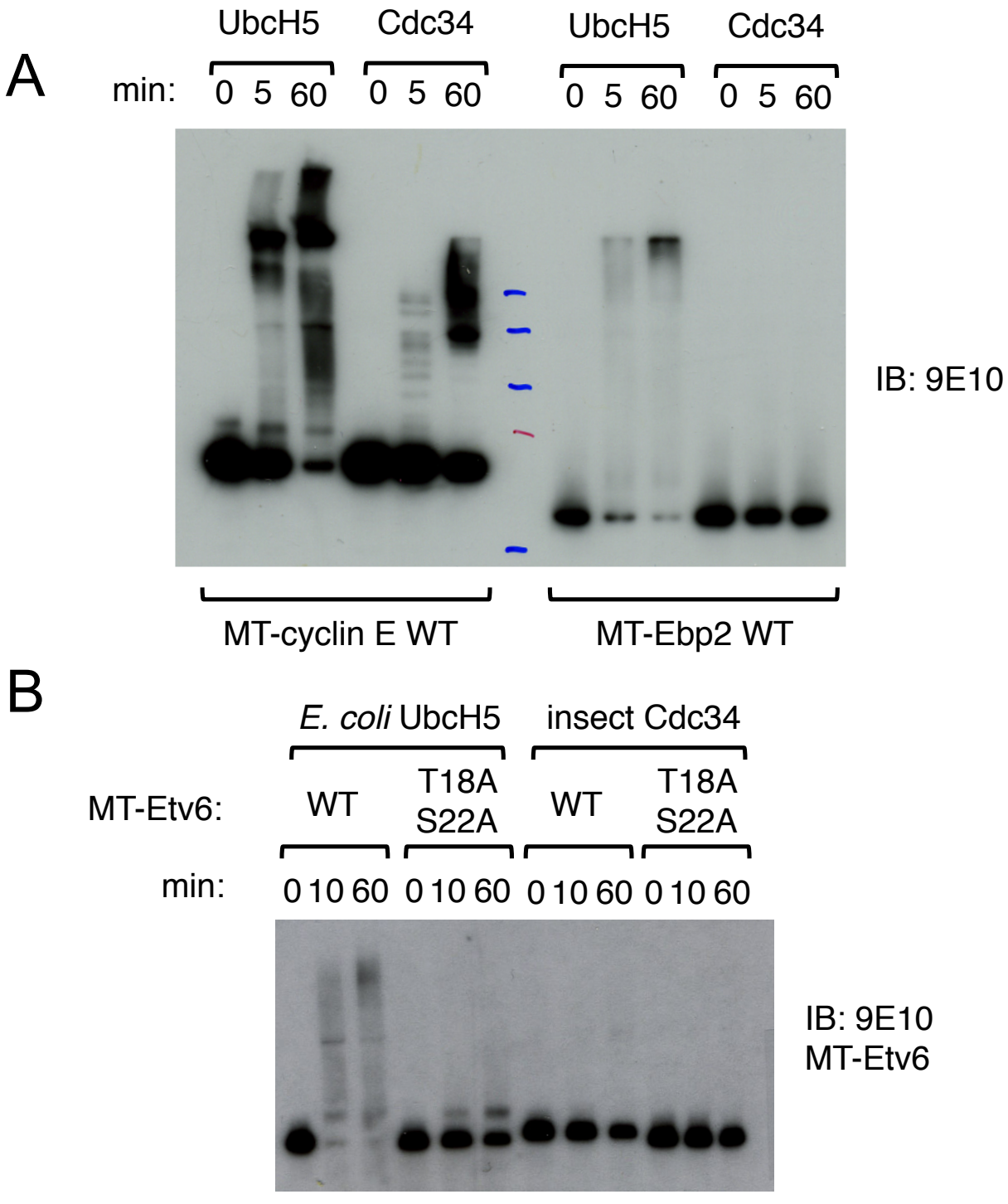

Figure 4.10: Pseudo-substrates are poly-ubiquitylated by UbcH5 but not Cdc34

A) Comparison of poly-ubiquitylation of cyclin E and Ebp2 by both E2s.
B) Poly-ubiquitylation of Etv6 is dependent on the CPD-like sequence, and only occurs with UbcH5.

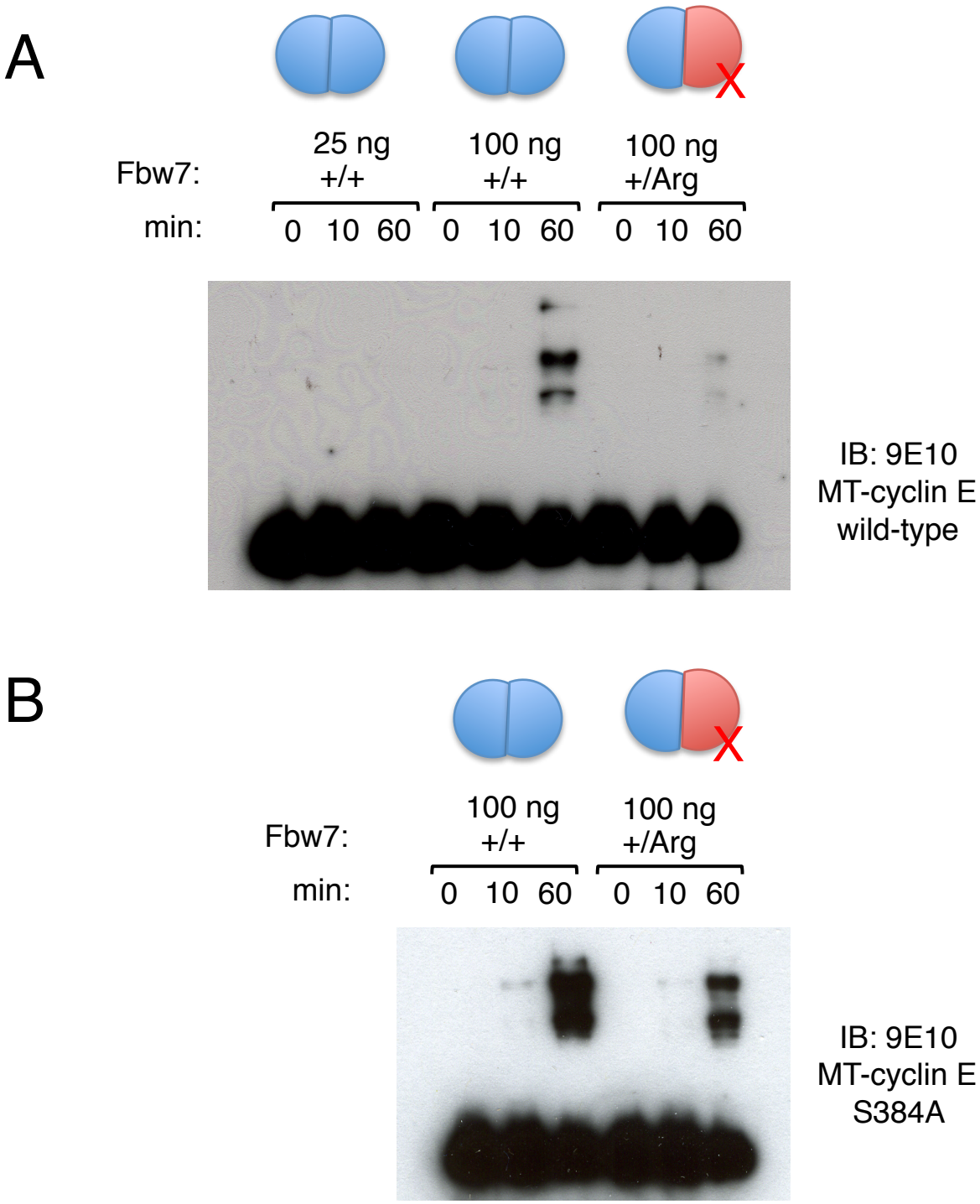

Figure 4.11: Fbw7 hetero-dimer is deficient in leading to poly-ubiquitylation of cyclin E

A) Fbw7 wild-type dimer and hetero-dimer activities compared against wild-type cyclin E. The reaction with 25% wild-type dimer serves as a control for re-shuffling of the dimer.
B) Hetero-dimer is also compromised in poly-ubiquitylation of S384A mutant cyclin .

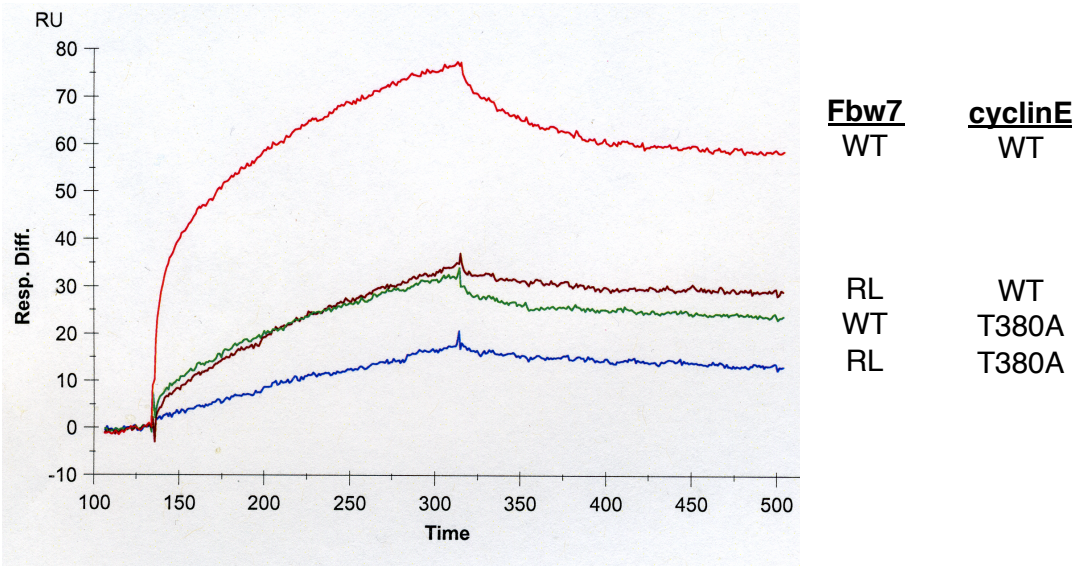

Figure 4.12: Qualitative comparison of Fbw7/cyclin E binding by SPR

Biacore sensorgrams using cyclin E captured from transfected HEK29A lysate (via an anti-Myc-tag antibody, captured on the chip by amine-coupled anti-mouse IgG) as ligand and purified Fbw7 as analyte.

CHAPTER 5

Conclusions and Future Directions

The work presented in this dissertation has centered on the attempt to understand the effect of SCF^{Fbw7} dimerization on substrate regulation. As described in Chapter 2, I used gene-targeting to create a human cell line expressing only Fbw7 monomers. The cells were not largely affected by this perturbation. We saw moderate deregulation of cyclin E, and significant stabilization of c-Myc protein. The stabilization of Myc in these cells is a fairly major result, one not predicted from our over-expression data. The fact that Myc appears to be a substrate dependent on Fbw7 dimerization in cells argues that our over-expression studies may underestimate the number of substrates that rely on Fbw7 dimerization for proper regulation *in vivo*, and validates the importance using a gene-targeting approach to study modifications of endogenous proteins.

In Chapter 3, I successfully generated a recombinant Fbw7 expression and purification system, the first in the field. I discussed at length my varied efforts toward solving the structure of an Fbw7 dimer. In the course of these efforts, I purified the other SCF components and was able to reconstitute the entire SCF dimeric ligase.

Chapter 4 discusses the various *in vitro* assays I developed to study Fbw7 using the purified components I generated during my crystallography efforts. I was able to recapitulate *in vitro* our two-degron model of the engagement of cyclin E by Fbw7. I also was able to study interesting aspects of SCF biology, probing the activities of different E2s, of different forms of Cul-1, and different ubiquitin chain extensions. The reagents I generated during the course of this dissertation work will continue to be extremely useful in the lab for *in vitro* studies.

Although the SCF may be the most-studied Cullin-RING ligase, new facets of its regulation are continually being discovered and discussed. The dimerization of substrate-adapter proteins is a very interesting and not well-understood aspect of this superfamily of ligases. The ability of Fbw7 (and other F-box proteins as well as other Cullin-RING ligase substrate adaptor proteins) to self-associate is

evolutionarily conserved, seen from yeast to worm to fly to human. This strongly suggests that substrate-adaptor proteins dimerize for an important reason. We still do not know whether the dimerized SCF^{Fbw7} complex is capable of simultaneously binding two Cul-1 molecules. Although a seemingly small point, it is an important question, because it is still only conjecture as to whether a dimeric ligase is more efficient because it simultaneously contains two active E2s.

Aside from homo-dimerization, there is also the question of F-box protein hetero-dimerization. It has been suggested that different Fbw7 isoforms are able to hetero-dimerize [62], but if the species are truly spatially separated in cells, this is unlikely to be a physiologic phenomenon. But what about hetero-dimerization of two completely independent F-box proteins, to create a completely mixed SCF dimer? This is a very intriguing possibility, but it has been reported that various yeast F-box proteins do not associate with one another [93], and my limited work on β-TrCP dimerization did not show formation of Fbw7/β-TrCP mixed dimers.

Even if Fbw7 associates with no other F-box protein, the dimerization domain is still a protein-protein interaction domain. It could be possible that some novel protein is able to bind this surface. Or, once could even imagine the interface could make contact with a non-CPD portion of one or more Fbw7 substrates. We have evidence not presented in this dissertation that this phenomenon may be occurring in the regulation of c-Myc, but not N- or L-Myc.

Another possibility along this same line that cannot be ruled out by the studies performed above is the idea of a novel protein binding to the *dimer*, not just the interface. The interlocked dimerization domains could create another interface that allows for the association of another component, a novel regulator of the SCF. Hypothetically, such a protein could serve to lock the WD propellers into a particular conformation, thereby modifying SCF activity.

To explore these lines of reasoning, I was at one time interested in performing a yeast two-hybrid screen to look for proteins that interact with the dimerization domain of Cdc4. I constructed the parental strains and the positive control plasmids to perform the pilot experiment for this screen, but it was deemed too risky an approach, too far outside our lab expertise. Perhaps a series of mass spectrometry experiments would be worthwhile, to see what proteins specifically bound a polypeptide consisting of the

Fbw7 dimerization domain. Of course, we would expect to pull out Fbw7, but what else would we find? An interesting control for this experiment could be a polypeptide containing the ΔD mutation described in Chapter 2. We would expect to lose Fbw7 binding, but what effect would the mutation have on the associated proteins? These results could also be compared to a polypeptide corresponding to the β-TrCP dimerization domain, to see if there are any factors that appear to bind to both domains.

Using the purified Fbw7 in small molecule screens (as briefly mentioned in the Conclusions section of Chapter 4) is a tantalizing approach to identify drugs that could be useful for patients suffering from Fbw7 mutant tumors. As mentioned in Chapter 1, as many as 10% of human malignancies display Fbw7 mutations, and approximately half of these are point mutations of three key arginine residues that result in abrogated substrate binding. As long as gene-targeting to correct such somatic mutations in patients remains a far-off proposition, the idea of rescuing the protein/protein interaction with a small molecule is an attractive avenue. Use of a small molecule as a 'molecular glue' to hold an SCF to its substrate is seen in nature, in an *Arabidopsis* SCF complex [106].

Knowing now that the majority of cellular Fbw7 exists as a dimer, these types of *in vitro* experiments ought to be performed with the dimeric form of the protein. The studies of the past decade that have looked at Fbw7 monomer have been extremely valuable in understanding the function of the protein. However, now it is time to focus on the physiologically relevant form of the protein, the dimer. The impact that F-box protein dimerization has on the overall SCF structure (and, likely, function) cannot be understated. As mentioned briefly in the previous chapters, understanding the impact of isoform identify on substrate regulation is another challenge for the coming decade.

BIBLIOGRAPHY

1. Ciechanover, A., *Proteolysis: from the lysosome to ubiquitin and the proteasome.* Nat Rev Mol Cell Biol, 2005. **6**(1): p. 79-87.

2. Hilt, W. and D.H. Wolf, *Proteasomes : the world of regulatory proteolysis edited by Wolfgang Hilt, Dieter H. Wolf.* 2000, Georgetown, Tx
Austin, Tex.: Landes Bioscience ;
Eurekah.com. 391.

3. Hershko, A. and A. Ciechanover, *The ubiquitin system.* Annu Rev Biochem, 1998. **67**: p. 425-79.

4. Ye, Y. and M. Rape, *Building ubiquitin chains: E2 enzymes at work.* Nat Rev Mol Cell Biol, 2009. **10**(11): p. 755-64.

5. Deshaies, R.J. and C.A. Joazeiro, *RING domain E3 ubiquitin ligases.* Annu Rev Biochem, 2009. **78**: p. 399-434.

6. Schulman, B.A. and J.W. Harper, *Ubiquitin-like protein activation by E1 enzymes: the apex for downstream signalling pathways.* Nat Rev Mol Cell Biol, 2009. **10**(5): p. 319-31.

7. van Wijk, S.J. and H.T. Timmers, *The family of ubiquitin-conjugating enzymes (E2s): deciding between life and death of proteins.* FASEB J. **24**(4): p. 981-93.

8. Hershko, A. and A. Ciechanover, *The ubiquitin system.* Annu Rev Biochem, 1998. **67**: p. 425-79.

9. Spence, J., et al., *A ubiquitin mutant with specific defects in DNA repair and multiubiquitination.* Mol Cell Biol, 1995. **15**(3): p. 1265-73.

10. Sun, L. and Z.J. Chen, *The novel functions of ubiquitination in signaling.* Curr Opin Cell Biol, 2004. **16**(2): p. 119-26.

11. Sadowski, M., et al., *Protein monoubiquitination and polyubiquitination generate structural diversity to control distinct biological processes.* IUBMB Life. **64**(2): p. 136-42.

12. Pickart, C.M., *Mechanisms underlying ubiquitination.* Annu Rev Biochem, 2001. **70**: p. 503-33.

13. Ohta, T., et al., *ROC1, a homolog of APC11, represents a family of cullin partners with an associated ubiquitin ligase activity.* Mol Cell, 1999. **3**(4): p. 535-41.

14. Vodermaier, H.C., *APC/C and SCF: controlling each other and the cell cycle.* Curr Biol, 2004. **14**(18): p. R787-96.

15. Zheng, N., et al., *Structure of the Cul1-Rbx1-Skp1-F boxSkp2 SCF ubiquitin ligase complex.* Nature, 2002. **416**(6882): p. 703-9.

16. Skowyra, D., et al., *F-box proteins are receptors that recruit phosphorylated substrates to the SCF ubiquitin-ligase complex.* Cell, 1997. **91**(2): p. 209-19.

17. Bai, C., et al., *SKP1 connects cell cycle regulators to the ubiquitin proteolysis machinery through a novel motif, the F-box.* Cell, 1996. **86**(2): p. 263-74.

18. Willems, A.R., M. Schwab, and M. Tyers, *A hitchhiker's guide to the cullin ubiquitin ligases: SCF and its kin.* Biochim Biophys Acta, 2004. **1695**(1-3): p. 133-70.

19. Koff, A., et al., *Formation and activation of a cyclin E-cdk2 complex during the G1 phase of the human cell cycle.* Science, 1992. **257**(5077): p. 1689-94.

20. Ohtsubo, M. and J.M. Roberts, *Cyclin-dependent regulation of G1 in mammalian fibroblasts.* Science, 1993. **259**(5103): p. 1908-12.

21. Resnitzky, D., et al., *Acceleration of the G1/S phase transition by expression of cyclins D1 and E with an inducible system.* Mol Cell Biol, 1994. **14**(3): p. 1669-79.

22. Spruck, C.H., K.A. Won, and S.I. Reed, *Deregulated cyclin E induces chromosome instability.* Nature, 1999. **401**(6750): p. 297-300.

23. Strohmaier, H., et al., *Human F-box protein hCdc4 targets cyclin E for proteolysis and is mutated in a breast cancer cell line.* Nature, 2001. **413**(6853): p. 316-22.

24. Keyomarsi, K., et al., *Deregulation of cyclin E in breast cancer.* Oncogene, 1995. **11**(5): p. 941-50.

25. Porter, P.L., et al., *Expression of cell-cycle regulators p27Kip1 and cyclin E, alone and in combination, correlate with survival in young breast cancer patients.* Nat Med, 1997. **3**(2): p. 222-5.

26. Keyomarsi, K., et al., *Cyclin E and survival in patients with breast cancer.* N Engl J Med, 2002. **347**(20): p. 1566-75.

27. Bortner, D.M. and M.P. Rosenberg, *Induction of mammary gland hyperplasia and carcinomas in transgenic mice expressing human cyclin E.* Mol Cell Biol, 1997. **17**(1): p. 453-9.

28. Keyomarsi, K. and A.B. Pardee, *Redundant cyclin overexpression and gene amplification in breast cancer cells.* Proc Natl Acad Sci U S A, 1993. **90**(3): p. 1112-6.

29. Cassia, R., et al., *Cyclin E gene (CCNE) amplification and hCDC4 mutations in endometrial carcinoma.* J Pathol, 2003. **201**(4): p. 589-95.

30. Koepp, D.M., et al., *Phosphorylation-dependent ubiquitination of cyclin E by the SCFFbw7 ubiquitin ligase.* Science, 2001. **294**(5540): p. 173-7.

31. Won, K.A. and S.I. Reed, *Activation of cyclin E/CDK2 is coupled to site-specific autophosphorylation and ubiquitin-dependent degradation of cyclin E.* EMBO J, 1996. **15**(16): p. 4182-93.

32. Clurman, B.E., et al., *Turnover of cyclin E by the ubiquitin-proteasome pathway is regulated by cdk2 binding and cyclin phosphorylation.* Genes Dev, 1996. **10**(16): p. 1979-90.

33. Welcker, M., et al., *Multisite phosphorylation by Cdk2 and GSK3 controls cyclin E degradation.* Mol Cell, 2003. **12**(2): p. 381-92.

34. Ye, X., et al., *Recognition of phosphodegron motifs in human cyclin E by the SCF(Fbw7) ubiquitin ligase.* J Biol Chem, 2004. **279**(48): p. 50110-9.

35. Singer, J.D., et al., *Cullin-3 targets cyclin E for ubiquitination and controls S phase in mammalian cells.* Genes Dev, 1999. **13**(18): p. 2375-87.

36. McEvoy, J.D., et al., *Constitutive turnover of cyclin E by Cul3 maintains quiescence.* Mol Cell Biol, 2007. **27**(10): p. 3651-66.

37. Moberg, K.H., et al., *Archipelago regulates Cyclin E levels in Drosophila and is mutated in human cancer cell lines.* Nature, 2001. **413**(6853): p. 311-6.

38. Moberg, K.H., et al., *The Drosophila F box protein archipelago regulates dMyc protein levels in vivo.* Curr Biol, 2004. **14**(11): p. 965-74.

39. Welcker, M., et al., *The Fbw7 tumor suppressor regulates glycogen synthase kinase 3 phosphorylation-dependent c-Myc protein degradation.* Proc Natl Acad Sci U S A, 2004. **101**(24): p. 9085-90.

40. Yada, M., et al., *Phosphorylation-dependent degradation of c-Myc is mediated by the F-box protein Fbw7.* EMBO J, 2004. **23**(10): p. 2116-25.

41. Nateri, A.S., et al., *The ubiquitin ligase SCFFbw7 antagonizes apoptotic JNK signaling.* Science, 2004. **303**(5662): p. 1374-8.

42. Wei, W., et al., *The v-Jun point mutation allows c-Jun to escape GSK3-dependent recognition and destruction by the Fbw7 ubiquitin ligase.* Cancer Cell, 2005. **8**(1): p. 25-33.

43. Welcker, M., et al., *A nucleolar isoform of the Fbw7 ubiquitin ligase regulates c-Myc and cell size.* Curr Biol, 2004. **14**(20): p. 1852-7.

44. Tsunematsu, R., et al., *Mouse Fbw7/Sel-10/Cdc4 is required for notch degradation during vascular development.* J Biol Chem, 2004. **279**(10): p. 9417-23.

45. Tetzlaff, M.T., et al., *Defective cardiovascular development and elevated cyclin E and Notch proteins in mice lacking the Fbw7 F-box protein.* Proc Natl Acad Sci U S A, 2004. **101**(10): p. 3338-45.

46. Oberg, C., et al., *The Notch intracellular domain is ubiquitinated and negatively regulated by the mammalian Sel-10 homolog.* J Biol Chem, 2001. **276**(38): p. 35847-53.

47. Spruck, C.H., et al., *hCDC4 gene mutations in endometrial cancer.* Cancer Res, 2002. **62**(16): p. 4535-9.

48. Rajagopalan, H., et al., *Inactivation of hCDC4 can cause chromosomal instability.* Nature, 2004. **428**(6978): p. 77-81.

49. Sundqvist, A., et al., *Control of lipid metabolism by phosphorylation-dependent degradation of the SREBP family of transcription factors by SCF(Fbw7).* Cell Metab, 2005. **1**(6): p. 379-91.

50. Punga, T., M.T. Bengoechea-Alonso, and J. Ericsson, *Phosphorylation and ubiquitination of the transcription factor sterol regulatory element-binding protein-1 in response to DNA binding.* J Biol Chem, 2006. **281**(35): p. 25278-86.

51. Wertz, I.E., et al., *Sensitivity to antitubulin chemotherapeutics is regulated by MCL1 and FBW7.* Nature. **471**(7336): p. 110-4.

52. Inuzuka, H., et al., *SCF(FBW7) regulates cellular apoptosis by targeting MCL1 for ubiquitylation and destruction.* Nature. **471**(7336): p. 104-9.

53. Bengoechea-Alonso, M.T. and J. Ericsson, *Tumor suppressor Fbxw7 regulates TGFbeta signaling by targeting TGIF1 for degradation.* Oncogene. **29**(38): p. 5322-8.

54. Zhao, D., et al., *The Fbw7 tumor suppressor targets KLF5 for ubiquitin-mediated degradation and suppresses breast cell proliferation.* Cancer Res. **70**(11): p. 4728-38.

55. Liu, N., et al., *The Fbw7/human CDC4 tumor suppressor targets proproliferative factor KLF5 for ubiquitination and degradation through multiple phosphodegron motifs.* J Biol Chem. **285**(24): p. 18858-67.

56. Wood, L.D., et al., *The genomic landscapes of human breast and colorectal cancers.* Science, 2007. **318**(5853): p. 1108-13.

57. Hubbard, E.J., et al., *sel-10, a negative regulator of lin-12 activity in Caenorhabditis elegans, encodes a member of the CDC4 family of proteins.* Genes Dev, 1997. **11**(23): p. 3182-93.

58. Orlicky, S., et al., *Structural basis for phosphodependent substrate selection and orientation by the SCFCdc4 ubiquitin ligase.* Cell, 2003. **112**(2): p. 243-56.

59. Akhoondi, S., et al., *FBXW7/hCDC4 is a general tumor suppressor in human cancer.* Cancer Res, 2007. **67**(19): p. 9006-12.

60. O'Neil, J., et al., *FBW7 mutations in leukemic cells mediate NOTCH pathway activation and resistance to gamma-secretase inhibitors.* J Exp Med, 2007. **204**(8): p. 1813-24.

61. Kimura, T., et al., *hCDC4b, a regulator of cyclin E, as a direct transcriptional target of p53.* Cancer Sci, 2003. **94**(5): p. 431-6.

62. Zhang, W. and D.M. Koepp, *Fbw7 isoform interaction contributes to cyclin E proteolysis.* Mol Cancer Res, 2006. **4**(12): p. 935-43.

63. Welcker, M. and B.E. Clurman, *Fbw7/hCDC4 dimerization regulates its substrate interactions.* Cell Div, 2007. **2**: p. 7.

64. Schwob, E., et al., *The B-type cyclin kinase inhibitor p40SIC1 controls the G1 to S transition in S. cerevisiae.* Cell, 1994. **79**(2): p. 233-44.

65. Verma, R., R.M. Feldman, and R.J. Deshaies, *SIC1 is ubiquitinated in vitro by a pathway that requires CDC4, CDC34, and cyclin/CDK activities.* Mol Biol Cell, 1997. **8**(8): p. 1427-37.

66. Meimoun, A., et al., *Degradation of the transcription factor Gcn4 requires the kinase Pho85 and the SCF(CDC4) ubiquitin-ligase complex.* Mol Biol Cell, 2000. **11**(3): p. 915-27.

67. Blondel, M., et al., *Nuclear-specific degradation of Far1 is controlled by the localization of the F-box protein Cdc4.* EMBO J, 2000. **19**(22): p. 6085-97.

68. Drury, L.S., G. Perkins, and J.F. Diffley, *The Cdc4/34/53 pathway targets Cdc6p for proteolysis in budding yeast.* EMBO J, 1997. **16**(19): p. 5966-76.

69. Nash, P., et al., *Multisite phosphorylation of a CDK inhibitor sets a threshold for the onset of DNA replication.* Nature, 2001. **414**(6863): p. 514-21.

70. Tang, X., et al., *Composite low affinity interactions dictate recognition of the cyclin-dependent kinase inhibitor Sic1 by the SCFCdc4 ubiquitin ligase.* Proc Natl Acad Sci U S A, 2012. **109**(9): p. 3287-92.

71. Klein, P., T. Pawson, and M. Tyers, *Mathematical modeling suggests cooperative interactions between a disordered polyvalent ligand and a single receptor site.* Curr Biol, 2003. **13**(19): p. 1669-78.

72. Mittag, T., et al., *Dynamic equilibrium engagement of a polyvalent ligand with a single-site receptor.* Proc Natl Acad Sci U S A, 2008. **105**(46): p. 17772-7.

73. Hao, B., et al., *Structure of a Fbw7-Skp1-cyclin E complex: multisite-phosphorylated substrate recognition by SCF ubiquitin ligases.* Mol Cell, 2007. **26**(1): p. 131-43.

74. Kominami, K., I. Ochotorena, and T. Toda, *Two F-box/WD-repeat proteins Pop1 and Pop2 form hetero- and homo-complexes together with cullin-1 in the fission yeast SCF (Skp1-Cullin-1-F-box) ubiquitin ligase.* Genes Cells, 1998. **3**(11): p. 721-35.

75. Wolf, D.A., F. McKeon, and P.K. Jackson, *F-box/WD-repeat proteins pop1p and Sud1p/Pop2p form complexes that bind and direct the proteolysis of cdc18p.* Curr Biol, 1999. **9**(7): p. 373-6.

76. Tang, X., et al., *Suprafacial orientation of the SCFCdc4 dimer accommodates multiple geometries for substrate ubiquitination.* Cell, 2007. **129**(6): p. 1165-76.

77. Suzuki, H., et al., *Homodimer of two F-box proteins betaTrCP1 or betaTrCP2 binds to IkappaBalpha for signal-dependent ubiquitination.* J Biol Chem, 2000. **275**(4): p. 2877-84.

78. Barbash, O., et al., *Mutations in Fbx4 inhibit dimerization of the SCF(Fbx4) ligase and contribute to cyclin D1 overexpression in human cancer.* Cancer Cell, 2008. **14**(1): p. 68-78.

79. Dixon, C., et al., *Overproduction of polypeptides corresponding to the amino terminus of the F-box proteins Cdc4p and Met30p inhibits ubiquitin ligase activities of their SCF complexes.* Eukaryot Cell, 2003. **2**(1): p. 123-33.

80. Mingozzi, F. and K.A. High, *Therapeutic in vivo gene transfer for genetic disease using AAV: progress and challenges.* Nat Rev Genet. **12**(5): p. 341-55.

81. Michelfelder, S. and M. Trepel, *Adeno-associated viral vectors and their redirection to cell-type specific receptors.* Adv Genet, 2009. **67**: p. 29-60.

82. Wang, J., S.M. Faust, and J.E. Rabinowitz, *The next step in gene delivery: molecular engineering of adeno-associated virus serotypes.* J Mol Cell Cardiol. **50**(5): p. 793-802.

83. Khan, I.F., R.K. Hirata, and D.W. Russell, *AAV-mediated gene targeting methods for human cells.* Nat Protoc, 2011. **6**(4): p. 482-501.

84. Wang, X.S., S. Ponnazhagan, and A. Srivastava, *Rescue and replication signals of the adeno-associated virus 2 genome.* J Mol Biol, 1995. **250**(5): p. 573-80.

85. Hirata, R.K. and D.W. Russell, *Design and packaging of adeno-associated virus gene targeting vectors.* J Virol, 2000. **74**(10): p. 4612-20.

86. Grim, J.E., et al., *Isoform- and cell cycle-dependent substrate degradation by the Fbw7 ubiquitin ligase.* J Cell Biol, 2008. **181**(6): p. 913-20.

87. Kohli, M., et al., *Facile methods for generating human somatic cell gene knockouts using recombinant adeno-associated viruses.* Nucleic Acids Res, 2004. **32**(1): p. e3.

88. Topaloglu, O., et al., *Improved methods for the generation of human gene knockout and knockin cell lines.* Nucleic Acids Res, 2005. **33**(18): p. e158.

89. Ericson, K., et al., *Genetic inactivation of AKT1, AKT2, and PDPK1 in human colorectal cancer cells clarifies their roles in tumor growth regulation.* Proc Natl Acad Sci U S A. **107**(6): p. 2598-603.

90. Hirata, R.K., et al., *Efficient PRNP gene targeting in bovine fibroblasts by adeno-associated virus vectors.* Cloning Stem Cells, 2004. **6**(1): p. 31-6.

91. Yeh, E., et al., *A signalling pathway controlling c-Myc degradation that impacts oncogenic transformation of human cells.* Nat Cell Biol, 2004. **6**(4): p. 308-18.

92. Orlicky, S., et al., *Structural basis for phosphodependent substrate selection and orientation by the SCFCdc4 ubiquitin ligase.* Cell, 2003. **112**(2): p. 243-56.

93. Tang, X., et al., *Suprafacial orientation of the SCFCdc4 dimer accommodates multiple geometries for substrate ubiquitination.* Cell, 2007. **129**(6): p. 1165-76.

94. Honda, R., et al., *The structure of cyclin E1/CDK2: implications for CDK2 activation and CDK2-independent roles.* EMBO J, 2005. **24**(3): p. 452-63.

95. Schulman, B.A., et al., *Insights into SCF ubiquitin ligases from the structure of the Skp1-Skp2 complex.* Nature, 2000. **408**(6810): p. 381-6.

96. Walter, T.S., et al., *Lysine methylation as a routine rescue strategy for protein crystallization.* Structure, 2006. **14**(11): p. 1617-22.

97. Kim, Y., et al., *Large-scale evaluation of protein reductive methylation for improving protein crystallization.* Nat Methods, 2008. **5**(10): p. 853-4.

98. Tsai, L.H., E. Harlow, and M. Meyerson, *Isolation of the human cdk2 gene that encodes the cyclin A- and adenovirus E1A-associated p33 kinase.* Nature, 1991. **353**(6340): p. 174-7.

99. Gu, Y., J. Rosenblatt, and D.O. Morgan, *Cell cycle regulation of CDK2 activity by phosphorylation of Thr160 and Tyr15.* EMBO J, 1992. **11**(11): p. 3995-4005.

100. Espinoza, F.H., et al., *A cyclin-dependent kinase-activating kinase (CAK) in budding yeast unrelated to vertebrate CAK.* Science, 1996. **273**(5282): p. 1714-7.

101. Kitagawa, K., et al., *SGT1 encodes an essential component of the yeast kinetochore assembly pathway and a novel subunit of the SCF ubiquitin ligase complex.* Mol Cell, 1999. **4**(1): p. 21-33.

102. Su, Y., et al., *The acidity of protein fusion partners predominantly determines the efficacy to improve the solubility of the target proteins expressed in Escherichia coli.* J Biotechnol, 2007. **129**(3): p. 373-82.

103. Duda, D.M., et al., *Structural insights into NEDD8 activation of cullin-RING ligases: conformational control of conjugation.* Cell, 2008. **134**(6): p. 995-1006.

104. Wu, K., J. Kovacev, and Z.Q. Pan, *Priming and extending: a UbcH5/Cdc34 E2 handoff mechanism for polyubiquitination on a SCF substrate.* Mol Cell. **37**(6): p. 784-96.

105. Emberley, E.D., R. Mosadeghi, and R.J. Deshaies, *Deconjugation of Nedd8 from Cul1 is directly regulated by Skp1-Fbox and substrate, and CSN inhibits deneddylated SCF by a non-catalytic mechanism.* J Biol Chem.

106. Tan, X., et al., *Mechanism of auxin perception by the TIR1 ubiquitin ligase.* Nature, 2007. **446**(7136): p. 640-5.

CURRICULUM VITAE

Elizabeth Anne Larimore

EDUCATION

September 2006 – August 2012

University of Washington, Seattle WA

PhD, Molecular and Cellular Biology (MCB), advised by Dr. Bruce Clurman and Dr. Ning Zheng

- Dissertation title: "Dimerization of the Fbw7 ubiquitin ligase impacts substrate regulation, tumor suppressor activity"
- Cumulative GPA 3.62

August 2002 – May 2006

Cornell University, Ithaca NY

- BA, Biological Sciences, Molecular and Cell Biology concentration; East Asian Studies minor
- Cumulative GPA 3.76, *magna cum laude* graduate

EXPERIENCE

September 2006 – August 2012

Graduate Research Associate

University of Washington/Fred Hutchinson Cancer Research Center (FHCRC), Seattle WA

- Thesis research centered on the basic biology of a human protein called Fbw7, classified in recent years as the fifth most important tumor suppressor, and is mutated in approximately 10% of human cancers
- Used gene-targeting techniques to create a human cell line in which the Fbw7 protein cannot dimerize; studied the downstream cellular effects
- Extensive experience in protein purification: first in the field to purify Fbw7 in its physiologically relevant dimeric form
- Developed various *in vitro* and *in vivo* biochemical assays to test activity and properties of dimeric Fbw7
- Trained and advised a postdoc and staff scientist in carrying out small molecule drug screen (in collaboration with GlaxoSmithKline) to search for drugs that can restore Fbw7 function in tumors with Fbw7 mutations

Advisors: Dr. Bruce Clurman, Dr. Ning Zheng

January 2003 – May 2006

Undergraduate Researcher

Department of Molecular Biology and Genetics, Cornell University, Ithaca NY

- Research culminated in honors research thesis, awarded high honors
- Using *D. melanogaster* eye pigment deposition as a read-out of gene expression, correlated variation in pigment deposition to SNPs in second-chromosome genes known to affect chromatin remodeling
- Developed image-based software to quantitate area of eye pigment deposition

Advisor: Dr. Andrew Clark

June 2011 – September 2011

Summer Intern

Product & Process Development, Amgen Inc., Seattle WA

- Performed high-throughput screening to study the capability of chromatography resins to clear contaminating virus particles, a crucial aspect of filing for FDA approval of biotherapeutics
- Worked in a collaborative, industrial setting, at the interface of Purification and Biosafety departments
- Exposed to the challenges of producing biotherapeutics at commercial scales and the regulations governing their manufacture

- Presented data, analysis, conclusions and future directions in site-wide poster session and in oral presentation to Purification Process Development department

Supervisor: Dr. Lisa Connell-Crowley

October 2009 – May 2010

Volunteer Intern
Immusoft Corporation, Seattle WA

- Volunteered part-time doing market research for a Seattle start-up company co-founded by a recent graduate
- Analyzed potential indications for Immusoft's technology; compiled a list of California biotechnology companies that would be potential customers

PUBLICATIONS

Larimore EA, Welcker M, Zheng N & Clurman BE. Dimerization of Fbw7 contributes to proper regulation of oncogenic substrates cyclin E and c-Myc. In preparation.

Connell-Crowley L, **Larimore EA**, Gillespie R. High throughput screening to define virus clearance on chromatography resins. In preparation.

Welcker M, **Larimore EA**, Frappier L & Clurman BE. Nucleolar targeting of the Fbw7 ubiquitin ligase by a pseudosubstrate and glycogen synthase kinase 3. *Molecular & Cellular Biology*, March 2011.

SELECTED PRESENTATIONS

Larimore EA, Welcker M & Clurman BE. "The Fbw7 tumor suppressor: genetic and biochemical approaches to study a dimeric ubiquitin ligase." American Association for Cancer Research (AACR) Annual Meeting, 2012. Highly rated poster.

Connell-Crowley L, **Larimore B**, Gillespie R & Vunnum S. "High throughput process development: Identifying key operating parameters for retrovirus clearance by AEX and mixed mode resins." American Chemical Society National Meeting, 2012.

FELLOWSHIPS & HONORS

Highly rated poster award, AACR annual meeting	**March 2012**
Cell & Molecular Biology Training Grant	**July 2009 – June 2011**
Ruth L. Kirschstein National Service Research Award	**August 2008 – June 2009**
High honors, undergraduate research honors thesis	**May 2006**
HHMI Hughes Scholar	**June 2005 – August 2005**
Cornell Asian Studies Department Travel Fellowship, Japan	**May 2004 – August 2004**
Cornell University Dean's List	**Fall 2002 – Spring 2006**

TEACHING EXPERIENCE

Summer 2008

Science Education Partnership mentor, FHCRC

Paired with a Washington public high school science teacher who shadowed me in the lab for two weeks; along with the other participating graduate students, I also gave lectures and demonstrations for the participating educators

Fall 2007

Teaching assistant, Biochemistry 440, "Protein Structure and Intermediary Metabolism"

Provided weekly recitation section and one-on-one help for sixty UW undergraduate students

VOLUNTEER EXPERIENCE (SELECTED)

Washington Biotechnology and Biomedical Association's Governor's Life Sciences Summit volunteer
Led annual DNA isolation activity for high school students, FHCRC
Evaluated high school student summer intern posters, FHCRC
Judged science ethics presentations and science project oral defenses at Seattle area high schools

CONFERENCE PRESENTATIONS

Ubiquitin Drug Discovery Conference, Philadelphia PA	**2012**
American Association for Cancer Research Annual Meeting, Chicago IL	**2012**
"The Cell Cycle," Cold Spring Harbor Laboratories NY	**2008**

ACADEMIC LEADERSHIP

Selection committee: McDougall Award, for excellence in mentoring at FHCRC	**2010**
Planning committee: MCB Student Symposium, "Evolution: from molecules to mammals"	**2009**

PROFESSIONAL ASSOCIATION MEMBERSHIPS

Association for Women in Science
Washington Biotechnology and Biomedical Association